University of California
Santa Barbara

Soft-Reset Control and Optimization

A dissertation submitted in partial satisfaction
of the requirements for the degree

Doctor of Philosophy
in
Electrical and Computer Engineering

by

Justin Huynh Le

Committee in charge:

Professor Andrew R. Teel, Chair
Professor João P. Hespanha
Professor Francesco Bullo
Professor Jorge I. Poveda

June 2023

The Dissertation of Justin Huynh Le is approved.

Professor João P. Hespanha

Professor Francesco Bullo

Professor Jorge I. Poveda

Professor Andrew R. Teel, Committee Chair

June 2023

Soft-Reset Control and Optimization

by

Justin Huynh Le

To my parents.

Acknowledgements

I would like to thank Professor Andrew Teel for his kindness and patience as a mentor and for giving me guidance and encouragement to pursue my interests. I would like to thank the Air Force Office of Scientific Research for supporting Professor Teel's research and thereby supporting mine. I would like to thank Professor Teel, along with the other dissertation committee members, Professor João Hespanha, Professor Francesco Bullo, and Professor Jorge Poveda, as well as Professor Jason Marden and Professor Mahnoosh Alizadeh, for their thoughtfulness and for taking the time to share their incredible wealth of knowledge through many discussions, lectures, and reading recommendations. I would like to thank all of the students, researchers, and staff members who I have had the privilege of knowing at the CCDC and at UCSB for their friendship, support, and insights. Finally, I would like to thank my family, especially my parents and my brother, for their unending love and support.

Curriculum Vitæ

Justin Huynh Le

Education

2023	Ph.D. in Electrical and Computer Engineering (Expected), University of California, Santa Barbara.
2018	M.S. in Electrical Engineering, University of Nevada, Las Vegas.
2016	B.S. in Electrical Engineering, Minor in Mathematics, University of Nevada, Las Vegas.

Publications

1. M. Baradaran Hosseini, J. H. Le, and A. R. Teel, *Input-to-state stability of soft-reset systems with nonlinear data*, *Mathematics of Control, Signals, and Systems* (Feb, 2023).
2. J. H. Le and A. R. Teel, *Concurrent learning in high-order tuners for parameter identification*, in *2022 IEEE 61st Conference on Decision and Control (CDC)*, pp. 2159–2164, 2022.
3. J. H. Le and A. R. Teel, *Passive soft-reset controllers for nonlinear systems*, in *2021 60th IEEE Conference on Decision and Control (CDC)*, pp. 5320–5325, 2021.
4. J. H. Le and A. R. Teel, *Hybrid heavy-ball systems: Reset methods for optimization with uncertainty*, in *2021 American Control Conference (ACC)*, pp. 2236–2241, 2021.
5. M. Baradaran Hosseini, J. H. Le, and A. R. Teel, *Analyzing the effect of persistent asset switches on a class of hybrid-inspired optimization algorithms*, in *2021 American Control Conference (ACC)*, pp. 3422–3427, 2021.
6. A. R. Teel, J. I. Poveda, and J. H. Le, *First-order optimization algorithms with resets and Hamiltonian flows*, in *58th IEEE Conference on Decision and Control*, pp. 5838–5843, 2019.
7. J. H. Le, A. P. Yazdanpanah, E. E. Regentova, and V. Muthukumar, *A deep belief network for classifying remotely-sensed hyperspectral data*, in *Advances in Visual Computing*, pp. 682–692, Springer International Publishing, 2015.

Abstract

Soft-Reset Control and Optimization

by

Justin Huynh Le

Reset control is a technique that augments traditional dynamic feedback controllers with a mechanism to adaptively or periodically reset a memory state in such a way as to improve transient closed-loop behaviors such as overshoot and settling time. It has been shown to overcome inherent limitations of linear time-invariant controllers, enabling performance improvements in a wide variety of applications, including industrial high-precision motion systems and electromechanical automotive systems. As reset control finds broader applications, it faces challenges in implementation and analysis, especially due to the prevalence of nonlinearities, such as those arising in the dynamics of robotic and vehicular systems, as well as those arising in the cost functions that are to be optimized in such systems. One challenge lies in the need for a feature known as temporal regularization, which is generally necessary to guarantee robust stability properties of reset control systems and can be difficult to implement effectively while preserving benefits of resets. Another challenge lies in the inherent discontinuity of control signals produced by reset controllers, which can be detrimental to hardware in physical systems.

This dissertation studies the recently introduced notion of soft resetting, which addresses the above limitations by implementing reset behaviors in an approximate sense, allowing resets to occur gradually rather than instantaneously and doing so with tunable fidelity of approximation. It is shown that, if a traditional reset controller admits a strongly convex energy function that certifies passivity, there exists a soft-reset controller that approximates the behavior of the traditional controller while inheriting its

passivity properties. The implications of this result are discussed for nonlinear and multi-agent problems having nonlinear cost functions to be optimized in steady state. Then, connections are drawn between discrete-time analogues of soft-reset systems and accelerated gradient methods for numerical optimization, for which resetting has historically been referred to as restarting and has been shown to improve convergence behaviors in applications such as machine learning. Specifically, for convex problems, linear matrix inequalities are constructed for numerically certifying exponential convergence, while for nonconvex problems, asymptotic stability in probability of global minima is studied for a class of stochastically perturbed accelerated gradient methods with resets. Soft resetting is numerically demonstrated on various problems, including vehicular formation control and online parameter identification.

Contents

Chapter 1

Introduction

A reset controller is a dynamical system whose state jumps to a new value when a prescribed condition, involving controller states and plant states, is realized. One of the earliest known reset controllers is due to Clegg, who introduced an integrating circuit that, for all intents and purposes, resets its state to zero when the product of the input and the output of the integrator attempts to become negative [1]. The Clegg integrator was extended by Horowitz and co-authors some twenty years later to more general "first-order reset elements" (FOREs) [2], [3]. After another two decades, stability and performance results for linear reset control systems began to receive significant attention, starting with the work of Hollot and co-authors [4], [5], [6], [7], [8], [9]. This work was continued and expanded upon within the hybrid systems framework of [10] in [11] and [12], for example. Other contributions pertaining to linear reset control systems include [13] and [14]. A recent overview, perspective, and applications of linear reset control systems are found in [15]. For nonlinear reset control systems, Haddad and co-authors made noteworthy contributions, especially for lossless interconnections [16], [17], using an alternative hybrid systems framework [18]. In all of this work, controller resets are typically triggered by the closed-loop system state hitting a surface or attempting to enter a sector. Other reset control system mechanisms include those found in event-triggered control, where a control signal is typically held constant until a change to its value is required to maintain

closed-loop stability or other properties [19], [20]. These types of resets are beyond the scope of our work. We focus instead on sector-based resets, which are resets riggered by the closed-loop system state attempting to enter a sector.

More recently, reset controllers are finding increasingly broad applications, including, but not limited to, industrial high-precision motion systems with unknown friction characteristics [21], [22], longitudinal motion in a coordinated platoon of automatically cruising vehicles [23], [24], exhaust gas recirculation valves [15, Ch. 8], and electromechanical valves in power-split transmission systems [15, Ch. 9]. In all of these cases, the transient performance of a linear feedback controller is significantly improved by augmenting that controller with a reset mechanism.

However, reset control continues to face challenges in implementation and analysis, especially due to the prevalence of nonlinearities, such as those arising in the dynamics of robotic and vehicular systems, as well as those arising in the cost functions that are to be optimized in such systems. One specific challenge lies in implementing a feature referred to as temporal regularization, which enforces a positive lower bound on the time elapsed between instances of resetting and has been shown to be essential for stability/robustness guarantees in reset control [12]. Another challenge lies in the inherent discontinuity of control signals produced by reset controllers, which can be detrimental to hardware in physical systems, especially the aforementioned systems in which nonlinearities abound.

To address these challenges, we consider an alternative implementation, referred to as a soft-reset implementation, of control systems with sector-based resets. In contrast with previously studied reset systems modeled by hybrid systems, which we refer to as hard-reset systems, soft-reset systems are modeled as differential inclusions. (Differential inclusions have appeared in other works related to reset control systems, including [25], [26], and [27].) Soft-reset systems allow resets to occur gradually rather than instantaneously, doing so with tunable fidelity of approximation. In this way, they avoid the need

for regularization and prevent discontinuity of control signals.

In Chapter 3, we give conditions under which such a reset control system can be implemented using a differential inclusion rather than a hybrid system that involves resets, focusing on nonlinear control problems in which passivty characterizes both plant and controller, inspired by results for linear systems given in [28]. Soft-reset control is numerically demonstrated on some systems commonly studied in nonlinear control theory, including a robotic manipulator and a translational oscillator with a rotational actuator.

In Chapter 5, the problem of steady-state optimization is considered, in which a plant is to be driven asymptotically toward the solution of an optimization problem using feedback measurement of the plant state and knowledge of the plant's steady-state input-output relation. We restrict our focus to specific soft-reset controllers which can be numerically demonstrated to improve on the performance of standard controllers that lack resets, showing that steady-state optimality is achieved in a sense for linear time-invariant plants and for a class of nonlinear passive plants having only filtered gradient information available.

In Chapter 4, we examine implications of passivity for reset control in multi-agent settings, in which multiple plants sharing information through a graph-structured network are to be driven toward consensus or toward the solution of a network-wide optimization problem. We give conditions involving passivity on the agent-level dynamics under which soft resets can be implemented for such systems and numerically demonstrate the benefits of resets.

The connections between reset control and gradient-based optimization motivate the application of resets to parameter identification methods, many of which can be interpreted as dynamics that optimize an objective function representing the parameter estimation error. One such method that has seen recent attention in the literature is

the high-order tuner, which aims to improve on the performance of standard gradient methods for identification by filtering the gradient and thereby introducing additional tuning parameters. Chapter 6 lays some groundwork to enable future applications of soft resets in high-order tuners, beginning with a novel analysis via Matrosov theorem to establish uniform global asymptotic stability properties of high-order tuners without resets under a persistent excitation condition. It is then shown that the incorporation of online data in the sense of "concurrent learning" can relax the persistent excitation condition and enable the use of soft resets without much modification to the analysis or implementation.

Chapters 7 and 8 consider the discrete-time perspective, in which connections can be made between reset control and the notion referred to as "restarting" in numerical optimization. In Chapter 7, a technique inspired by reset control is demonstrated on convex optimization algorithms, which are algorithms that are widely used in statistical data analysis, among many other applications, and can be modeled as nonlinear systems. Specifically, a numerical approach is developed, based on linear matrix inequalities, to certify exponential rates of convergence for reset-based optimization algorithms that are implemented in the discrete-time domain. In addition, it is demonstrated through numerical experiments that resets can greatly improve the efficiency of optimization algorithms when applied to statistical problems such as logistic regression. In Chapter 8, we introduce a stochastic difference inclusion to model a class of nonconvex optimization algorithms derived from accelerated gradient methods in which resets are combined with stochastic perturbations with the intention of efficiently seeking global optima. We show that a probabilistic notion of global asymptotic stability holds for the set of global solutions to a minimization problem having appropriate smoothness conditions but without requiring convexity.

Chapter 2

Mathematical Preliminaries

The set of (nonnegative) real numbers is denoted by ($\mathbb{R}_{\geq 0}$) $\mathbb{R}$. The set of (nonnegative) integers is denoted by ($\mathbb{Z}_{\geq 0}$) $\mathbb{Z}$. For any two vectors $u, v \in \mathbb{R}^n$, we use $\langle u, v \rangle \coloneqq u^T v$. For $x \in \mathbb{R}^n$, we use $|x| \coloneqq \sqrt{\langle x, x \rangle}$. Given $x \in \mathbb{R}^n$ and a nonempty set $\mathcal{A} \subset \mathbb{R}^n$, the distance of x to $\mathcal{A}$ is denoted $|x|_{\mathcal{A}}$ and is defined by $|x|_{\mathcal{A}} \coloneqq \inf_{y \in \mathcal{A}} |x - y|$. A vector having all entries equal to 1 is denoted $\mathbb{1}$.

Given a pair $(x, u) \in \mathbb{R}^n \times \mathbb{R}^m$, by abuse of notation we consider $z := (x, u)$ to be a vector in $\mathbb{R}^{n+m}$. By the same abuse of notation, we sometimes write a function defined on $\mathbb{R}^n \times \mathbb{R}^m$ as a function defined on $\mathbb{R}^{n+m}$. That is, $f(x, u)$ may be written as $f(z)$ with $z = (x, u)$.

We denote by $\mathcal{G}$ the set of functions from $\mathbb{R}_{\geq 0}$ to $\mathbb{R}_{\geq 0}$ that are continuous, nondecreasing, and zero at zero. The subset of strictly increasing functions in $\mathcal{G}$ is denoted by $\mathcal{K}$. The subset of unbounded functions in $\mathcal{K}$ is denoted by $\mathcal{K}_\infty$. Moreover, $\beta : \mathbb{R}_{\geq 0} \times \mathbb{R}_{\geq 0} \to \mathbb{R}_{\geq 0}$ is said to belong to class $\mathcal{KL}$ if $\beta(\cdot, s)$ belongs to class $\mathcal{K}$ for each $s \geq 0$, and for each fixed $r \geq 0$, the mapping $\beta(r, \cdot)$ is decreasing to zero.

For any set $\mathcal{A} \subseteq \mathbb{R}^n$, the closure of $\mathcal{A}$ is denoted $\overline{\mathcal{A}}$. A set-valued mapping $F : \mathbb{R}^n \rightrightarrows \mathbb{R}^m$ is said to be outer semicontinuous if, for every $x \in \mathbb{R}^n$ and every sequence $\{x_i\}_{i=1}^{\infty}$ with $\lim_{i \to \infty} x_i = x$, it holds that $\limsup_{i \to \infty} F(x_i) \subseteq F(x)$. The graph of F is defined as $\text{graph}(F) \coloneqq \{(x, y) \in \mathbb{R}^n \times \mathbb{R}^m : \ y \in F(x)\}$. The mapping F is outer semicontinuous

if and only if its graph is closed [10, Lemma 5.10]. It is said to be locally bounded if, for every $x \in \mathbb{R}^n$, there exists a neighborhood U_x of x such that $F(U_x) \subseteq \mathbb{R}^m$ is bounded. It is said to be *sector bounded near the origin* if there exist $\delta > 0$ and $L > 0$ such that $|f| \leq L|z|$ for all $z \in \mathbb{R}^n$ satisfying $|z| \leq \delta$ and all $f \in F(z)$. It is said to be *quadratically bounded near the origin* if there exist $\delta > 0$ and $L > 0$ such that $|f| \leq L|z|^2$ for all $z \in \mathbb{R}^n$ satisfying $|z| \leq \delta$ and all $f \in F(z)$. It is said to be homogeneous of degree $k \in \mathbb{Z}_{\geq 0}$ if $F(\lambda x) = \lambda^k F(x)$ for all $x \in \mathbb{R}^n$ and $\lambda > 0$.

We use C^1 for any function that is continuously differentiable. A function $V : \mathbb{R}^n \to \mathbb{R}$ is said to be *convex* if

$$V\left(\lambda x_1 + (1-\lambda)x_2\right) \leq \lambda V(x_1) + (1-\lambda)V(x_2)$$

for all $x_1, x_2 \in \mathbb{R}^n$ and all $\lambda \in [0, 1]$. A C^1 function $V : \mathbb{R}^n \to \mathbb{R}$ is called *strongly convex* if there exists a $\mu > 0$ such that, for all $x, y \in \mathbb{R}^n$, we have

$$V(y) \geq V(x) + \langle \nabla V(x), y - x \rangle + \mu |x - y|^2. \tag{2.1}$$

A differentiable function $V : \mathbb{R}^n \to \mathbb{R}$ is called *invex* if the there exists a function $\eta : \mathbb{R}^{2n} \to \mathbb{R}^n$ such that a $V(x) - V(y) \geq \eta(x, y)^T \nabla V(y)$ for all $x, y \in \mathbb{R}^n$. The function V is invex if and only if the set of minimizers is equivalent to the set of points x for which $\nabla V(x) = 0$ [29, Thm. 1].

The origin of the system $\dot{x} \in F(x)$ is said to be *(Lyapunov) stable* if, for each $\varepsilon > 0$, there exists $\delta > 0$ such that $|x(0)| \leq \delta$ implies $|x(t)| \leq \varepsilon$ for all $t \geq 0$. It is said to be *globally attractive* if every solution x satisfies $\lim_{t \to \infty} |x(t)| = 0$. It is said to be *globally asymptotically stable (GAS)* if it is both stable and globally attractive. It is said to be *globally exponentially stable (GES)* if there exist positive constants c_0 and c_1 such that

every solution x satisfies $|x(t)| \leq c_0|x(0)|\exp(-c_1 t)$ for all $t \geq 0$.

A map $\varphi : \mathbb{R}^n \times \mathbb{R}_{\geq 0} \to \mathbb{R}^m$ is said to be locally bounded in x uniformly in t if there exist numbers $\delta > 0$ and $M > 0$ not dependent on t such that $|\varphi(x,t)| \leq M$ for all t and for all x such that $|x| \leq \delta$. For a locally bounded function $f : \mathbb{R}^n \times \mathbb{R}_{\geq 0} \to \mathbb{R}^n$ such that $x \mapsto f(x,t)$ is continuous uniformly in t and $t \mapsto f(x,t)$ is piecewise continuous, the origin of the system $\dot{x} = f(x,t)$ is said to be uniformly globally stable (UGS) if there exists a class-$\mathcal{K}_\infty$ function γ such that, for each initial condition $(x_\circ, t_\circ) \in \mathbb{R}^n \times \mathbb{R}_{\geq 0}$, each solution $x(\cdot)$ satisfies $|x(t)| \leq \gamma(|x_\circ|)$ for all $t \geq t_\circ$. The origin is said to be uniformly globally attractive (UGA) if for each $r > 0$ and $\sigma > 0$ there exists $T > 0$ such that, if the initial condition $(x_\circ, t_\circ) \in \mathbb{R}^n \times \mathbb{R}_{\geq 0}$ satisfies $|x_\circ| \leq r$, $|x(t)| \leq \sigma$ for all $t \geq t_\circ + T$. The origin is said to be uniformly globally asymptotically stable (UGAS) if it is UGS and UGA. The origin is said to be uniformly globally exponentially stable (UGES) if there exist $c > 0$ and $\alpha > 0$ such that, for each initial condition $(x_\circ, t_\circ) \in \mathbb{R}^n \times \mathbb{R}_{\geq 0}$, $|x(t)| \leq c|x_\circ|\exp(-\alpha(t - t_0))$ for all $t \geq t_\circ$.

The open and closed unit balls in $\mathbb{R}^n$ are denoted $\mathbb{B}^\circ$ and $\mathbb{B}$, respectively. We write $v \sim \mu(\cdot)$ to indicate that a random vector v has probability distribution μ. For the stochastic difference inclusion

$$x^+ \in G(x, v^+), \quad v \sim \mu(\cdot), \tag{2.2}$$

a compact set $\mathcal{A} \subseteq \mathbb{R}^n$ is said to be uniformly Lyapunov stable in probability for (2.2) if, for each $\varepsilon > 0$ and $\rho > 0$, there exists a $\delta > 0$ such that, for every initial condition in $\mathcal{A} + \delta\mathbb{B}$,

$$\mathbb{P}\left[\text{graph}(x) \subseteq (\mathbb{Z} \times (\mathcal{A} + \varepsilon\mathbb{B}^\circ))\right] \geq 1 - \rho, \tag{2.3}$$

where $\text{graph}(x) \coloneqq \cup_{i \in \mathbb{Z}_{\geq 0}}(\{i\} \times x(i))$. The compact set $\mathcal{A}$ is uniformly Lagrange stable in probability for (2.2) if, for each $\delta > 0$ and $\rho > 0$, there exists a $\varepsilon > 0$ such that (2.3) holds. The compact set $\mathcal{A}$ is uniformly globally stable in probability for (2.2) if it is both uniformly Lyapunov stable in probability and uniformly Lagrange stable in probability.

A compact set $\mathcal{A}$ is uniformly globally attractive in probability for (2.2) if, for each $\varepsilon > 0$, $\rho > 0$, and $R > 0$, there exists $\tau \geq 0$ such that, for every initial condition in $\mathcal{A} + R\mathbb{B}$,

$$\mathbb{P}\left[\text{graph}(x) \cap (\mathbb{Z}_{\geq \tau} \times \mathbb{R}^n) \subseteq (\mathbb{Z} \times (\mathcal{A} + \varepsilon \mathbb{B}^\circ))\right] \geq 1 - \rho,$$

where $\mathbb{Z}_{\geq \tau}$ is the set of nonnegative integers greater than or equal to τ. The compact set $\mathcal{A}$ is uniformly globally asymptotically stable in probability for (2.2) if it is uniformly globally stable in probability and uniformly globally attractive in probability.

Chapter 3

Passive Soft-Reset Controllers for Nonlinear Systems

In this chapter, we focus on implementing reset controllers that are (strictly) passive and on analyzing their interconnection with passive plants. We show that a passive hard-reset controller that has a strongly convex energy function can be approximated as a soft-reset controller. The considered soft-reset controller contains a parameter that can be adjusted to better approximate the action of the hard-reset controller. Closed-loop asymptotic stability is established for the interconnection of a passive soft-reset controller with a passive plant, under appropriate detectability assumptions. Several examples are used to illustrate the efficacy of soft-reset controllers.

3.1 Introduction

In [28], conditions were given under which a linear reset control system can be implemented using a differential inclusion rather than a hybrid system that involves resets. Here, we instead focus on nonlinear control problems, especially those where passivity plays a role, both in characterizing a nonlinear plant and also in characterizing a reset controller. In Section 3.2, we specify the passive, hard-reset controllers that we aim to implement as soft-reset controllers. We emphasize that such passive hard-reset con-

trollers should admit a strongly convex energy function in order to be implementable as a soft-reset controller. In particular, it is shown that, if a hard-reset controller admits a strongly convex energy function that certifies passivity, there exists a soft-reset implementation that inherits its passivity properties, enabling the soft-reset controller to achieve desired closed-loop stability and passivity properties when placed in feedback interconnection with a passive nonlinear system. Our passive soft-reset controllers are introduced in Section 3.3. In Section 3.4, we discuss the interconnection of a passive soft-reset controller with a passive plant. Section 3.5 contains several illustrations of the developed theory.

3.2 Passive hard-reset controllers

A (square) hard-reset control system is a hybrid system with state $x_c \in \mathbb{R}^{n_c}$, input $u_c \in \mathbb{R}^{m_c}$, and output $y_c \in \mathbb{R}^{m_c}$ with the following model:

$$(x_c, u_c) \in C \qquad \dot{x}_c = f_c(x_c, u_c) \tag{3.1a}$$

$$(x_c, u_c) \in D \qquad x_c^+ = g_c(x_c, u_c) \tag{3.1b}$$

$$y_c = h_c(x_c, u_c) \tag{3.1c}$$

where, typically,

$$C := \{(x_c, u_c) \in \mathbb{R}^{n_c} \times \mathbb{R}^{m_c} : \varphi(x_c, u_c) \leq 0\} \tag{3.2a}$$

$$D := \{(x_c, u_c) \in \mathbb{R}^{n_c} \times \mathbb{R}^{m_c} : \varphi(x_c, u_c) \geq 0\}\,. \tag{3.2b}$$

We impose the following assumptions on the functions that prescribe the model.

Assumption 1 *The following conditions hold for the functions f_c, g_c, h_c, and φ that*

appear in (3.1)-(3.2):

1. *(*Continuous, locally sector bounded data and quadratic jump condition*)*

   There exists $M = M^T$ such that $\varphi(z_c) = z_c^T M z_c$ for all $z_c \in \mathbb{R}^{n_c+m_c}$; also, f_c, g_c, and h_c are sector bounded near the origin and continuous.

2. *(*Jumps land in flow set*)*

   $(x_c, u_c) \in D$ implies $(g_c(x_c, u_c), u_c) \in C$.

3. (Passivity via a strongly convex energy function*)*

   There exist a strongly convex, positive definite, continuously differentiable function $V_c : \mathbb{R}^{n_c} \to \mathbb{R}_{\geq 0}$, a continuous, positive definite, quadratically bounded near the origin function $\rho : \mathbb{R}^{m_c} \to \mathbb{R}_{\geq 0}$, and $\varepsilon > 0$ such that, with the definition

$$C_\varepsilon := \left\{ z_c \in \mathbb{R}^{n_c+m_c} : z_c^T M z_c \leq \varepsilon z_c^T z_c \right\}, \tag{3.3}$$

   we have

$$\langle \nabla V_c(x_c), f_c(x_c, u_c) \rangle \leq y_c^T u_c - \rho(y_c) \quad \forall (x_c, u_c) \in C_\varepsilon \tag{3.4a}$$

$$V_c(g_c(x_c, u_c)) \leq V_c(x_c) \qquad \forall (x_c, u_c) \in D \tag{3.4b}$$

   where $y_c = h_c(x_c, u_c)$.

4. *(*Minimum phase and detectable*)*

   Any absolutely continuous, bounded solution $(x_c, u_c) : [0, \infty) \to \mathbb{R}^{n_c} \times \mathbb{R}^{m_c}$ of (3.1a), i.e., for almost all $t \in [0, \infty)$,

$$(x_c(t), u_c(t)) \in C, \quad \dot{x}_c(t) = f_c(x_c(t), u_c(t)), \tag{3.5}$$

that satisfies $y_c(t) = 0$ *for all* $t \in [0, \infty)$ *also satisfies* $\lim_{t\to\infty} u_c(t) = 0$ *and* $\lim_{t\to\infty} x_c(t) = 0$. ■

Assumption 1.2 implies that, after a jump, the solution of the hard-reset system (3.1)-(3.2) has the potential to flow without immediately jumping again. However, it is possible that $(g_c(x_c, u_c), u_c) \in C \cap D$, in which case the solution also has the potential to jump immediately. That is, there is no guarantee that all of the complete solutions of the hard-reset control system (3.1)-(3.2) have time domains that are unbounded in the ordinary time direction. This is one of the primary motivations for considering a "soft" implementation of the reset control system (3.1)-(3.2), as we do in the next section.

The crux of Assumption 1 is Assumption 1.3, which imposes a type of strict passivity condition on the hard-reset control system (3.1)-(3.2). For more context, compare with Assumption 2.2, where strict passivity of a continuous-time, passive plant is characterized. In addition, we use (3.4b) and the strong convexity of V_c in the next section to propose the soft-reset implementation of the hard-reset system (3.1).

The following example illustrates a class of systems satisfying Assumption 1.

Example 1 *Consider a hard-reset control system (3.1)-(3.2) with* $(x_c, u_c) \in \mathbb{R} \times \mathbb{R}$*, the following data:*

$$f_c(x_c, u_c) := a_c x_c + b_c u_c \tag{3.6a}$$

$$g_c(x_c, u_c) := r_c x_c + p_c u_c \tag{3.6b}$$

$$h_c(x_c, u_c) := c_c x_c + d_c u_c \tag{3.6c}$$

$$M := \begin{bmatrix} m_{11} & m_{12} \\ m_{12} & m_{22} \end{bmatrix} \tag{3.6d}$$

and the energy function

$$V_c(x_c) := \kappa x_c^2 \tag{3.7}$$

where $\kappa > 0$. *There are no assumptions yet on the signs of the parameters in (3.6). Define*

$$M_0 := \begin{bmatrix} 2\kappa a_c + \rho c_c^2 & \kappa b_c + \rho c_c d_c - 0.5 c_c \\ \kappa b_c + \rho c_c d_c - 0.5 c_c & -d_c + \rho d_c^2 \end{bmatrix} \tag{3.8}$$

and note that if

$$\begin{bmatrix} x_c \\ u_c \end{bmatrix}^T M_0 \begin{bmatrix} x_c \\ u_c \end{bmatrix} \leq 0 \tag{3.9}$$

then

$$\begin{aligned} \langle \nabla V_c(x_c), f_c(x_c, u_c) \rangle &= 2\kappa a_c x_c^2 + 2\kappa b_c x_c u_c \\ &\leq (c_c x_c + d_c u_c) u_c - \rho (c_c x_c + d_c u_c)^2 \\ &= y_c u_c - \rho y_c^2. \end{aligned} \tag{3.10}$$

Let $\varepsilon > 0$. *By the S-procedure [30, p. 655], if there exists* $\lambda \in [0, \infty)$ *such that*

$$\lambda (M - \varepsilon I) - M_0 \geq 0 \tag{3.11}$$

and there exists $z_c \neq 0$ *such that* $z_c^T M z_c \leq 0$, *i.e., the flow set* C *contains more points than just the origin, then (3.10) holds for* $z_c \in C_\varepsilon$ *where* C_ε *is defined in (3.3). For example, when* $d_c > 0$, *we can take* $M = M_0 + \varepsilon I$, *with* $\varepsilon > 0$ *and* $\rho > 0$ *small, and*

$\lambda = 1$. *In this case, there exists* $z_c \neq 0$ *of the form* $z_c = (0, u_c)$ *with* $u_c \neq 0$ *such that* $z_c^T M z_c \leq 0$ *so that the S-procedure applies. It also follows that, with the zero reset map, i.e.,* $r_c = p_c = 0$, $(x_c, u_c) \in D$ *implies* $(g(x_c, u_c), u_c) \in C$, *i.e., Assumption 1.2 holds. If* $d_c > 0$ *and* $b_c c_c > a_c d_c$ *then the minimum phase and detectability properties hold.*

3.3 Passive soft-reset controllers

Using (2.1), the strong convexity assumption on V_c in Assumption 1.3 and the bound in (3.4b) imply that there exists $\mu > 0$ such that

$$\begin{aligned} &(x_c, u_c) \in D \quad \Longrightarrow \\ &\langle \nabla V_c(x_c), x_c - g_c(x_c, u_c) \rangle \geq \mu |x_c - g_c(x_c, u_c)|^2. \end{aligned} \tag{3.12}$$

With (3.2b), another way to write this condition is as

$$\begin{aligned} s \in \mathrm{SGN}(\varphi(x_c, u_c)) \Longrightarrow \\ \langle \nabla V_c(x_c), (s+1)(g_c(x_c, u_c) - x_c) \rangle \\ \leq -(s+1)\mu |x_c - g_c(x_c, u_c)|^2, \end{aligned} \tag{3.13}$$

where the set-valued mapping $\mathrm{SGN} : \mathbb{R} \rightrightarrows \mathbb{R}$ is defined as $\mathrm{SGN}(s) := \mathrm{sign}(s)$ for $s \neq 0$ and $\mathrm{SGN}(0) := [-1, 1]$. Thus, we can add a term of the form

$$-\gamma(x_c, u_c) \Big(\mathrm{SGN} \Big(\varphi(x_c, u_c) \Big) + 1 \Big) \Big(x_c - g_c(x_c, u_c) \Big) \tag{3.14}$$

to the differential equation $\dot{x}_c = f_c(x_c, u_c)$ without increasing the directional derivative of V_c as long as γ takes nonnegative values. Moreover, due to Assumption 1.1 and Assumption 1.2, it can be shown that $|g_c(x_c, u_c) - x_c| > 0$ when $\varphi(x_c, u_c) > 0$, which

means that the additional term (3.14) can be used to enhance the negativity of the directional derivative of V_c outside of the set C_ε defined in (3.3), potentially obviating the need for hard resets.

Led by these observations, the soft-reset implementation of the hard-reset system (3.1) is given by the differential inclusion

$$\begin{aligned} \dot{x}_c \in\ & f_c(x_c, u_c) \\ & - \gamma(x_c, u_c) \left(\mathrm{SGN}\left(\varphi(x_c, u_c)\right) + 1 \right) \left(x_c - g_c(x_c, u_c) \right) \end{aligned} \tag{3.15}$$

where $\gamma : \mathbb{R}^{n_c} \times \mathbb{R}^{m_c} \to \mathbb{R}_{>0}$ is continuous, and the set-valued mapping $\mathrm{SGN} : \mathbb{R} \rightrightarrows \mathbb{R}$ is defined above (3.14). Notice that, within the set C defined in (3.1a), the soft-reset dynamics (3.15) match the dynamics (3.1a) of the hard-reset controller. Outside of C, the dynamics (3.15) imitate a reset (if $\gamma(x_c, u_c)$ is large) by rapidly driving x_c towards $g_c(x_c, u_c)$.

We now show that the soft-reset control system (3.15) inherits a strict passivity property from its hard-reset control system inspiration (3.1)-(3.2) when γ is sufficiently large. In addition, we note that γ does not need to be large when the inequality in (3.4a) holds for all $(x_c, u_c) \in \mathbb{R}^{n_c} \times \mathbb{R}^{m_c}$, i.e., $\varepsilon \geq \overline{\sigma}(M)$ where $\overline{\sigma}(M)$ the maximum singular value of M.

Theorem 1 *If Assumption 1.1, 1.2, and 1.3 hold then there exists a continuous, positive definite function* $\sigma_1 : \mathbb{R}^{n_c} \times \mathbb{R}^{m_c} \to \mathbb{R}_{\geq 0}$ *and for each* $\gamma_0 > 0$ *there exists a continuous func-*

tion $\gamma : \mathbb{R}^{n_c \times m_c} \to \mathbb{R}_{>0}$ *such that, for each* $(x_c, u_c) \in \mathbb{R}^{n_c} \times \mathbb{R}^{m_c}$ *and* $s \in \mathrm{SGN}(\varphi(x_c, u_c))$,

$$\begin{aligned} &\langle \nabla V_c(x_c), f_c(x_c, u_c) - \gamma(x_c, u_c)(s+1)(x_c - g_c(x_c, u_c)) \rangle \\ &\quad \leq y_c^T u_c - \rho(y_c) \\ &\qquad - \gamma_0 \max\{0, \varphi(x_c, u_c)\} \frac{\varphi(x_c, u_c)}{\max\{1, \sigma_1(x_c, u_c)^2\}}. \end{aligned} \tag{3.16}$$

One can take γ *proportional to* γ_0 *in the case where the inequality in (3.4a) holds for all* $(x_c, u_c) \in \mathbb{R}^{n_c} \times \mathbb{R}^{m_c}$.

Proof: Define $\widehat{g}_c(z_c) := \begin{bmatrix} g_c(x_c, u_c)^T & u_c^T \end{bmatrix}^T$. Due to Assumption 1.1, which supposes that g_c is sector bounded near the origin and continuous, there exists a continuous function $\sigma_1 : D \to \mathbb{R}_{\geq 0}$ that is sector bounded near the origin and positive definite satisfying

$$|M(\widehat{g}_c(z_c) + z_c)| \leq \sigma_1(z_c) \qquad \forall z_c \in D. \tag{3.17}$$

Then using the Cauchy-Schwarz inequality, $M = M^T$, and Assumption 1.2, which gives that $\widehat{g}_c(z_c)^T M \widehat{g}_c(z_c) \leq 0$ when $z_c^T M z_c \geq 0$, it follows that

$$\begin{aligned} &z_c \neq 0,\ z_c^T M z_c \geq 0 \implies \\ &\qquad |g_c(x_c, u_c) - x_c|_2 \geq \frac{-(\widehat{g}(z_c) - z_c)^T M (\widehat{g}(z_c) + z_c)}{\sigma_1(z_c)} \\ &\qquad\qquad = \frac{z_c^T M z_c - \widehat{g}(z_c)^T M \widehat{g}(z_c)}{\sigma_1(z_c)} \\ &\qquad\qquad \geq \frac{z_c^T M z_c}{\sigma_1(z_c)}. \end{aligned} \tag{3.18}$$

Combining (3.13), (3.18), and Assumption 1.1 gives

$$\begin{aligned} &z_c \neq 0, s \in \mathrm{SGN}(z_c^T M z_c) \Longrightarrow \\ &\quad \langle \nabla V_c(x_c), (s+1)(g_c(x_c, u_c) - x_c) \rangle \\ &\qquad \leq -2\mu \max\left\{0, z_c^T M z_c\right\} \frac{z_c^T M z_c}{\sigma_1(z_c)^2}. \end{aligned} \tag{3.19}$$

Next, due to Assumption 1.1, which supposes that f_c and h_c are sector bounded near the origin and continuous, and due to Assumption 1.3 which supposes that V_c is continuously differentiable and zero at zero, so that ∇V_c is sector bounded near the origin and continuous, and also supposes that ρ is quadratically bounded near the origin, there exists a continuous function $\sigma_2 : \mathbb{R}^{n_c+m_c} \to \mathbb{R}_{\geq 0}$ that is quadratically bounded near the origin such that, for all $(x_c, u_c) \in \mathbb{R}^{n_c+m_c}$,

$$\langle \nabla V_c(x_c), f_c(x_c, u_c) \rangle - y_c^T u_c + \rho(y_c) \leq \sigma_2(z_c). \tag{3.20}$$

Note that, according to (3.4a), we can take $\sigma_2(z_c) = 0$ for all $z_c \in C_\varepsilon$. Also note that if $\varepsilon \geq \overline{\sigma}(M)$, the latter denoting the maximum singular value of M, then $C_\varepsilon = \mathbb{R}^{n_c} \times \mathbb{R}^{m_c}$. It follows from (3.20) that

$$\begin{aligned} &z_c \neq 0, z_c^T M z_c \geq \varepsilon |z_c|^2 \Longrightarrow \\ &\langle \nabla V_c(x_c), f_c(x_c, u_c) \rangle - y_c^T u_c + \rho(y_c) \leq \sigma_2(z_c) \\ &\leq \sigma_2(z_c) \max\left\{0, z_c^T M z_c\right\} \frac{z_c^T M z_c}{\varepsilon^2 |z_c|^4} \\ &= \frac{\sigma_1(z_c)^2 \sigma_2(z_c)}{\varepsilon^2 |z_c|^4} \max\left\{0, z_c^T M z_c\right\} \frac{z_c^T M z_c}{\sigma_1(z_c)^2}. \end{aligned} \tag{3.21}$$

We note that, since σ_1 is sector bounded near the origin and σ_2 is quadratically bounded

near the origin,

$$\limsup_{z_c \to 0, z_c \in D \setminus \{0\}} \frac{\sigma_1(z_c)^2 \sigma_2(z_c)}{|z_c|^4} < \infty. \tag{3.22}$$

Pick $\gamma : \mathbb{R}^{n_c+m_c} \to \mathbb{R}_{\geq 0}$ to be a continuous function such that, for all $z_c \in D \setminus \{0\}$,

$$\gamma(z_c) \geq \frac{1}{2\mu} \left(\gamma_0 + \frac{\sigma_1(z_c)^2 \sigma_2(z_c)}{\varepsilon^2 |z_c|^4} \right). \tag{3.23}$$

It then follows by combining (3.19), (3.21), and (3.23) that

$$\begin{aligned} &z_c \neq 0, s \in \mathrm{SGN}\left(z_c^T M z_c\right) \Longrightarrow \\ &\langle V_c(x_c), f_c(x_c, u_c) - \gamma(x_c, u_c)(s+1)(x_c - g_c(x_c, u_c)) \rangle \\ &\leq y_c^T u_c - \rho(y_c) - \gamma_0 \max\left\{0, z_c^T M z_c\right\} \frac{z_c^T M z_c}{\sigma_1(z_c)^2} \end{aligned} \tag{3.24}$$

and thus

$$\begin{aligned} &s \in \mathrm{SGN}\left(z_c^T M z_c\right) \Longrightarrow \\ &\langle V_c(x_c), f_c(x_c, u_c) - \gamma(x_c, u_c)(s+1)(x_c - g_c(x_c, u_c)) \rangle \\ &\leq y_c^T u_c - \rho(y_c) - \gamma_0 \max\left\{0, z_c^T M z_c\right\} \frac{z_c^T M z_c}{\max\left\{1, \sigma_1(z_c)^2\right\}}. \end{aligned} \tag{3.25}$$

Since $\varphi(x_c, u_c) = z_c^T M z_c$, this bound gives the result. ■

3.4 Negative feedback interconnection with a passive plant

In this section, we consider the negative feedback interconnection of (3.15) with a continuous-time, passive, detectable plant that has state $x_p \in \mathbb{R}^{n_p}$, input $u_p \in \mathbb{R}^{m_p}$, and output $y_p \in \mathbb{R}^{m_p}$, and can be modeled as

$$\dot{x}_p = f_p(x_p, u_p) \qquad y_p = h_p(x_p). \tag{3.26}$$

A negative feedback interconnection is produced via the conditions

$$u_c = -y_p = -h_p(x_p) \tag{3.27a}$$

$$u_p = y_c = h(x_c, u_c) = h(x_c, -h_p(x_p)). \tag{3.27b}$$

The resulting closed-loop system has state variable denoted $x \coloneqq (x_p, x_c)$.

Assumption 2 *The following conditions hold for the functions f_p and h_p that appear in (3.26):*

1. *(*Continuous data*)*

   The functions f_p and h_p are continuous.

2. *(*Passive dynamics*)*

   There exists a continuously differentiable, positive definite, radially unbounded function $V_p : \mathbb{R}^{n_p} \to \mathbb{R}_{\geq 0}$ such that, for all $(x_p, u_p) \in \mathbb{R}^{n_p} \times \mathbb{R}^{m_p}$,

   $$\langle \nabla V_p(x_p), f_p(x_p, u_p) \rangle \leq y_p^T u_p \tag{3.28}$$

   where $y_p = h_p(x_p)$.

*3. (*Detectability*)*

Each bounded solution $x_p : [0, \infty) \to \mathbb{R}^{n_p}$ of (3.26) that satisfies $u_p(t) = y_p(t) = 0$ for all $t \in [0, \infty)$ also satisfies $\lim_{t\to\infty} x_p(t) = 0$. ■

Theorem 2 *Suppose Assumption 1 and Assumption 2 hold. Then the interconnection of the plant (3.26) with the soft-reset system (3.15) via negative feedback (3.27) has the origin globally asymptotically stable whenever the function $\gamma : \mathbb{R}^{n_c+m_c} \to \mathbb{R}_{>0}$ in (3.15) induces the inequality (3.16).*

Proof: We use $x := (x_p, x_c)$ for the composite state and $F(x)$ to denote the right-hand side of the closed-loop differential inclusion, so that $\dot{x} \in F(x)$.

Consider the composite Lyapunov function candidate

$$V(x) := V_p(x_p) + V_c(x_c) \quad \forall (x_p, x_c) \in \mathbb{R}^{n_p} \times \mathbb{R}^{n_c} \tag{3.29}$$

where V_p comes from Assumption 2.2 and V_c comes from Assumption 1.3. This function is continuously differentiable and positive definite by these assumptions. It is radially unbounded since V_p is assumed to be radially unbounded and V_c is assumed to be strongly convex. Using (3.28) and (3.16) together with (3.27), we get, for all $x \in \mathbb{R}^{n_p+n_c}$ and all $f \in F(x)$,

$$\begin{aligned} \langle \nabla V(x), f \rangle &\leq -\rho(y_c) \\ &\quad - \gamma_0 \max\{0, \varphi(x_c, -y_p)\} \frac{\varphi(x_c, -y_p)}{\max\{1, \sigma_1(x_c, -y_p)^2\}} \end{aligned} \tag{3.30}$$

where $\gamma_0 > 0$, ρ is positive definite, and $y_p = h_p(x_p)$. It follows that the right-hand side of (3.30) is never positive and so the origin is stable and all solutions are bounded.

To establish global convergence to the origin, we use the invariance principle for differential inclusions [31, 32], which applies due to Assumption 1.1 and 2.1 and the fact that the set-valued mapping SGN is outer semicontinuous and bounded with nonempty convex values. According to the invariance principle, every solution converges to the origin if and only if there does not exist a solution $x : [0, \infty) \to \mathbb{R}^n$ and constant $c > 0$ satisfying $V(x(t)) = c$ for all $t \in [0, \infty)$. To rule out such a solution, we decompose F so that

$$\dot{x} \in F(x) =: g(x) + \Big(\mathrm{SGN}(\phi(x)) + 1\Big)\, \omega(x) \tag{3.31}$$

for appropriate, continuous functions g, ϕ and ω and note that

$$|\omega(x)| = \gamma(x_c, -h_p(x_p))|x_c - g_c(x_c, -h_p(x_p))| \tag{3.32}$$

and

$$\begin{aligned} &\langle \nabla V(x), \omega(x) \rangle \\ &= -\gamma\left(x_c, -h_p(x_p)\right) \langle \nabla V_c(x_c), \Big(x_c - g_c(x_c, -h_p(x_p))\Big) \rangle. \end{aligned} \tag{3.33}$$

Now suppose there exists a solution $x : [0, \infty) \to \mathbb{R}^n$ and constant $c > 0$ satisfying $V(x(t)) = c$ for all $t \in [0, \infty)$. Being a solution of (3.31), $x(\cdot)$ satisfies, for almost all $t \in [0, \infty)$,

$$\dot{x}(t) = g(x(t)) + \Big(s(t) + 1\Big)\, \omega(x(t)) \tag{3.34a}$$

$$s(t) \in \mathrm{SGN}\left(\phi(x(t))\right). \tag{3.34b}$$

Since ρ is positive definite and $\gamma_0 > 0$, it follows from (3.30) that such a solution requires

$y_c(t) = u_p(t) = 0$ for all $t \in [0, \infty)$ and $\varphi(x_c(t), -y_p(t)) \leq 0$ for all $t \in [0, \infty)$, i.e., for almost all $t \geq 0$,

$$(x_c(t), u_c(t)) \in C. \tag{3.35}$$

In turn, it follows from (3.4a), (3.28), (3.33), (3.13) and the positivity of $\gamma(\cdot)$ that, for almost all $t \geq 0$,

$$0 = \langle \nabla V(x(t)), g(x(t)) \rangle \tag{3.36a}$$

$$0 = \langle \nabla V(x(t)), (s(t) + 1)\omega(x(t)) \rangle. \tag{3.36b}$$

Again with (3.13), the positivity of μ and the strict positivity of $\gamma(\cdot)$, it follows that, for almost all $t \geq 0$,

$$(s(t) + 1)|x_c(t) - g_c(x_c(t), -y_p(t))|^2 = 0 \tag{3.37}$$

and thus, from (3.32), for almost all $t \geq 0$,

$$(s(t) + 1)\omega(x(t)) = 0. \tag{3.38}$$

It then follows from (3.34) that $x(\cdot)$ is a solution of $\dot{x} = g(x)$, with g defined via (3.31). In particular, with (3.35), $x_c(\cdot)$ is a solution of (3.1a). Then, according to Assumption 1.4, it follows that $\lim_{t\to\infty} u_c(t) = \lim_{t\to\infty} -y_p(t) = 0$ and $\lim_{t\to\infty} x_c(t) = 0$. We thus have $\lim_{t\to\infty} V_p(x_p(t)) = c$. Again, by the invariance principle, there must exist a solution $\hat{x}_p : [0, \infty) \to \mathbb{R}^n$ of (3.26) with $V_p(\hat{x}_p(t)) = c$ and $\hat{u}_p(t) = \hat{y}_p(t) = 0$ for all $t \geq 0$. However, the existence of such a solution contradicts Assumption 2.3. Hence, there is no solution that keeps V equal to a non-zero constant. Thus, the origin is globally attractive

and global asymptotic stability is established. ■

While our assumptions focus on guaranteeing global results, it is clear that local results accrue from local assumptions. For example, the plant considered in Section 3.5.2 satisfies local detectability instead of global detectability, and hence Theorem 2 guarantees a local asymptotic stability result for the closed-loop system.

It is also easy to show that, by introducing a closed-loop input $u \coloneqq (u_1, u_2)$ of appropriate dimension and considering the feedback interconnection produced by the conditions

$$u_c = u_1 - y_p, \tag{3.39a}$$

$$u_p = u_2 + y_c, \tag{3.39b}$$

the channel $(u_1, u_2) \mapsto (y_c, y_p)$ is passive with the storage function being the function V from the proof of Theorem 2.

3.5 Illustrations

3.5.1 TORA

We consider the translational oscillator with rotating actuator (TORA) from [33] and [34]. The dynamics have the form

$$\begin{bmatrix} 1 & \sigma\cos(\theta) \\ \sigma\cos(\theta) & 1 \end{bmatrix} \begin{bmatrix} \ddot{\theta} \\ \ddot{x} \end{bmatrix} = \begin{bmatrix} u \\ -x + \sigma\dot{\theta}^2\sin(\theta) \end{bmatrix} \tag{3.40}$$

where $\sigma \in (0, 1)$, θ is an angular position, and x is a dimensionless translational position. Following [35, Problem 5.10(b)], the preliminary control choice $u = -\theta + w$ renders

the system passive (in fact, lossless) from w to $\dot{\theta}$, as established by the continuously differentiable, positive definite, radially unbounded energy function

$$V_p(\theta, \dot{\theta}, x, \dot{x}) := \frac{1}{2}\left(x^2 + \theta^2\right) + \frac{1}{2}\begin{bmatrix} \dot{\theta} \\ \dot{x} \end{bmatrix}^T \begin{bmatrix} 1 & \sigma\cos(\theta) \\ \sigma\cos(\theta) & 1 \end{bmatrix} \begin{bmatrix} \dot{\theta} \\ \dot{x} \end{bmatrix}. \tag{3.41}$$

Figures 3.1 and 3.2 show the performance of a soft-reset controller using the system data from Example 1, with $a_c = b_c = c_c = 1$, $d_c = 0.01$, $r_c = p_c = 0$, $\kappa = 1/4$, $\rho = 10^{-3}$, $\varepsilon = 10^{-2}$, and $M = M_0 + \varepsilon I$ controlling the TORA with $\sigma = 0.1$. The controller is an unstable FORE implemented with soft resets and having the energy function $V_c(x) = 0.5|x_c|^2$. We do not simulate the behavior for $\gamma = 0$ since it is immediate that the time derivative of

$$t \mapsto V_p(x_p(t)) + V_c(x_c(t))$$

is $2\kappa a_c x_p^2(t) \geq 0$ for all $t \geq 0$ in this case, so that asymptotic stability of the origin is impossible. The performance for sufficiently large, positive values of γ is shown. The oscillations in the translational position decrease and the convergence rate increases as γ increases.

3.5.2 Multi-link robotic manipulator

We consider the planar 2-link robotic manipulator from [35, App. A.10]. The state variable is $q = (q_1, q_2)$, where q_1 is the angular position of the first link, measured with respect to the horizontal axis of the plane, and q_2 is the angular position of the second link, measured with respect to the line segment from the first joint to the second joint.

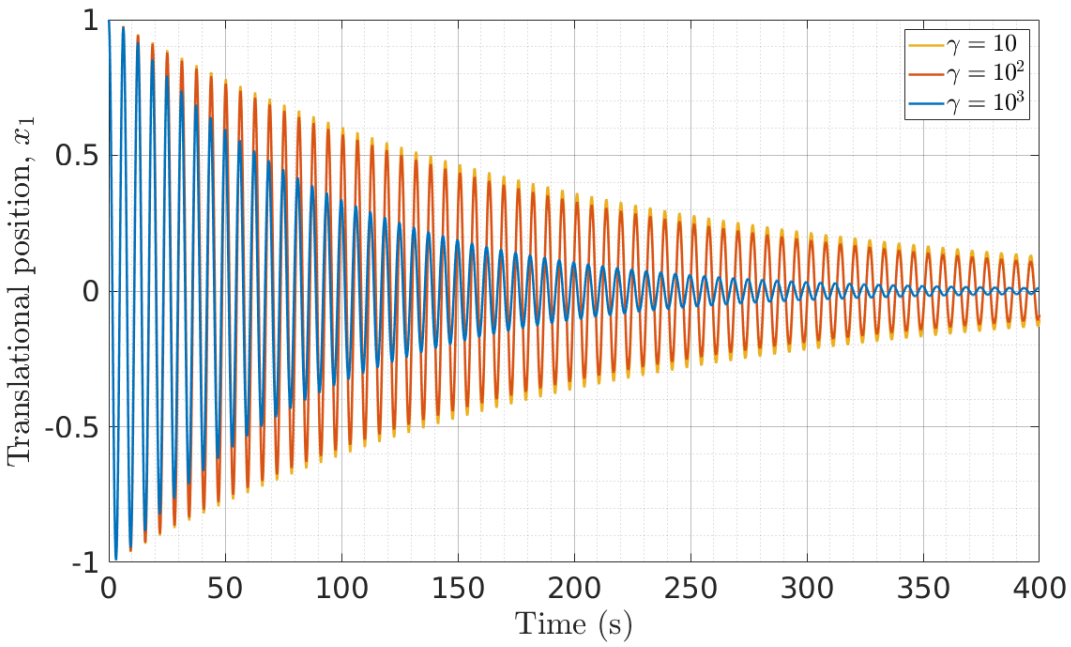

Figure 3.1: Evolution of the translational position of the TORA system ($\sigma = 0.1$) controlled by an unstable FORE with soft resets and various values of the soft-reset parameter γ. With $\gamma = 0$ the origin is not asymptotically stable. With $\gamma > 0$ large enough, the origin is asymptotically stable; oscillations are smaller and the convergence is faster for larger γ.

We define the potential energy as

$$P(q) \coloneqq 784.8 \sin(q_1) + 245.25 \sin(q_1 + q_2) + \frac{\varrho}{2} \left(\left| q_1 + \frac{\pi}{2} \right|^2 + |q_2|^2 \right),$$

where ϱ is a small positive number to ensure radial unboundedness and positive definiteness of $q \mapsto P(q) - P(q^*)$ with respect to $q^* \coloneqq (-\frac{\pi}{2}, 0)$. With $g(q) \coloneqq \partial P(q)/\partial q$ for all $q \in \mathbb{R}^n$, the dynamic equation of the manipulator is

$$\ddot{q} = M^{-1}(q)[u - C(q, \dot{q})\dot{q} - g(q)], \tag{3.42}$$

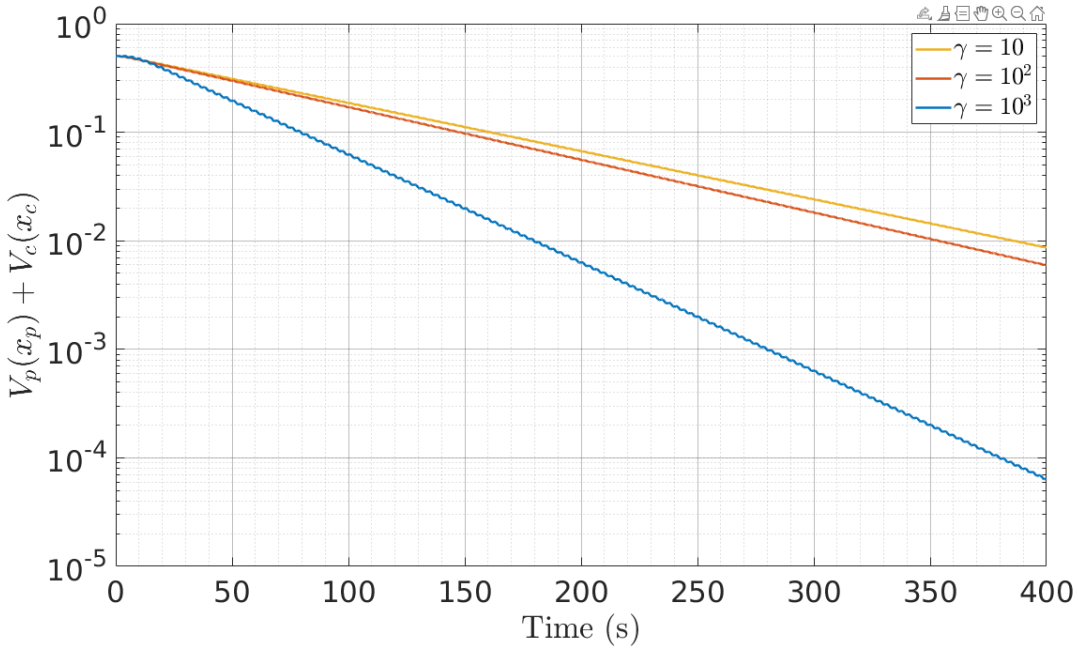

Figure 3.2: Evolution of the total energy for the TORA system ($\sigma = 0.1$) controlled by an unstable FORE with soft resets and various values of the soft-reset parameter γ. The convergence rate increases as γ increases.

with u being the system input, and with M and C given by [35, Eqs. A.36-A.38]. Defining the state $x_p = (q, \dot{q})$, passivity from u to $\dot{q}$ can be shown using the continuously differentiable, positive definite, radially unbounded energy function

$$V_p(x_p) = \frac{1}{2}\dot{q}^T M(q)\dot{q} + P(q) - P(q^*). \tag{3.43}$$

For the system having the translated state $\tilde{x}_p \coloneqq (\tilde{q}, \dot{q})$ with $\tilde{q} \coloneqq q - q^*$, global detectability does not hold because, for small ϱ, $g(q)$ can be zero at some points where $q \neq q^*$. However, $g(q)$ is uniquely zero at q^* in the region where $q - q^* \in [-\pi, \pi]^2$. Thus, local detectability holds for trajectories $\tilde{x}_p$ for which $\tilde{q}(t) \in [-\pi, \pi]^2$ for all t. Figure 3.3 shows the trajectory of q_1 and Figure 3.4 shows the evolution of the energy when the system is controlled using

measurements of $\dot{q}$, with the controller having input $u_c = -\dot{q}$ and having the form

$$f_c(z_c) = A_c x_c + B_c u_c, \tag{3.44a}$$

$$g_c(z_c) = 0, \tag{3.44b}$$

$$h_c(z_c) = C_c x_c, \tag{3.44c}$$

with $A_c = -I_{n_c}$, $B_c = 100 I_{n_c}$, and $C_c = I_{n_c}$. With the chosen system matrices, the controller's energy function is given by $V_c(x) = 0.005|x_c|^2$. The initial condition is $(\pi/2, -\pi/4)$, which we have chosen so that, via the closed-loop stability verified by the Lyapunov function $V_p(x_p) + V_c(x_c)$, the trajectories satisfy $\tilde{q}(t) \in [-\pi, \pi]^2$ for all t. The soft resets are implemented with $\gamma = 10^3$ and

$$M = \begin{bmatrix} 0 & -\frac{1}{2} I_{n_c} \\ -\frac{1}{2} I_{n_c} & 0 \end{bmatrix}. \tag{3.45}$$

3.5.3 Strongly convex, non-quadratic accelerated optimization

We consider the strongly convex function $\phi : \mathbb{R}^{n_p} \to \mathbb{R}$ from [36, Eq. 17], given by

$$\phi(x) = \sum_{i=1}^{p} \hat{\phi}(a_i^T x - b_i) + \frac{1}{2}|x|^2, \tag{3.46}$$

$$\hat{\phi}(\alpha) = \begin{cases} \frac{1}{2}\alpha^2 \exp(-r/\alpha), & \alpha > 0 \\ 0 & \alpha \leq 0, \end{cases} \tag{3.47}$$

with $r = 10^{-6}$. We randomly generate the entries of A and b as described in [36], such that $|A| = \sqrt{L-1}$, where $L = 10^4$ is the Lipschitz constant of $\nabla\phi$. To apply our proposed

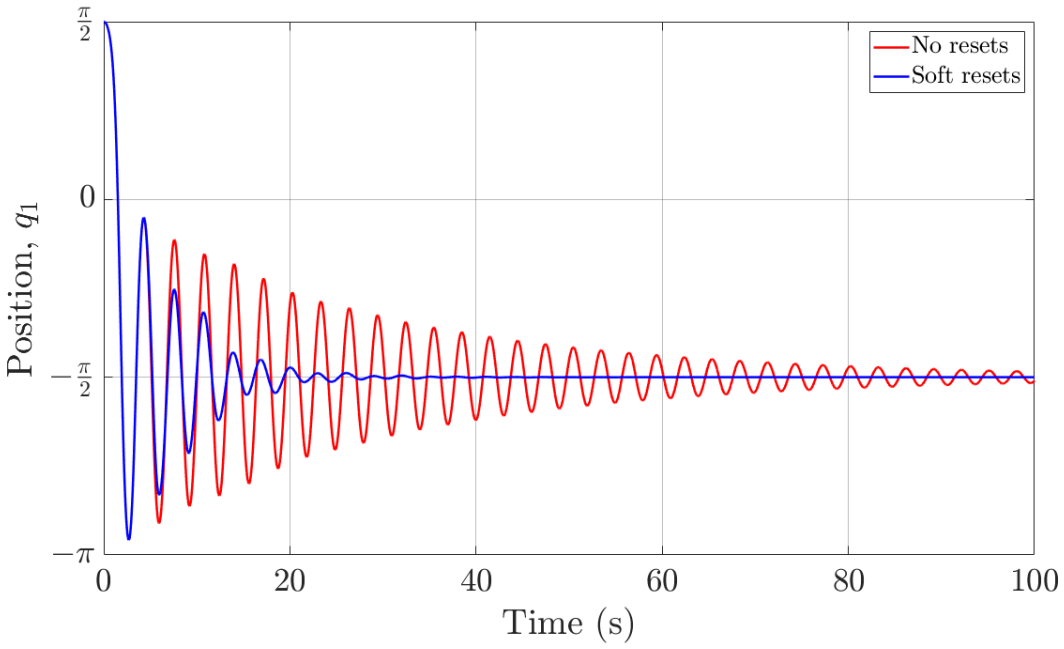

Figure 3.3: Angular position trajectory of the first link in a 2-link robotic manipulator, controlled using a stable FORE with angular velocities as inputs and using soft resets.

reset control approach toward the minimization of ϕ, we define the plant system

$$f_p(x_p, u_p) = u_p, \tag{3.48}$$

$$h_p(x_p, u_p) = \nabla\phi(x_p), \tag{3.49}$$

and we take the control system to be defined by (3.44) with $n_c = n_p$, $A_c = -KI_{n_c}$, $B_c = I_{n_c}$, and $C_c = I_{n_c}$, where $K \in \mathbb{R}_{>0}$ is a tuning parameter. The top plot in Figure 3.5 shows the evolution of $|\nabla\phi(x_p)|$ for the case of $n_p = 5$, $p = 10$, and $K = 2$. The soft resets are implemented with $K = 1$, $\gamma = 30$, and M given by (3.45). The bottom plot in Figure 3.5 shows the evolution of $|\nabla\phi(x_p)|$ for the case of $n_p = 50$, $p = 5$, and $K = 2$. The soft resets are implemented with $K = 2$, $\gamma = 20$, and M given by (3.45).

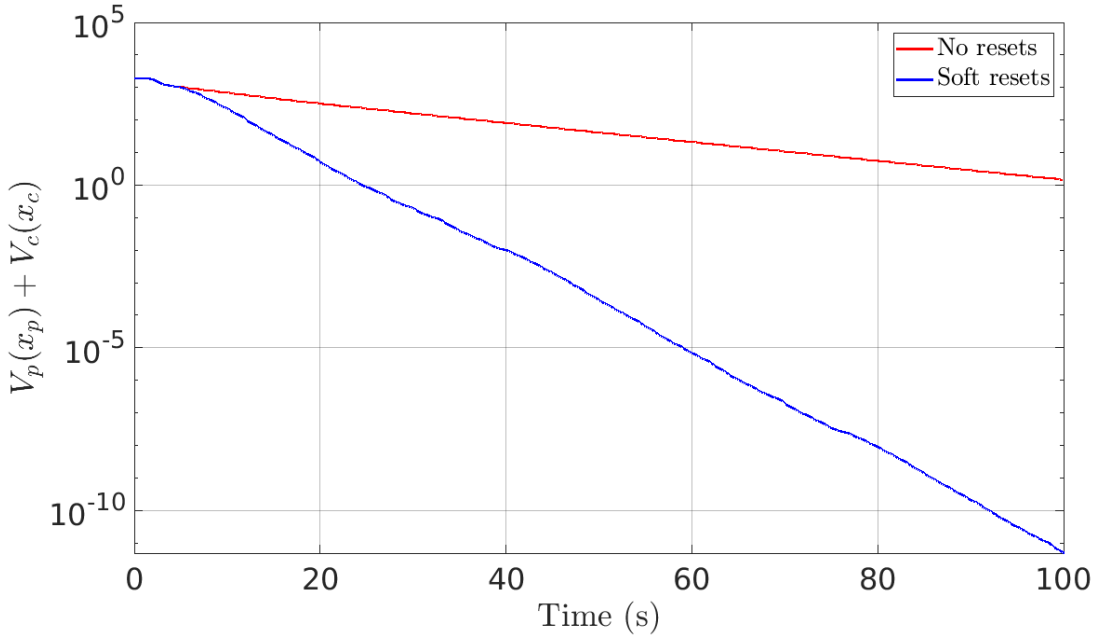

Figure 3.4: Evolution of the total energy of a 2-link robotic manipulator, controlled using a stable FORE with angular velocities as inputs and using soft resets.

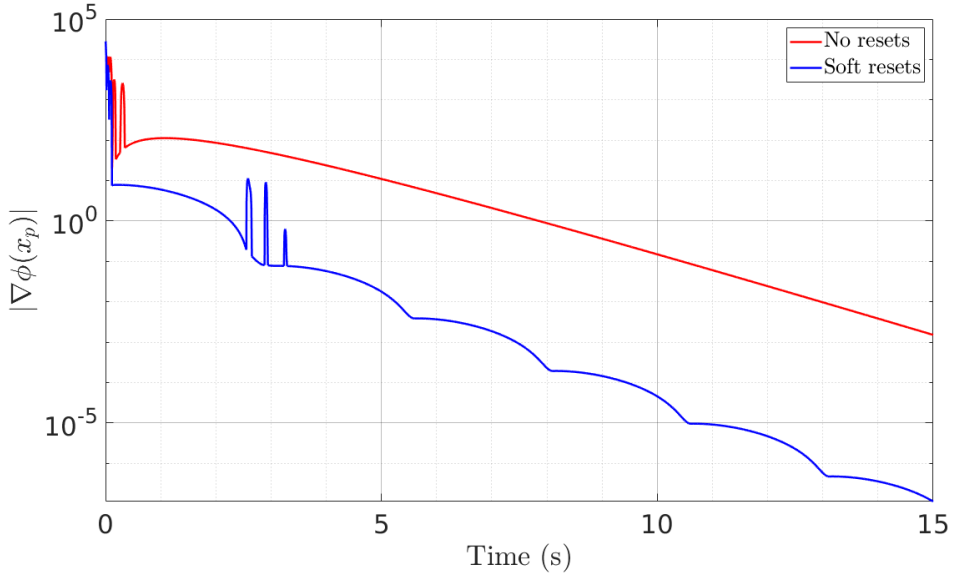

(a)

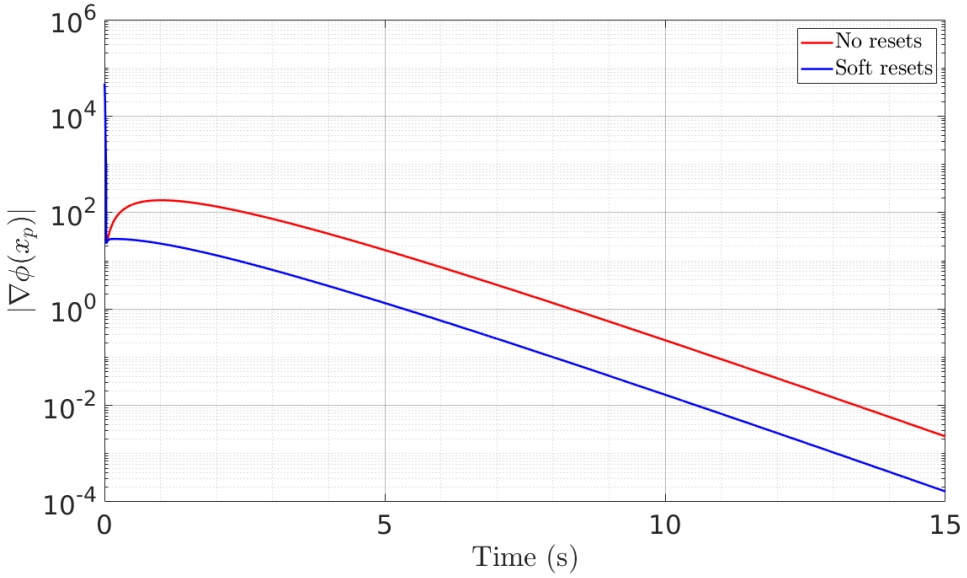

(b)

Figure 3.5: Performance of reset control for strongly convex optimization.

Chapter 4

Soft Resetting in Multi-Agent Optimization and Formation Control

Leveraging results for the single-agent case, this chapter introduces passive soft-reset control for multi-agent problems, namely for leader-follower formation control problems with not-necessarily-convex cost functions to be optimized by leader agents. Agents are assumed to have nonlinear passive dynamics and to share position but not velocity information with neighboring agents in a communication network represented by an undirected connected graph. The target-seeking formation is shown to be achieved in the sense of global asymptotic stability of the desired formation anchored at a desired target. Passivity properties and reset mechanisms are specified at the agent (nodal) level to preserve the decentralized nature of the control system implementation while also inducing the desired stability properties at the network level.

4.1 Introduction

Reset mechanisms have the potential to improve on the performance of existing continuous-time controllers in several ways without greatly affecting the complexity of implementation. In the setting of multi-agent systems, resets may be able to significantly reduce severe fluctuations in the agents' trajectories that result from uncertainty

about real-world operating conditions. Such uncertainties include the communication graph topology, number of agents in the network, and the target-seeking dynamics of the leader agents. In addition, reset methods may also yield similar benefits in settings where the uncertainties pertain to exogenous disturbances such as wind and payload in an unmanned aerial vehicle (UAV). These disturbances have presented challenges in designing robust controllers for multi-UAV systems, for example those that are tasked with collaboratively transporting a payload suspended by cables [37], [38]. The fluctuations typically must be addressed by appropriately tuning the gain parameters of the continuous-time controllers according to properties of, for example, the Laplacian of the communication graph or the dynamics of neighboring agents and disturbances. It is often unreasonable to assume that such information will be available in practice or that an opportunity will be available, before deployment of the multi-agent system, for precisely tuning parameters to unknown environments. Hence, we propose that reset control can play a crucial role in coping with uncertainty in multi-agent systems, like the role played by reset methods in convex optimization [26], where improvements are seen not only in the reduction of fluctuations but also in asymptotic convergence rates. For UAV systems, among other vehicular and robotic systems, the particular advantage of reduced fluctuations may be especially important in mitigating the wear of actuators and reducing the consumption of energy, and reset methods can potentially offer this advantage without introducing much additional cost or complexity to the controller implementation.

We focus on a type of multi-agent optimization problem referred to as a leader-follower formation control problem [39], of which the problem of multi-agent consensus is a special case. Many studies on this topic focus on agents modeled by double-integrator dynamics or having strongly convex quadratic cost functions to be optimized. We avoid these limitations by working within the framework of passivity, which furthermore facilitates the application of passive soft-reset control techniques developed in [40]. Although the

stability properties of formation controllers for double-integrator agents can be analyzed using the approach of [41, Ch. 3], in contrast, the passivity-based approach of [42] enables a unified study of stability when extending the algorithm to account for the following: more general models than double integrators (including nonlinear models), nonlinear optimization objectives that encode formation properties, and adaptive estimation of a network-wide reference velocity. The more general models can capture the nonlinear dynamics of systems such as marine vessels [43], [44], robotic manipulators [45], satellites [46], and sensor networks [46]. See [42] and [46] for overviews of passivity-based multi-agent control systems. We make use of the passivity framework of [42], as it is especially compatible with existing passivity-based analyses of reset control systems.

The benefit of reset control has been demonstrated in a variety of multi-agent systems. Reset methods for consensus of single-integrator networks are studied in [47] and [48], where the use of proportional-integral control gives rise to an integrator state to which resets can be applied. In addition to improvements in disturbance rejection properties, it is also shown in [47] that the use of integral control can improve the exponential rate of convergence. However, to our knowledge, reset methods have not been applied in double-integrator networks, where the benefits can potentially be more significant than those seen in the single-integrator setting. Several of these benefits are demonstrated in the numerical example of Section 4.4 of this chapter. Other multi-agent systems to which reset control has been applied include vehicle platoons, particularly those with lane-changing requirements [23], [24]. In all of the existing work on reset control for multi-agent systems, hard resets are considered. However, because the agents in these systems are often vehicles and robots with passive nonlinear dynamics, they stand to benefit greatly from soft resetting, which is applicable to passive systems and avoids the discontinuity of control signals that can be detrimental to hardware in mechanical systems.

In this chapter, we introduce soft resetting for leader-follower formation control, with target-seeking objectives encoded by not-necessarily-convex but invex cost functions, assuming an undirected connected communication graph for convenience. In Section 4.2, we introduce the basic leader-follower formation control system which is to be augmented with resets. In Section 4.3, we develop a reset mechanism and a corresponding soft-reset implementation, establishing a closed-loop asymptotic stability result to show that the target-seeking formation is achieved. We obtain a Lyapunov function for showing closed-loop stability properties via storage functions that verify passivity at the nodal level. This approach somewhat resembles the approaches taken in, for example, [49], [50], and [51]. However, we employ a more traditional notion of passivity, in contrast with the notion of equilibrium independent passivity [50] employed those works.

4.2 The basic multi-agent optimization dynamics

Consider a network of agents, with $\mathcal{N} \coloneqq \{1, \dots, N\}$ denoting the set of agent indices and each agent having state variable $x_i \coloneqq (q_i, p_i) \in \mathbb{R}^{2n}$ with position q_i and velocity p_i. Denote the network-wide states by $q \coloneqq (q_1, \dots, q_N)$ and $p \coloneqq (p_1, \dots, p_N)$. For each agent $i \in \mathcal{N}$, the control input is denoted u_i, and the system model is given by

$$\dot{q}_i = p_i, \tag{4.1a}$$

$$\dot{p}_i = f_i(p_i, u_i), \tag{4.1b}$$

$$y_i = p_i, \tag{4.1c}$$

under the following conditions.

Assumption 3 *For each $i \in \mathcal{N}$, the following conditions hold.*

1. *f_i is sector bounded near the origin and continuous.*

2. *There exist a strongly convex, positive definite, continuously differentiable function* $V_{p,i} : \mathbb{R}^n \to \mathbb{R}_{\geq 0}$*, a continuous, positive definite, quadratically bounded near the origin function* $\rho_i : \mathbb{R}^n \to \mathbb{R}_{\geq 0}$*,* $\varepsilon > 0$*, and a matrix* $M_i = M_i^T$ *such that, with the definition*

$$C_{\varepsilon,i} \coloneqq \left\{ z_i \coloneqq (p_i, u_i) \in \mathbb{R}^{2n} : z_i^T M_i z_i \leq \varepsilon z_i^T z_i \right\}, \tag{4.2}$$

we have

$$\langle \nabla V_{p,i}(p_i),\ f_i(p_i, u_i) \rangle \leq y_i^T u_i - \rho_i(y_i) \qquad \forall (p_i, u_i) \in C_{\varepsilon,i}. \tag{4.3}$$

3. *Any absolutely continuous, bounded solution* $(p_i, u_i) : [0, \infty) \to \mathbb{R}^{2n}$ *of*

$$\dot{p}_i = f_i(p_i, u_i), \quad (p_i, u_i) \in C_{0,i} \tag{4.4}$$

that satisfies $p_i(t) = 0$ *for all* $t \in [0, \infty)$ *also satisfies* $\lim_{t\to\infty} u_i(t) = 0$*. Here,* $C_{0,i}$ *is given by* (4.2) *with* $\varepsilon = 0$*.*

The control objective is to drive the agents to reach a formation which is centered at a point known only to the leader agent(s), assuming that each agent can communicate information only with a subset of other agents, according to the following conditions.

Assumption 4 *The agents' communication network topology is described by a static undirected graph* $\mathcal{G}$ *having Laplacian matrix* $\mathcal{L}$*, with vertices (nodes) indexed by* $i \in \mathcal{N} \coloneqq \{1, \ldots, N\}$ *and edges indexed by* $l \in \mathcal{E} \coloneqq \{1, \ldots, E\}$*. Furthermore, the agents can communicate information about their positions but not about their velocities or relative velocities.*

Given Assumption 4, for each edge $l \in \mathcal{E}$ of the graph $\mathcal{G}$, we arbitrarily assign one node to be the head and the other to be the tail, so that the incidence matrix $D \in \mathbb{R}^{N\times E}$ may be defined as follows:

$$D_{il} = \begin{cases} 1 & \text{if } i \text{ is the head of } l \\ -1 & \text{if } i \text{ is the tail of } l \\ 0 & \text{otherwise.} \end{cases}$$

Note that the Laplacian $\mathcal{L}$ satisfies $\mathcal{L} = DD^T$ [52, Prop. 4.8]. Let $\tilde{D} \coloneqq D \otimes I_n$ and $\tilde{\mathcal{L}} \coloneqq \mathcal{L} \otimes I_n$. Note that, for all $q \coloneqq (q_1, \ldots, q_N) \in \mathbb{R}^{nN}$,

$$\tilde{D}^T q = 0 \text{ if and only if } q_i = q_j \ \forall (i,j) \in \mathcal{N}^2. \tag{4.5}$$

Let $q_i^r \in \mathbb{R}^n$ denote the desired position of agent i. Let q^c denote the "center" of the desired formation, in the sense that, for each i, we may write $q_i^r = q^c + q_i^f$ for some vector q_i^f referred to as the "formation vector" of agent i. A formation is said to be asymptotically achieved if, for all $(i,j) \in \mathcal{N}^2$, $q_i - q_i^f \to q_j - q_j^f$ as $t \to \infty$.

We define sets $\mathcal{N}_L \subseteq \mathcal{N}$ and $\mathcal{N}_F \subseteq \mathcal{N}$ representing the sets of leader and follower agents, respectively. Assume $\mathcal{N} = \mathcal{N}_L \cup \mathcal{N}_F$ and $\mathcal{N}_L \cap \mathcal{N}_F = \emptyset$. For convenience, we assume that the agents are indexed in such a way that $\mathcal{N}_L = \{1, \ldots, |\mathcal{N}_L|\}$. Denote the leader positions by $q_L \coloneqq (q_1, \ldots, q_{|\mathcal{N}_L|})$ and the follower positions by q_F, so that we have $q = (q_L, q_F)$.

We consider the leaders to be tasked with *target seeking*. That is, they are tasked with converging to a point that minimizes a certain cost function that is unknown to the follower agents and which can be designed according to the needs of the application at hand. For each leader $i \in \mathcal{N}_L$, denote the cost function by $\phi_{L,i} : \mathbb{R}^n \to \mathbb{R}$. The total cost

function $\phi_L : \mathbb{R}^{n|\mathcal{N}_L|} \to \mathbb{R}$ is given by

$$\phi_L(q_L) \coloneqq \sum_{i=1}^{|\mathcal{N}_L|} \phi_{L,i}(q_{L,i}). \tag{4.6}$$

The following conditions are assumed to hold.

Assumption 5 *For each $i \in \mathcal{N}_L$, $\phi_{L,i}$ has a unique minimizer at q_i^r, with the minimal value of $\phi_{L,i}$ denoted $\phi_{L,i}^*$. Furthermore, the functions $\phi_{L,i}$ are such that ϕ_L*

- *has a unique minimizer at $q_L^r \coloneqq (q_1^r, \ldots, q_{|\mathcal{N}_L|}^r)$ and minimal value denoted ϕ_L^*,*
- *is continuously differentiable,*
- *is positive definite and radially unbounded with respect to q_L^r,*
- *and satisfies $\nabla\phi_L(q_L) = 0$ if and only if $q_L = q_L^r$.*

Defining

$$\gamma_i^q \coloneqq \begin{cases} 1 & \text{if } i \in \mathcal{N}_L, \\ 0 & \text{if } i \notin \mathcal{N}_L, \end{cases}$$

let $\gamma^q \coloneqq (\gamma_1, \ldots, \gamma_N)$. Observing that the matrix $\operatorname{diag}(\gamma^q)$ has rank $|\mathcal{N}_L|$, we consider a factorization of $\operatorname{diag}(\gamma^q)$ given by $\Gamma\Gamma^T$ with the matrix $\Gamma \in \mathbb{R}^{N\times|\mathcal{N}_L|}$ having orthonormal columns. Letting $\tilde{\Gamma} \coloneqq \Gamma \otimes I_n$, we have $q_L = \tilde{\Gamma}q$. Then, letting $\tilde{\mathcal{L}} \coloneqq \mathcal{L} \otimes I_n$, $q^f \coloneqq (q_1^f, \ldots, q_N^f)$, $q^r \coloneqq (q_1^r, \ldots, q_N^r)$, and $f(p,u) \coloneqq (f_1(p_1,u_1), \ldots, f_N(p_N,u_N))$, the leader-

follower formation control system is given by

$$q \coloneqq \begin{bmatrix} q_L \\ q_F \end{bmatrix} \in \mathbb{R}^{nN}, \qquad q_L = \tilde{\Gamma} q, \tag{4.7a}$$

$$u \coloneqq \begin{bmatrix} u_1 \\ \vdots \\ u_N \end{bmatrix} = -\tilde{\mathcal{L}}(q - q^f) - \tilde{\Gamma} \nabla \phi_L(q_L), \tag{4.7b}$$

$$\dot{q} = p, \tag{4.7c}$$

$$\dot{p} = f(p, u), \tag{4.7d}$$

under the following condition.

Assumption 6 *The matrix* $\begin{bmatrix} -\tilde{D} & -\tilde{\Gamma} \end{bmatrix}$ *has full column rank.*

To give an example satisfying Assumption 6, consider $n = 1$ and $N = 3$, with agent 1 being the only leader and $\mathcal{G}$ being a simple path from agent 1 to agent N, in which case we may write

$$\tilde{D} = \begin{bmatrix} 1 & 0 \\ -1 & 1 \\ 0 & -1 \end{bmatrix}, \qquad \tilde{\Gamma} = \begin{bmatrix} 1 \\ 0 \\ 0 \end{bmatrix}. \tag{4.8}$$

More generally, Assumption 6 can be satisfied as follows.

Proposition 4.2.1 *Suppose that there is exactly one leader agent and that the graph* $\mathcal{G}$ *is undirected, connected, and acyclic. Then, Assumption 6 holds.*

Proof: The undirected, connected, and acyclic properties of $\mathcal{G}$ together ensure that D has $N - 1$ columns and has full column rank [52, Prop. 4.3]. The presence of exactly

one leader ensures that Γ has exactly one column with exactly one non-zero entry. By definition, each column of D has more than one non-zero entry, and therefore each column of D is linearly independent of Γ. It follows that $\begin{bmatrix} -D & -\Gamma \end{bmatrix} \in \mathbb{R}^{N\times N}$ has full column rank and therefore that $\begin{bmatrix} -\tilde{D} & -\tilde{\Gamma} \end{bmatrix}$ has full column rank. ■

4.3 Soft-reset multi-agent optimization

4.3.1 The reset mechanism

Resets are incorporated into (4.1) as follows. For each agent $i \in \mathcal{N}$, given a matrix $M_i = M_i^T$ satisfying Assumption 3, the reset condition is described by the set

$$D_i \coloneqq \left\{ z_i \coloneqq (p_i, u_i) \in \mathbb{R}^{2n} : z_i^T M_i z_i \geq 0 \right\}. \tag{4.9}$$

For each agent $i \in \mathcal{N}$, the desired state value after resetting is specified by a function $g_i : \mathbb{R}^{2n} \to \mathbb{R}^n$ that satisfies the following conditions.

Assumption 7 *For each $i \in \mathcal{N}$, the following conditions hold.*

1. *g_i is sector bounded near the origin and continuous.*

2. *$(p_i, u_i) \in D_i$ implies $(g_i(p_i, u_i), u_i) \in C_{0,i}$, where $C_{0,i}$ is given by (4.2) with $\varepsilon = 0$.*

3. *For some function $V_{p,i}$ satisfying Assumption 3, it holds that*

$$V_{p,i}(g_i(p_i, u_i)) \leq V_{p,i}(p_i) \qquad \forall (p_i, u_i) \in D_i. \tag{4.10}$$

4.3.2 The soft-reset implementation

For each agent $i \in \mathcal{N}$, with

$$\varphi_i(p_i, u_i) \coloneqq \begin{bmatrix} p_i \\ u_i \end{bmatrix}^T M_i \begin{bmatrix} p_i \\ u_i \end{bmatrix},$$

soft resets are implemented in (4.1) as follows:

$$\begin{aligned} &\dot{p}_i \in F_i(p_i, u_i) \\ &\quad \coloneqq f_i(p_i, u_i) - \gamma_i(p_i, u_i) \left(\mathrm{SGN}\left(\varphi_i(p_i, u_i)\right) + 1 \right) \left(p_i - g_i(p_i, u_i) \right), \end{aligned} \tag{4.11}$$

where $\gamma_i : \mathbb{R}^{2n} \to \mathbb{R}_{>0}$ is continuous, and the set-valued mapping $\mathrm{SGN} : \mathbb{R} \rightrightarrows \mathbb{R}$ is defined as $\mathrm{SGN}(s) := \mathrm{sign}(s)$ for $s \neq 0$ and $\mathrm{SGN}(0) := [-1, 1]$. The following lemma is a direct consequence of Theorem 1 in Chapter 3.

Lemma 4.3.1 *Under Assumptions 3 and 7, for each $i \in \mathcal{N}$, there exists a continuous, positive definite function $\sigma_{1,i} : \mathbb{R}^{2n} \to \mathbb{R}_{\geq 0}$ and for each $\gamma_0 > 0$ there exists a continuous function $\gamma_i : \mathbb{R}^{2n} \to \mathbb{R}_{>0}$ such that, for each $(p_i, u_i) \in \mathbb{R}^{2n}$ and each $f_i \in F_i(p_i, u_i)$,*

$$\langle \nabla V_{p,i}(p_i), f_i \rangle \leq y_i^T u_i - \rho_i(y_i) - \gamma_0 \max\{0, \varphi_i(p_i, u_i)\} \frac{\varphi_i(p_i, u_i)}{\max\{1, \sigma_{1,i}(p_i, u_i)^2\}}. \tag{4.12}$$

Moreover, due to Assumption 7.3 and the strong convexity of each $V_{p,i}$, there exists $\mu > 0$ such that, for all $i \in \mathcal{N}$,

$$\begin{aligned} &s_i \in \mathrm{SGN}(\varphi_i(p_i, u_i)) \implies \\ &\quad \langle \nabla V_{p,i}(p_i),\ (s_i + 1)(g_i(p_i, u_i) - p_i) \rangle \leq -(s_i + 1)\mu |p_i - g_i(p_i, u_i)|^2. \end{aligned} \tag{4.13}$$

Without loss of generality, μ may be taken to be independent of i.

The soft-reset leader-follower formation control system is given by

$$q \coloneqq \begin{bmatrix} q_L \\ q_F \end{bmatrix} \in \mathbb{R}^{nN}, \qquad q_L = \tilde{\Gamma} q, \tag{4.14a}$$

$$u \coloneqq \begin{bmatrix} u_1 \\ \vdots \\ u_N \end{bmatrix} = -\tilde{\mathcal{L}}(q - q^f) - \tilde{\Gamma} \nabla \phi_L(q_L), \tag{4.14b}$$

$$\dot{q} = p, \tag{4.14c}$$

$$\dot{p} \in F(p, u), \tag{4.14d}$$

where, for each $(p, u) \in \mathbb{R}^{2nN}$, $F(p, u)$ is defined as the set of points $f^\circ \coloneqq (f_1^\circ, \ldots, f_N^\circ) \in \mathbb{R}^{nN}$ such that $f_i^\circ \in F_i(p_i, u_i)$ for all $i \in \mathcal{N}$, with F_i defined by (4.11). The formation control and target seeking objectives are achieved in the following sense.

Theorem 3 *Suppose Assumptions 3, 4, 5, 6, and 7 hold. Then, whenever the function* $\gamma \coloneqq (\gamma_1, \ldots, \gamma_N)$ *induces the inequality* (4.12) *for all* $i \in \mathcal{N}$*, the point* $(q^r, 0)$ *is globally asymptotically stable for the system having state* (q, p) *with dynamics given by* (4.14)*.*

Proof: With (4.5) and the definition of q_L^r from Assumption 5, the result follows by showing that the origin is globally asymptotically stable for the system given by

$$z \coloneqq \tilde{D}^T (q - q^f) \in \mathbb{R}^{nE}, \tag{4.15a}$$

$$\tilde{q}_L \coloneqq q_L - q_L^r \in \mathbb{R}^{n|\mathcal{N}_L|}, \tag{4.15b}$$

$$u \coloneqq \begin{bmatrix} u_1 \\ \vdots \\ u_N \end{bmatrix} = -\tilde{D} z - \tilde{\Gamma} \nabla \phi_L(\tilde{q}_L + q_L^r), \tag{4.15c}$$

$$\dot{z} = \tilde{D}^T p, \tag{4.15d}$$

$$\dot{p} \in F(p, u), \tag{4.15e}$$

$$\dot{\tilde{q}}_L = \tilde{\Gamma} p, \tag{4.15f}$$

where q_L^r comes from Assumption 5. We use $x \coloneqq (z, p, \tilde{q}_L)$ for the composite state and $\overline{F}(x)$ to denote the right-hand side of the closed-loop differential inclusion, so that $\dot{x} \in \overline{F}(x)$. Let

$$\begin{aligned} V_z(z) &\coloneqq \frac{1}{2}|z|^2 \\ V_p(p) &\coloneqq \sum_{i=1}^{N} V_{p,i}(p_i), \\ V_L(\tilde{q}_L) &\coloneqq \phi_L(\tilde{q}_L + q_L^r) - \phi_L^*, \end{aligned}$$

where $\{V_{p,i}\}_{i=1}^N$ comes from Assumption 3, ϕ_L comes from (4.6), and ϕ_L^* comes from Assumption 5. Consider the composite Lyapunov function candidate

$$V(x) \coloneqq V_z(z) + V_p(p) + V_L(\tilde{q}_L) \qquad \forall x \in \mathbb{R}^{n(E+N+|\mathcal{N}_L|)},$$

which is continuously differentiable, positive definite, and radially unbounded due to Assumptions 3, 4, and 5. Using Assumption 3 and Lemma 4.3.1, we have, for all $x \in$

$\mathbb{R}^{n(E+N+|\mathcal{N}_L|)}$ and all $\overline{f} \in \overline{F}(x)$,

$$\begin{aligned}\left\langle \nabla V(x), \overline{f} \right\rangle &\leq \left\langle z, \tilde{D}^T p \right\rangle \\ &\quad + \sum_{i=1} \left[y_i^T u_i - \rho_i(y_i) - \gamma_0 \max\left\{0, \varphi_i(p_i, u_i)\right\} \frac{\varphi_i(p_i, u_i)}{\max\left\{1, \sigma_{1,i}(p_i, u_i)^2\right\}} \right] \\ &\quad + \left\langle \nabla \phi_L(\tilde{q}_L + q_L^r), \tilde{\Gamma} p \right\rangle \\ &= \sum_{i=1} \left[-\rho_i(y_i) - \gamma_0 \max\left\{0, \varphi_i(p_i, u_i)\right\} \frac{\varphi_i(p_i, u_i)}{\max\left\{1, \sigma_{1,i}(p_i, u_i)^2\right\}} \right]. \end{aligned} \tag{4.16}$$

where $\gamma_0 > 0$, ρ_i is positive definite for all $i \in \mathcal{N}$, and $y_i = p_i$ for all $i \in \mathcal{N}$. It follows that the right-hand side of (4.16) is never positive and so the origin is stable and all solutions are bounded.

To establish global convergence to the origin, we use the invariance principle for differential inclusions [31, 32], which applies due to Assumptions 3.1 and 7.1 and the fact that the set-valued mapping SGN is outer semicontinuous and bounded with nonempty convex values. According to the invariance principle, every solution converges to the origin if and only if there does not exist a solution $x : [0, \infty) \to \mathbb{R}^{n(E+N+|\mathcal{N}_L|)}$ and constant $c > 0$ satisfying $V(x(t)) = c$ for all $t \in [0, \infty)$. To rule out such a solution, we decompose $\overline{F}$ so that solutions of $\dot{x} \in \overline{F}(x)$ satisfy, for almost all $t \in [0, \infty)$,

$$\dot{x}(t) \in \eta(x(t)) + \begin{bmatrix} 0_{nE \times nN} \\ \operatorname{diag}(s(t)) + I \\ 0_{n|\mathcal{N}_L| \times nN} \end{bmatrix} \omega(x(t)), \tag{4.17a}$$

$$s(t) \coloneqq (s_1(t), \ldots, s_N(t)), \tag{4.17b}$$

$$s_i(t) \in \mathrm{SGN}(\varphi_i(p_i(t), u_i(t))), \qquad \forall i \in \mathcal{N}, \tag{4.17c}$$

for appropriate, continuous functions η and ω, and note that

$$|\omega(x)|^2 = \sum_{i=1}^{N} \gamma_i^2(p_i, u_i)|p_i - g_i(p_i, u_i)|^2 \tag{4.18}$$

and

$$\begin{aligned}
&\left\langle \nabla V(x), \begin{bmatrix} 0_{nE\times nN} \\ \operatorname{diag}(s) + I \\ 0_{n|\mathcal{N}_L|\times nN} \end{bmatrix} \omega(x) \right\rangle \\
&= -\sum_{i=1}^{N} \gamma_i(p_i, u_i) \left\langle \nabla V_{p,i}(p_i),\ (s_i + 1)\left(p_i - g_i(p_i, u_i)\right) \right\rangle .
\end{aligned} \tag{4.19}$$

Now suppose there exists a solution $x : [0, \infty) \to \mathbb{R}^{n(E+N+|\mathcal{N}_L|)}$ and constant $c > 0$ satisfying $V(x(t)) = c$ for all $t \in [0, \infty)$. Since ρ_i is positive definite for each $i \in \mathcal{N}$, and $\gamma_0 > 0$, it follows from (4.16) that such a solution requires $y_i(t) = 0$ for all $i \in \mathcal{N}$ and $t \in [0, \infty)$, as well as $\varphi_i(p_i(t), u_i(t)) \leq 0$ for all $i \in \mathcal{N}$ and $t \in [0, \infty)$. That is,

$$V_p(p(t)) = 0 \qquad \forall t \in [0, \infty), \tag{4.20}$$

and for all $i \in \mathcal{N}$ and almost all $t \geq 0$,

$$(p_i(t), u_i(t)) \in C_{0,i}. \tag{4.21}$$

In turn, it follows from (4.3), (4.19), (4.13), and the positivity of γ_i for all $i \in \mathcal{N}$ that,

for almost all $t \geq 0$,

$$0 = \langle \nabla V(x(t)), \eta(x(t)) \rangle,$$
$$0 = \left\langle \nabla V(x), \begin{bmatrix} 0_{nE \times nN} \\ \operatorname{diag}(s) + I \\ 0_{n|\mathcal{N}_L| \times nN} \end{bmatrix} \omega(x) \right\rangle.$$

Again with (4.13), the positivity of μ, and the strict positivity of γ_i for all $i \in \mathcal{N}$, it follows that, for all $i \in \mathcal{N}$ and for almost all $t \geq 0$,

$$(s_i(t) + 1)|p_i(t) - g_i(p_i(t), u_i(t))|^2 = 0 \tag{4.23}$$

and thus, from (4.18), for almost all $t \geq 0$,

$$\begin{bmatrix} 0_{nE \times nN} \\ \operatorname{diag}(s) + I \\ 0_{n|\mathcal{N}_L| \times nN} \end{bmatrix} \omega(x) = 0.$$

It then follows from (4.17) that $x(\cdot)$ is a solution of $\dot{x} = \eta(x)$. In particular, for each $i \in \mathcal{N}$, with (4.21), $p_i(\cdot)$ is a solution of (4.4). Then, according to Assumption 3.3, it follows that, for all $i \in \mathcal{N}$, $\lim_{t \to \infty} u_i(t) = 0$. That is,

$$\lim_{t \to \infty} u(t) = 0. \tag{4.24}$$

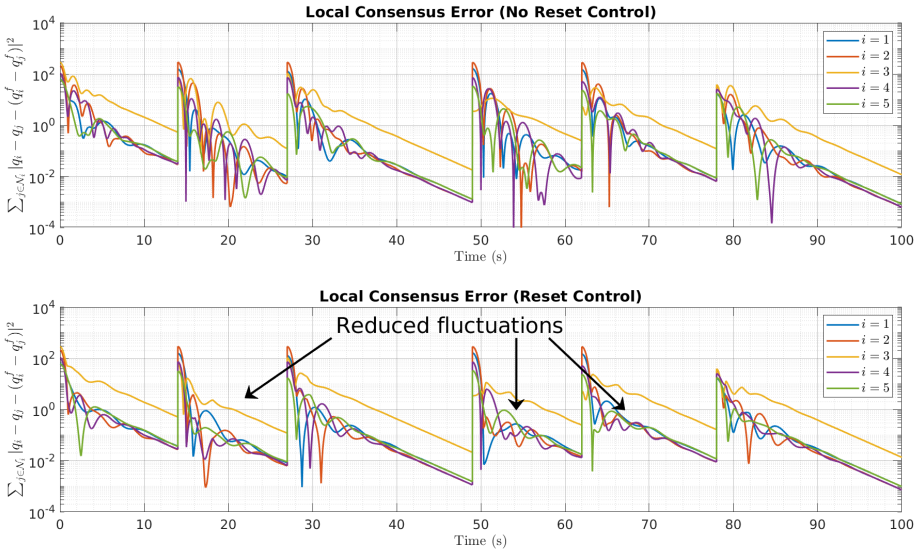

Figure 4.1: Evolution of the *local consensus error*, measuring the deviation from a desired formation. Denoting the ith-row of $\mathcal{L}$ by $\mathcal{L}_i$, the local consensus error can be expressed as $|(\mathcal{L}_i \otimes I_n)(q - q^f)|^2$.

Due to Assumptions 4, 5, and 6,

$$u = \begin{bmatrix} -\tilde{D} & -\tilde{\Gamma} \end{bmatrix} \begin{bmatrix} z \\ \nabla\phi_L(\tilde{q}_L + q_L^r) \end{bmatrix} = 0$$

if and only if $(z, \nabla\phi_L(\tilde{q}_L + q_L^r)) = (0, 0)$. Hence, (4.24) implies that $\lim_{t\to\infty}(z, \tilde{q}_L)(t) = (0, 0)$ and $\lim_{t\to\infty} V_z(z(t)) + V_L(\tilde{q}_L(t)) = 0$. However, due to (4.20), this contradicts the premise that $V(x(t)) = c$ for all $t \in [0, \infty)$. Hence, there is no solution that keeps V equal to a non-zero constant. We conclude that the origin of (4.15) is globally attractive and global asymptotic stability is established. ■

4.4 Numerical results

4.4.1 Experiments

Figure 4.1 compares the transient behaviors of the standard formation controller (4.7) and the soft-reset formation controller (4.14), for an experiment where $n = 2$, $N = 5$, agent 3 is the only leader, and $\mathcal{G}$ is a simple path from agent 1 to agent N. We choose

$$f_i(p_i, u_i) = -K_i p_i + u_i, \tag{4.25}$$
$$g_i(p_i, u_i) = 0,$$
$$M_i = \begin{bmatrix} 0 & -I_{nN} \\ 0 & -I_{nN} \end{bmatrix}$$

for all $i \in \mathcal{N}$. With (4.25), we focus on the case of double-integrator agents to make our figures more easily interpretable. One way to motivate the double-integrator model is to assume, as in [38] for example, that a low-level controller handles the roll, pitch, and yaw variables in a multirotor UAV. For the case of fixed-wing UAVs, the double-integrator model can be motivated by the use of feedback linearization, as described in [53, Section 3] for example.

Figure 4.2 shows the same experiment, displaying the traces of the agents' trajectories in $\mathbb{R}^2$. Initial positions are randomly drawn vectors with uniformly distributed entries (independently and identically distributed). The signal (q^c, q^f) is piecewise constant in time, with a switching signal that has dwell-time parameter $\delta = 0.08$, yielding a sequence of six different formations. For each $i \in \mathcal{N}$, we use "coarsely" chosen values of parameters, i.e., values that are not tailored to the specific experiment: for all $i \in \mathcal{N}$, $K_i = 1$ and $\gamma_i(p_i, u_i) = 10^4$. However, similar performance (and, in fact, oftentimes better performance) can be achieved by using much smaller values for $\gamma_i(p_i, u_i)$ such as

10.

4.4.2 Discussion

In Figure 4.1, the focus is not on the actual values of local consensus errors but on the *variance* of those values. In other words, the figure gives a quantitative sense of how resets reduce fluctuations in transient behaviors. On the other hand, in terms of the asymptotic performance with respect to network-wide consensus and target-seeking, the controller behaves similarly with and without resets, and hence, the resets are shown to improve transient behaviors while still preserving desirable asymptotic behaviors.

In Figure 4.2, the traces of the agents' trajectories illustrate how resets can consistently reduce the unhelpful and wasteful behaviors of the standard controller: at certain times, the "overshoot" behaviors are reduced, while at other times, the redundant "backtracking" behaviors are reduced. Overall, the reset method yields trajectories that are more regular and more akin to what a human operator might produce when manually controlling UAVs with full knowledge of the desired positions. Recall, however, that the agents here are severely information-restricted in the sense that they do not know the desired positions associated with each formation (with the exception of the leader agent, which only knows its own desired position), nor do they anticipate the times at which the desired formation switches.

Although the communication graph in our experiment does not vary with time, we anticipate that the setting of time-varying graphs will reveal novel benefits of resets. In particular, resets may reduce costly fluctuations that can typically be prevented only by carefully (possibly adaptively) tuning the parameters of existing controllers according to graph properties, such as the eigenvalues of the Laplacian, at the time of each switch. Especially when such properties are uncertain in practice, resets can offer a way

to improve transient behaviors without introducing much complexity to the controller implementation.

It is worth emphasizing that the incorporation of the reset method does not introduce any significant computational cost to the standard controller (4.7). Indeed, one recognized benefit of reset control is that it simply and cost-effectively augments the control systems that are already standard or currently implemented in practice, as explained in the introductory sections of [21] and [22]. Although other advanced control methods may be available for motion control and trajectory planning in multi-agent systems, they can be challenging to implement in distributed systems with low-cost hardware and with severely limited energy resources. In contrast, reset methods have the potential to achieve performance benefits in the presence of environmental uncertainty without compromising the real-time constraints on computing, sensing, actuation, communication, and power that arise in multi-agent systems that are mobile, spatially distributed, and driven by low-cost embedded computing platforms.

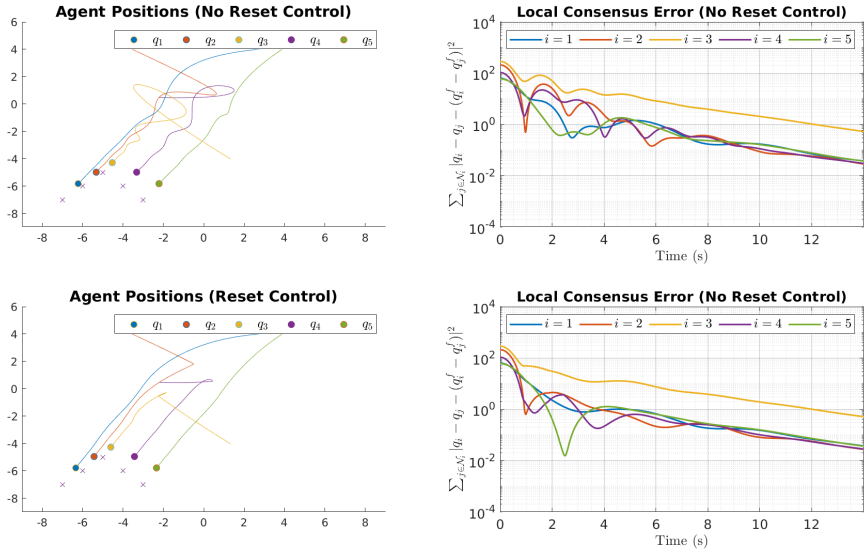

(a) First formation

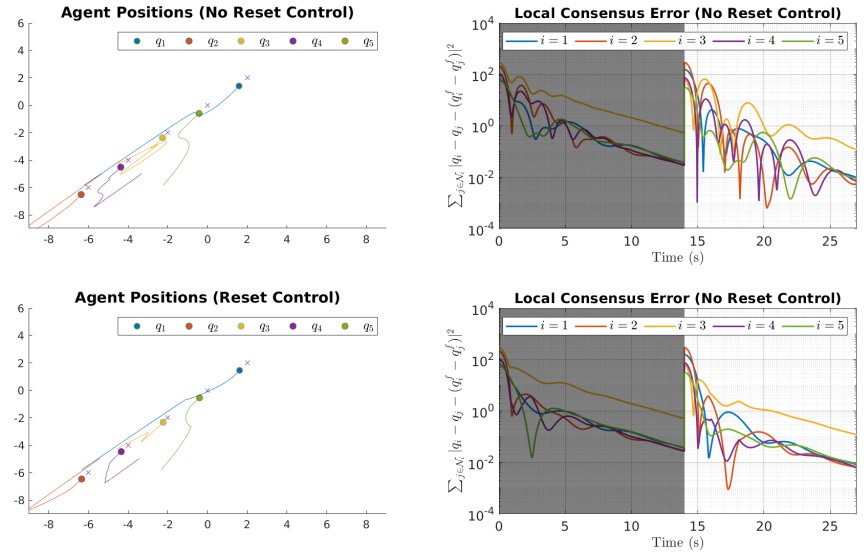

(b) Second formation

Figure 4.2: Traces of agent positions with and without reset control. Desired formations are indicated with 'x'-shaped markers.

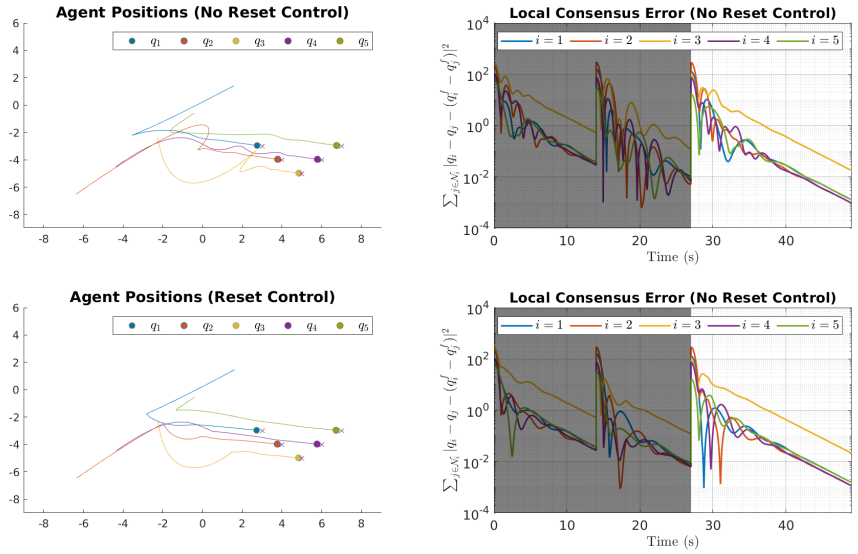

(c) Third formation

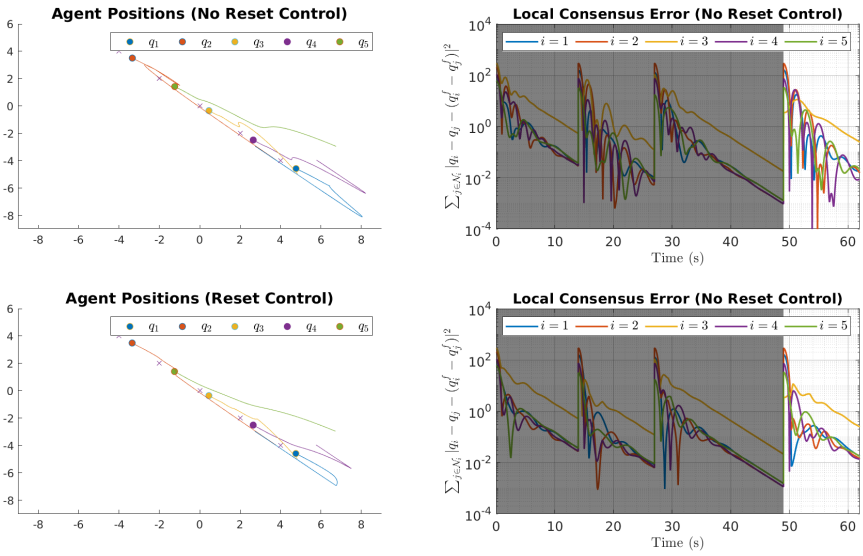

(d) Fourth formation

Figure 4.2: Traces of agent positions with and without reset control (continued).

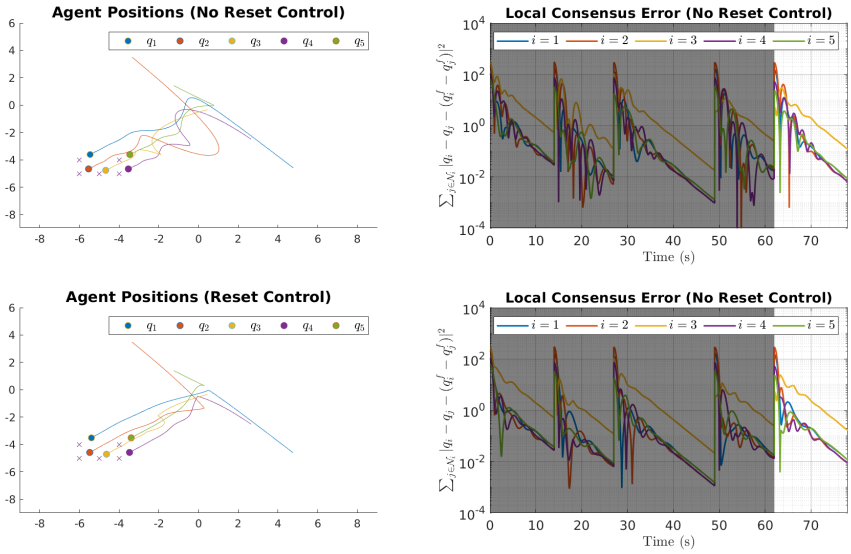

(e) Fifth formation

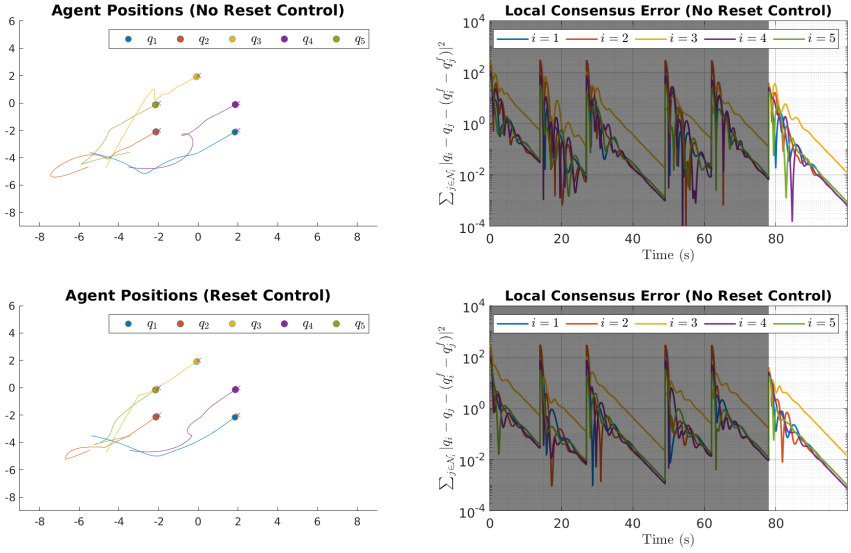

(f) Sixth formation

Figure 4.2: Traces of agent positions with and without reset control (continued).

Chapter 5

Soft-Reset Controllers for Steady-State Optimization with Feedback

One of the illustrations in Chapter 3 showed that soft-reset control is applicable to the problem of steady-state optimization, in which the goal is to drive a plant toward the solution of an optimization problem in steady state, assuming feedback measurement of the plant state and knowledge of the plant's steady-state input-output relation, as well as knowledge of the gradient of the optimization objective. In this chapter, we expand on this idea by constructing soft-reset controllers that show promise in improving on the performance of steady-state optimization controllers that lack resets. It is shown that steady-state optimality is achieved for linear time-invariant plants and for a class of nonlinear passive plants having only filtered gradient information available, in the sense that the solution of the online formulation for the desired optimization problem is globally asymptotically stable for the closed-loop system.

5.1 Introduction

In the problem of steady-state optimization with feedback, also referred to in the literature as the problem of feedback optimization or autonomous optimization, the control objective is to drive a plant toward a steady-state value that is the solution to an optimization problem, assuming feedback measurement of the plant state [54] [55] [56]. Here, the optimization problem encodes the relevant performance metrics and practical constraints, and the meaning of "steady-state value" may encompass the state-input pair or simply the plant state by itself, although the former case has seen much broader consideration in the literature. Both simulations and hardware experiments have demonstrated the benefits of steady-state optimization in such applications as power systems [57] [58] and transportation systems [59] [60]. In those applications, steady-state optimization with feedback plays an important role, due to the mismatch of plant models and the presence of time-varying input disturbances which make it infeasible to compute control strategies offline.

Many steady-state optimization strategies are based on first-order gradient methods for convex optimization. However, basic gradient methods may be insufficient for high-performance applications that demand rapid convergence. Some strategies have improved on the settling time of the basic gradient method by incorporating dynamics that are similar to the continuous-time notion of Nesterov acceleration studied in convex optimization, giving rise to a momentum state in the controller dynamics which has a time-varying damping parameter [54] [59]. As shown in [59], the time-dependence of the damping parameter must be designed in a specific way as to ensure robust stability properties without comprising efficiency of convergence. Namely, a form of temporal regularization is required, in which the momentum damping parameter decreases toward zero as a function of time but jumps to a large value periodically, with the period being

set in accordance with Lyapunov-like conditions for asymptotic stability. The stability conditions are obtained using a hybrid systems framework, which is natural for such systems that exhibit both flows and jumps.

In this chapter, we consider a novel perspective on momentum-based gradient methods for steady-state optimization with feedback, one in which the momentum parameter is adaptively tuned according to a sector-based condition on the state-input pair of the controller rather than a periodic or explicitly time-dependent mechanism. The result is a soft-reset controller for steady-state optimization that enjoys the same benefits of soft-reset control discussed in previous chapters: it avoids the need for temporal regularization and hybrid systems theory, while preventing discontinuity of control signals.

In Section 5.2, two soft-reset controllers inspired by momentum-based gradient methods are proposed: one for linear time-invariant plants and one for a class of passive nonlinear plants for which only filtered gradient information is available. In the latter case, the controller by itself does not have the form of a momentum-based gradient method but is designed to induce momentum-based gradient dynamics in the closed-loop system. Using analyses derived from singular perturbation methods, global asymptotic stability of the optimizer is established for both of the considered soft-reset control systems, assuming invexity and suitable smoothness conditions on the objective function. Section 5.3 numerically illustrates the potential for soft resets to significantly improve efficiency of convergence.

5.2 Stability analysis of soft-reset steady-state optimization

5.2.1 Linear time-variant systems

Consider a plant having state $x \in \mathbb{R}^{n_p}$ and input $u \in \mathbb{R}^{n_c}$, given by

$$\varepsilon \dot{x} = Ax + Bu \tag{5.1}$$

with $\varepsilon > 0$ and matrices A and B of appropriate dimension, under the following assumption.

Assumption 8 *The matrix A is Hurwitz. That is, all the eigenvalues of A have negative real part. Equivalently, for every symmetric matrix $Q > 0$, there exists a symmetric matrix $P > 0$ such that $A^T P + PA = -Q$.*

Given differentiable functions $\phi_x : \mathbb{R}^{n_p} \to \mathbb{R}$ and $\phi_u : \mathbb{R}^{n_c} \to \mathbb{R}$, the control objective is to steer (x, u) toward the solution of the optimization problem given by

$$\min_{x \in \mathbb{R}^{n_p},\, u \in \mathbb{R}^{n_c}} \phi_x(x) + \phi_u(u) \tag{5.2a}$$

$$\text{s.t.} \quad Ax + Bu = 0. \tag{5.2b}$$

Due to Assumption 8, A is Hurwitz and therefore invertible, and the steady-state relation of (5.1) can be written as $x = Gu$ with $G \coloneqq -A^{-1}B$. We reformulate (5.2) as

$$\min_{u \in \mathbb{R}^{n_c}} \Phi(u) \coloneqq \phi_x(Gu) + \phi_u(u) \tag{5.3}$$

under the following assumptions.

Assumption 9 *The matrix G has full column rank, and there exists a unique solution u^* to (5.3).*

Assumption 10 *There exists $L_x > 0$ such that, for all $x_1, x_2 \in \mathbb{R}^{n_p}$,*

$$|\nabla\phi_x(x_1) - \nabla\phi_x(x_2)| \leq L_x|x_1 - x_2|.$$

Assumption 11 *The function Φ is invex and radially unbounded.*

Assuming that x can be measured for feedback control and that the functions $(\nabla\phi_x, \nabla\phi_u)$ are known, the plant can be interconnected with a soft-reset controller having state $\overline{u} := (u_1, u_2) \in \mathbb{R}^{2n_c}$, output $u := u_1$, and dynamics given by

$$\dot{u}_1 = u_2, \tag{5.4a}$$

$$\dot{u}_2 \in -K_c u_2 - \psi(x, u_1) - \kappa \left(\mathrm{SGN}\left(\langle\psi(x, u_1),\, u_2\rangle\right) + 1\right) u_2, \tag{5.4b}$$

$$\psi(x, u_1) := G^T\nabla\phi_x(x) + \nabla\phi_u(u_1), \tag{5.4c}$$

where $K_c > 0$, $\kappa > 0$, and the set-valued mapping SGN is defined as

$$\mathrm{SGN(s)} := \begin{cases} \frac{s}{|s|} & s \neq 0 \\ [-1, 1] & s = 0. \end{cases} \tag{5.5}$$

The following result establishes that the control objective is achieved for sufficiently small values of ε in (5.1).

Theorem 4 *Under Assumptions 8, 9, 10, and 11, there exists $\varepsilon^* > 0$ such that, for all $\varepsilon \in (0, \varepsilon^*)$, the point $(Gu^*, u^*, 0)$ is globally asymptotically stable for the system having state $x_{cl} := (x, u_1, u_2)$ satisfying (5.1) and (5.4).*

Proof: Let $\tilde{x} \coloneqq x - Gu_1$, $\tilde{u}_1 \coloneqq u_1 - u^*$, and $\tilde{x}_{cl} \coloneqq (\tilde{x}, \tilde{u}_1, u_2)$. The result follows by showing that, under the given assumptions, the origin of the system given by

$$\begin{aligned}\dot{\tilde{x}}_{cl} &\in \tilde{F}(\tilde{x}_{cl}) \\ &\coloneqq \begin{bmatrix} (1/\varepsilon)A\tilde{x} - Gu_2 \\ u_2 \\ -K_c u_2 - \psi(\tilde{x} + Gu_1,\, \tilde{u}_1 + u^*) - \kappa \left(\mathrm{SGN}\left(\langle \psi(\tilde{x} + Gu_1,\, \tilde{u}_1 + u^*),\, u_2 \rangle\right) + 1\right) u_2 \end{bmatrix}\end{aligned} \tag{5.6}$$

is globally asymptotically stable. To this end, let (P, Q) be any pair of symmetric positive definite matrices satisfying the equation in Assumption 8, and let $\alpha > 0$. Consider the Lyapunov function candidate

$$V(\tilde{x}_{cl}) \coloneqq \tilde{x}^T P \tilde{x} + \alpha \left(\Phi(\tilde{u}_1 + u^*) - \Phi(u^*) + \frac{1}{2}|u_2|^2 \right),$$

which is positive definite due to Assumption 9 and radially unbounded due to Assumption 11. By Assumption 10, we have

$$\begin{aligned} &|\nabla\Phi(\tilde{u}_1 + u^*) - \psi(\tilde{x} + Gu_1,\, \tilde{u}_1 + u^*)| \\ &\quad = |G^T \nabla\phi_x(Gu_1) + \nabla\phi_u(u_1) \\ &\qquad - \left(G^T \nabla\phi_x(x) + \nabla\phi_u(u_1)\right)| \\ &\quad = |G^T(\nabla\phi_x(Gu_1) - \nabla\phi_x(x))| \\ &\quad \leq L_x |G| |Gu_1 - x| \\ &\quad = L_x |G| |\tilde{x}|. \end{aligned} \tag{5.7}$$

Furthermore, under Assumption 8,

$$2\langle P\tilde{x}, A\tilde{x}\rangle = \tilde{x}^T(A^TP + PA)\tilde{x} \leq -\lambda_{\min}(Q)|\tilde{x}|^2. \tag{5.8}$$

Using (5.7), (5.8), and the positivity of κ, we have that, for all $\tilde{x}_{cl} \in \mathbb{R}^{n_p+2n_c}$ and $\tilde{f} \in \tilde{F}(\tilde{x}_{cl})$, there exists $\sigma \in [-1, 1]$ such that

$$\begin{aligned}
&\langle \nabla V(\tilde{x}_{cl}),\, \tilde{f}\rangle \\
&\quad = \alpha\Big(\langle \nabla\Phi(\tilde{u}_1 + u^*), u_2\rangle - K_c|u_2|^2 \\
&\qquad - \langle \psi(\tilde{x} + Gu_1,\, \tilde{u}_1 + u^*), u_2\rangle - \kappa(\sigma+1)|u_2|^2\Big) \\
&\qquad + \frac{2}{\varepsilon}\langle P\tilde{x}, A\tilde{x}\rangle - 2\langle P\tilde{x}, Gu_2\rangle \\
&\quad \leq \alpha\Big(L_x|G||\tilde{x}||u_2| - K_c|u_2|^2\Big) + \frac{2}{\varepsilon}\langle P\tilde{x}, A\tilde{x}\rangle - 2\langle P\tilde{x}, Gu_2\rangle \\
&\quad \leq \alpha L_x|G||\tilde{x}||u_2| - \alpha K_c|u_2|^2 - \frac{1}{\varepsilon}\lambda_{\min}(Q)|\tilde{x}|^2 + 2|P||G||\tilde{x}||u_2| \\
&\quad = -\begin{bmatrix} |u_2| \\ |\tilde{x}| \end{bmatrix}^T \Lambda \begin{bmatrix} |u_2| \\ |\tilde{x}| \end{bmatrix}, \qquad (5.9) \\
&\Lambda \coloneqq \begin{bmatrix} \alpha K_c & -(\alpha L_x + 2|P|)|G|/2 \\ -(\alpha L_x + 2|P|)|G|/2 & \lambda_{\min}(Q)/\varepsilon \end{bmatrix}.
\end{aligned}$$

By requiring that

$$\epsilon < \frac{4\alpha K_c\lambda_{\min}(Q)}{(\alpha L_x|G| + 2|P||G|)^2} =: \varepsilon^*, \tag{5.10}$$

we have that Λ is positive definite, and (5.9) implies that the origin of (5.6) is globally stable. To show global asymptotic stability, we will apply the invariance principle for differential inclusions [32, Theorem 2.11] by showing that no complete solution of (5.6)

keeps V at a nonzero constant value. Observe that, due to (5.9), any solution that keeps V constant must satisfy $u_2 \equiv \tilde{x} \equiv 0$ and consequently $\dot{u}_2 \equiv 0$. Then, according to (5.6), such solutions also satisfy $\psi(\tilde{x} + Gu_1, \tilde{u}_1 + u^*) \equiv 0$. Moreover, because $\tilde{x} \equiv 0$, we have $\psi(\tilde{x} + Gu_1, \tilde{u}_1 + u^*) \equiv \nabla\Phi(u_1) \equiv 0$. It follows that $u_1 \equiv u^*$, due to the invexity in Assumption 11, which ensures that $\nabla\Phi(u_1) = 0$ if and only if $u_1 = u^*$. In summary, solutions that keep V constant must satisfy $(\tilde{x}, \tilde{u}_1, u_2) \equiv (0, 0, 0)$, and we conclude that the origin of (5.14) is globally asymptotically stable. ■

5.2.2 Passive systems

Consider a plant having states $\xi \in \mathbb{R}^{n_p}$ and $x \in \mathbb{R}^{n_p}$ with input $u \in \mathbb{R}^{n_c}$, parameter $K > 0$, and dynamics given by

$$\dot{\xi} = -K(\xi - \nabla\phi(x)), \tag{5.11a}$$

$$\dot{x} = f_p(x, u), \tag{5.11b}$$

where $\phi : \mathbb{R}^{n_p} \to \mathbb{R}$ and $f_p : \mathbb{R}^{n_p} \times \mathbb{R}^{n_c} \to \mathbb{R}^{n_p}$ satisfy the following.

Assumption 12 *The function ϕ is twice continuously differentiable, $\nabla\phi$ has locally Lipschitz partial derivatives, and there exists $\overline{H} > 0$ such that*

$$|\nabla^2\phi(x)| \leq \overline{H}, \quad \forall x \in \mathbb{R}^{n_p}.$$

Assumption 13 *The function ϕ is invex, radially unbounded, and has a unique minimizer over $\mathbb{R}^{n_p}$ denoted x^*.*

Assumption 14 *The function f_p is continuous and satisfies*

$$\langle \nabla\phi(x),\, f_p(x,u)\rangle \leq \langle \nabla\phi(x),\, u\rangle$$

for all $(x,u) \in \mathbb{R}^{n_p} \times \mathbb{R}^{n_c}$.

The control objective is to steer x toward the solution of the optimization problem given by

$$\min_{x\in\mathbb{R}^{n_p}} \phi(x).$$

Assuming that ξ can be measured for feedback control, we interconnect the plant with a soft-reset controller having input $-\xi$ and output u, given by

$$\dot{u} \in F_c(u,-\xi) \coloneqq -K_c u - \xi - \kappa(u,-\xi)\left(\mathrm{SGN}\left(\langle \xi, u\rangle\right)+1\right)u, \tag{5.13}$$

where $K_c > 0$, κ is a continuous function taking positive values, and SGN is defined as in (5.5). The following result establishes that the control objective is achieved for sufficiently large values of K in (5.11).

Theorem 5 *Under Assumptions 12, 13, and 14, if $K > \overline{H}/K_c$ then the point $(0,x^*,0)$ is globally asymptotically stable for the system having state $x_{cl} \coloneqq (\xi,x,u)$ satisfying* (5.11) *and* (5.13).

Proof: Let $\tilde{\xi} \coloneqq \xi - \nabla\phi(x)$, $\tilde{x} \coloneqq x - x^*$, and $\tilde{x}_{cl} \coloneqq (\tilde{\xi},\tilde{x},u)$. The result follows by

showing that, under the given assumptions, the origin of the system given by

$$\begin{aligned}\dot{\tilde{x}}_{cl} &\in \tilde{F}(\tilde{x}_{cl}) \\ &\coloneqq \begin{bmatrix} -K\tilde{\xi} - \nabla^2\phi(\tilde{x}+x^*)u \\ f_p(\tilde{x}+x^*,u) \\ -K_c u - \left(\tilde{\xi} + \nabla\phi(\tilde{x}+x^*)\right) - \kappa(u,-\xi)\left(\mathrm{SGN}\left(\left\langle \tilde{\xi} + \nabla\phi(\tilde{x}+x^*),\, u\right\rangle\right)+1\right)u \end{bmatrix}\end{aligned} \tag{5.14}$$

is globally asymptotically stable. Consider, for some $\alpha > 0$ to be chosen later, the positive definite Lyapunov function candidate

$$V(\tilde{x}_{cl}) \coloneqq \frac{1}{2}|\tilde{\xi}|^2 + \alpha\left(\phi(\tilde{x}+x^*) - \phi(x^*) + \frac{1}{2}|u|^2\right), \tag{5.15}$$

which is radially unbounded due to Assumption 13. For all $\tilde{x}_{cl} \in \mathbb{R}^{2n_p+n_c}$ and $\tilde{f} \in \tilde{F}(\tilde{x}_{cl})$, there exists $\sigma \in [-1,1]$ such that

$$\begin{aligned}&\langle \nabla V(\tilde{x}_{cl}), \tilde{f}\rangle \\ &\quad= \alpha\left(\langle \nabla\phi(\tilde{x}+x^*),\, f_p(\tilde{x}+x^*,u)\rangle - \langle \xi, u\rangle - K_c|u|^2 - \kappa(u,-\xi)(\sigma+1)|u|^2\right) \\ &\qquad - K|\tilde{\xi}|^2 - \langle \tilde{\xi}, \nabla^2\phi(\tilde{x}+x^*)u\rangle \\ &\quad\le \alpha\left(\langle \nabla\phi(\tilde{x}+x^*), u\rangle - \langle \xi, u\rangle - K_c|u|^2\right) - K|\tilde{\xi}|^2 + \overline{H}|\tilde{\xi}||u| \qquad (5.16a) \\ &\quad= \alpha\left(-K_c|u|^2 - \langle \tilde{\xi}, u\rangle\right) - K|\tilde{\xi}|^2 + \overline{H}|\tilde{\xi}||u| \\ &\quad\le -\alpha K_c|u|^2 + \alpha|\tilde{\xi}||u| - K|\tilde{\xi}|^2 + \overline{H}|\tilde{\xi}||u| \\ &\quad= -\begin{bmatrix} |u| \\ |\tilde{\xi}| \end{bmatrix}^T \Lambda \begin{bmatrix} |u| \\ |\tilde{\xi}| \end{bmatrix}, \qquad (5.16b)\end{aligned}$$

$$\Lambda \coloneqq \begin{bmatrix} \alpha K_c & -(\alpha+\overline{H})/2 \\ -(\alpha+\overline{H})/2 & K \end{bmatrix},$$

where, in (5.16a), we have used Assumptions 12 and 14 and the positivity of κ. By requiring that

$$K > \frac{(\alpha+\overline{H})^2}{4K_c\alpha} =: \underline{K}(\alpha), \tag{5.17}$$

we have that Λ is positive definite, and (5.16b) implies that the origin of (5.14) is globally stable. Note that

$$\frac{d\underline{K}(\alpha)}{d\alpha} = \frac{(\alpha-\overline{H})(\alpha+\overline{H})}{4K_c\alpha^2},$$
$$\frac{d^2\underline{K}(\alpha)}{d\alpha^2} = \frac{2\overline{H}^2}{4K_c\alpha^3},$$

and $\underline{K} : \mathbb{R}_{>0} \to \mathbb{R}_{>0}$ is minimized at $\alpha = \overline{H}$. For this choice of α, (5.17) is equivalent to the constraint that $K > \overline{H}/K_c$.

To show global asymptotic stability, we will apply the invariance principle as done in the proof of Theorem 4. Due to (5.16b), any solution that keeps V at a nonzero constant must satisfy $u \equiv \tilde{\xi} \equiv 0$ and consequently $\dot{u} \equiv 0$. Then, according to (5.14), such solutions also satisfy $\tilde{\xi} + \nabla\phi(\tilde{x}+x^*) \equiv 0$ or, equivalently, $\xi \equiv 0$. Combining $\xi \equiv 0$ and $\tilde{\xi} \equiv 0$, we have $\nabla\phi(x) \equiv 0$. It follows that $x \equiv x^*$, due to the invexity in Assumption 13, which ensures that $\nabla\phi(x) = 0$ if and only if $x = x^*$. Therefore, solutions that keep V constant must satisfy $(\tilde{\xi}, \tilde{x}, u) \equiv (0,0,0)$, and we conclude that the origin of (5.14) is globally asymptotically stable. ■

5.3 Numerical results

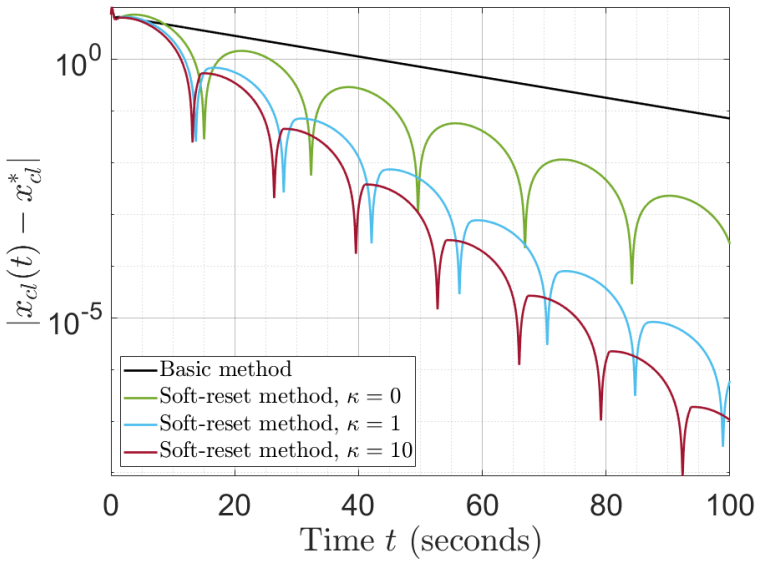

Figure 5.1: Evolution of the tracking error norm over time.

Defining the error $x_{cl} - x^*_{cl}$ with respect to $x^*_{cl} := (Gu^*, u^*, 0)$, Figure 5.1 shows the performance of the soft-reset controller (5.4) with $K_c = 1/4$ and compares it with the basic controller given by $\dot{u} = -\psi(x, u)$, where ψ is given by (5.4c) with

$$\phi_x(x) = \frac{1}{2} x^T Q x + b^T x, \tag{5.18a}$$

$$\phi_u(u) = 0.01|u|^2, \tag{5.18b}$$

where Q is randomly generated to have $\lambda_{\min}(Q) = 0.05$ and a condition number of 10^3, and the elements of b are randomly generated, independently uniformly distributed on $[-10, 10]^{n_p}$. Each controller in Figure 5.1 is placed in feedback interconnection with the

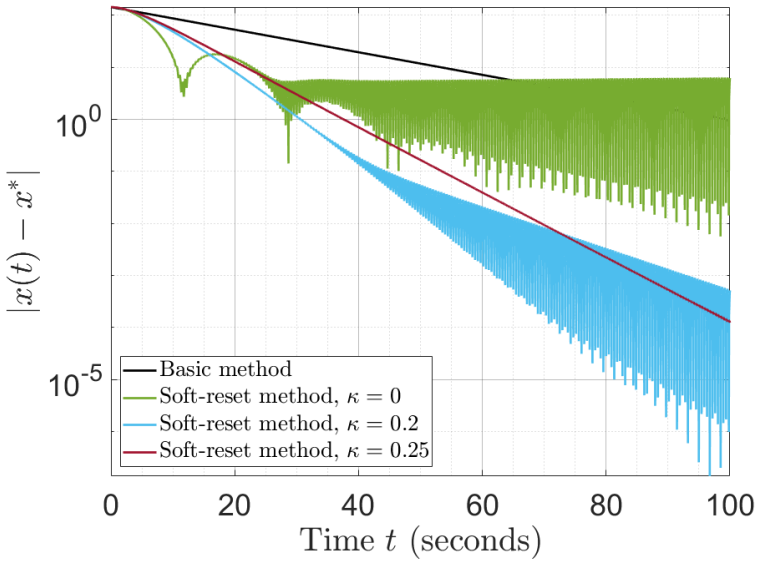

Figure 5.2: Evolution of the tracking error norm over time.

plant (5.1), setting $\varepsilon = 1$,

$$A = \begin{bmatrix} 0 & 1 & 0 \\ 0 & 0 & 1 \\ -48 & -44 & -12 \end{bmatrix}, \quad B = \begin{bmatrix} 0 \\ 0 \\ 5/3 \end{bmatrix}.$$

The eigenvalues of A are -2, -4, and -6, and thus Assumption 8 is satisfied [61, Thm. 8.2].

Figure 5.2 shows the performance of the soft-reset controller (5.13) with $K_c = 1/4$ and compares it with the basic controller given by $\dot{u} = -\xi$, with $n_p = 5$ and with ϕ having the same form as (5.18a), where Q and b are randomly generated as described previously. Each controller in Figure 5.2 is placed in feedback interconnection with the plant (5.11) with $K = 200$ and $f_p(x, u) = u$.

Chapter 6

Concurrent Learning in High-Order Tuners for Parameter Identification

High-order tuners are algorithms that show promise in achieving greater efficiency than classic gradient-based algorithms in identifying the parameters of parametric models and/or in facilitating the progress of a control or optimization algorithm whose adaptive behavior relies on such models. For high-order tuners, robust stability properties, namely uniform global asymptotic (and exponential) stability, currently rely on a persistent excitation (PE) condition. In this work, we establish such stability properties with a novel analysis based on a Matrosov theorem and then show that the PE requirement can be relaxed via a concurrent learning technique driven by sampled data points that are sufficiently rich. We show numerically that concurrent learning may greatly improve efficiency. We incorporate reset methods that preserve the stability guarantees while providing additional improvements that may be relevant in applications that demand highly accurate parameter estimates at relatively low additional cost in computation.

6.1 Introduction

The problem of identifying the parameters in a linear parametric model through the use of online measurements of input-output data has been studied extensively from the

standpoint of the continuous-time gradient algorithm, which plays an important role in adaptive control [62], [63] and has found broad applications in areas such as optimal nonlinear control [64], extremum seeking [65], and the analysis of machine learning algorithms [66]. The gradient algorithm has been shown to achieve uniform global asymptotic (and exponential) stability of the desired parameter value, under a condition of persistent excitation which has been shown to be both necessary and sufficient [67]. Here, the distinction between uniform and non-uniform asymptotic stability has crucial implications in practice: unlike the non-uniform notion of stability, the uniform notion ensures robustness, in the sense of achieving "total stability" in the presence of bounded additive disturbances ([68, Sec. 1B]) which are widely encountered in applications.

Although persistent excitation characterizes uniform asymptotic stability for the gradient algorithm, the incorporation of "concurrent learning" has been shown to enable uniform asymptotic stability in the absence of persistent excitation [69]. Concurrent learning involves an augmentation of the gradient, using discretely sampled data measurements that collectively satisfy a condition of "sufficient richness." Advantageously, sufficient richness can be characterized in terms of a rank condition on a matrix constructed from the data samples, a condition which can be computationally much simpler to verify in practice than the condition of persistent excitation.

In a separate thread of research, recent studies have shown that filtering the gradient can improve the performance of the gradient algorithm, sometimes significantly and in the absence of persistent excitation [70]. Namely, the use of filtering can improve the convergence rate of the parameter estimate toward the desired parameter value or, in adaptive control problems, the convergence rate of the tracking error toward zero. The filtering procedures considered in [70] and [71] give rise to algorithms referred to as high-order tuners, which take inspiration from algorithms introduced in [72]. In addition to offering improved performance in continuous-time settings, the recently developed

high-order tuners serve as a basis for deriving novel discrete-time algorithms for various problems of estimation and learning with online data, with guarantees of efficiency in the sense of Nesterov's method for convex optimization [73] and of robustness in noisy and adversarial environments [74], [75]. In continuous time, under a persistent excitation condition, uniform asymptotic stability properties of high-order tuners can be established using the method of analysis in [76, Sec. 4.6]. However, the use of concurrent learning in high-order tuners has not yet been explored.

In this work, we establish uniform global asymptotic stability (UGAS) properties of continuous-time high-order tuners for parameter identification under two different conditions: (1) persistent excitation and (2) concurrent learning with sufficiently rich data. In Section 6.2, UGAS is established under persistent excitation, using an approach that we claim to be simpler than that of [76, Sec. 4.6]. Whereas [76] shows uniform convergence by carefully examining solutions of a differential equation, we instead take advantage of a Matrosov theorem [77], which can be regarded as an analogue of the LaSalle invariance principle in the context of time-varying systems, with which uniform convergence is shown by combining infinitesimal conditions on Lyapunov-like functions together with observability-like conditions. In Section 6.3, we propose implementations of concurrent learning for high-order tuners in order to preserve UGAS in the absence of persistent excitation, given sufficiently rich data. We show that the resulting systems admit strict Lyapunov functions. In Section 6.4, we propose the use of a technique inspired by reset methods in control and optimization ([26], [40]), which shows promise in improving the efficiency of high-order tuners that make use of concurrent learning. In Section 6.5, numerical results show that concurrent learning can offer significant improvements in the convergence rate of high-order tuners for a parameter identification problem involving a regressor constructed from sinusoids.

6.2 Uniform global asymptotic stability in high-order tuners via persistent excitation

Suppose $y^*(t) = \phi^T(t)\theta^*$ for all $t \geq 0$, where $y^* : \mathbb{R}_{\geq 0} \to \mathbb{R}$ and $\phi : \mathbb{R}_{\geq 0} \to \mathbb{R}^n$ are known functions of time, and we wish to solve for $\theta^* \in \mathbb{R}^n$ online under the following assumption.

Assumption 15 *The regressor $\phi(\cdot)$ is piecewise continuous, bounded, and persistently exciting. That is, there exist $M > 0$, $T > 0$, and $\delta > 0$ such that $|\phi(t)| \leq M$ for all $t \geq 0$, and*

$$\int_t^{t+T} \phi(s)\phi^T(s)ds \geq \delta I \quad \forall t \geq 0.$$

As a means of determining θ^*, we follow the algorithmic development of [71], [70, Ch. 5]. Let $\theta \in \mathbb{R}^n$, $y(t) \coloneqq \phi^T(t)\theta$, $\tilde{\theta} \coloneqq \theta - \theta^*$, $e_y(t) \coloneqq y(t) - y^* = \phi^T(t)\tilde{\theta}$, and $L_t(\theta) \coloneqq (1/2)\tilde{\theta}^T\phi(t)\phi^T(t)\tilde{\theta}$, so that $\nabla_\theta L_t(\theta) = \phi(t)e_y(t)$, and consider the following differential equation in the variable $x \coloneqq (\theta, \vartheta)$:

$$\dot{x} = f(x,t) \coloneqq \begin{bmatrix} -\beta(\theta - \vartheta)\mathcal{N}_t \\ -\gamma\nabla_\theta L_t(\theta) \end{bmatrix}, \tag{6.1}$$

where $\beta \in \mathbb{R}_{>0}$, $\gamma \in \mathbb{R}_{>0}$, and $t \mapsto \mathcal{N}_t$ are to be selected for the purpose of achieving desired convergence properties for solutions of (6.1). Choosing $\mathcal{N}_t$ to be dependent on $\phi(t)$ will be crucial for establishing stability properties of (6.1). We focus on the case of

$$\mathcal{N}_t \coloneqq 1 + \mu\phi^T(t)\phi(t) \quad \forall t \geq 0, \quad \mu \in \mathbb{R}_{>0}, \tag{6.2}$$

although other choices may be feasible (see [78, Sec. 3] for an example to consider). Equation (6.1) is referred to as a high-order tuner and is identical to [71, Eq. 6] and [70,

Eq. 5.6].

Another high-order tuner of interest is given as follows:

$$\dot{x} = f(x,t) \coloneqq \begin{bmatrix} -\beta(\theta - \vartheta) \\ -\dfrac{\gamma}{\mathcal{N}_t}\nabla_\theta L_t(\theta) \end{bmatrix}. \tag{6.3}$$

Equation (6.3) is identical to [71, Eq. 6'] and [70, Eq. 5.6'].

For brevity, the dependence of ϕ and e_y on t will be suppressed hereafter.

Theorem 6 *Under Assumption 15, with $\mathcal{N}_t$ given by* (6.2)*, if $\beta \geq 2\gamma/\mu$, the point (θ^*, θ^*) is uniformly globally asymptotically stable for* (6.1)*.*

Proof: Recalling that $\tilde{\theta} = \theta - \theta^*$, let $p \coloneqq \vartheta - \theta$ and $\tilde{x} \coloneqq (\tilde{\theta}, p)$. We will use Matrosov's theorem [77] to establish that the origin is UGAS for the system

$$\dot{\tilde{x}} = \tilde{f}(\tilde{x},t) \coloneqq \begin{bmatrix} \beta\mathcal{N}_t p \\ -\beta\mathcal{N}_t p - \gamma\nabla_\theta L_t\left(\tilde{\theta} + \theta^*\right) \end{bmatrix}, \tag{6.4}$$

which will imply that (θ^*, θ^*) is UGAS for (6.1). To begin, consider the Lyapunov function candidate

$$V_0(\tilde{x}) \coloneqq \frac{1}{\gamma}\left|\tilde{\theta} + p\right|^2 + \frac{1}{\gamma}|p|^2. \tag{6.5}$$

which is radially unbounded, positive definite, and continuously differentiable. For all

$(\tilde{x}, t) \in \mathbb{R}^{2n} \times \mathbb{R}_{\geq 0}$, we have

$$\begin{aligned}\left\langle \nabla V_0(\tilde{x}), \tilde{f}(\tilde{x}, t) \right\rangle &= \frac{2}{\gamma}\Bigg[- \left\langle \tilde{\theta} + p,\ \gamma \nabla_\theta L_t \left(\tilde{\theta} + \theta^* \right) \right\rangle \\ &\quad - \left\langle p,\ \beta \mathcal{N}_t p + \gamma \nabla_\theta L_t \left(\tilde{\theta} + \theta^* \right) \right\rangle \Bigg] \\ &= -2 \left\langle \tilde{\theta}, \nabla_\theta L_t \left(\tilde{\theta} + \theta^* \right) \right\rangle - \frac{2\beta \mathcal{N}_t}{\gamma} |p|^2 \\ &\quad - 4 \left\langle p,\ \nabla_\theta L_t \left(\tilde{\theta} + \theta^* \right) \right\rangle.\end{aligned}$$

Substituting $\nabla_\theta L_t \left(\tilde{\theta} + \theta^* \right) = \phi \phi^T \tilde{\theta}$ and $e_y = \phi^T \tilde{\theta}$, followed by $\mathcal{N}_t = 1 + \mu \phi^T \phi$, we have

$$\begin{aligned}\left\langle \nabla V_0(\tilde{x}), \tilde{f}(\tilde{x}, t) \right\rangle &\leq -2 |e_y|^2 - \frac{2\beta \mathcal{N}_t}{\gamma} |p|^2 + 4|p||\phi||e_y| \\ &= -2 |e_y|^2 - \frac{2\beta}{\gamma} |p|^2 - \frac{2\beta\mu}{\gamma} |\phi|^2 |p|^2 + 4|p||\phi||e_y|.\end{aligned}$$

With $\beta \geq 2\gamma/\mu$, it follows that

$$\begin{aligned}&\left\langle \nabla V_0(\tilde{x}), \tilde{f}(\tilde{x}, t) \right\rangle \\ &\quad \leq -2 |e_y|^2 - \frac{2\beta}{\gamma} |p|^2 - 4|\phi|^2 |p|^2 + 4|p||\phi||e_y| \\ &\quad = -\frac{2\beta}{\gamma} |p|^2 - |e_y|^2 - \left[|e_y| - 2|p||\phi| \right]^2 \\ &\quad \leq -\frac{2\beta}{\gamma} |p|^2 - |e_y|^2 =: Y_0(\tilde{x}, e_y) \leq 0, \end{aligned} \tag{6.6}$$

and hence the origin of (6.4) is uniformly globally stable. Next, we establish uniform global attractivity by building Matrosov functions as follows. Let

$$V_1(\tilde{x}, t) \coloneqq -\tilde{\theta}^T \left(\int_t^\infty \exp(t - \tau) \phi(\tau) \phi^T(\tau) d\tau \right) \tilde{\theta}, \tag{6.7}$$

and note that Assumption 15 implies

$$V_1(\tilde{x},t) \leq -\exp(-T)\delta\tilde{\theta}^T\tilde{\theta} \quad \forall(\tilde{x},t) \in \mathbb{R}^{2n} \times \mathbb{R}_{\geq 0}.$$

Then, for all $(\tilde{x},t) \in \mathbb{R}^{2n} \times \mathbb{R}_{\geq 0}$, it holds that

$$\begin{aligned}
&\frac{\partial V_1(\tilde{x},t)}{\partial t} + \frac{\partial V_1(\tilde{x},t)}{\partial \tilde{x}} f(\tilde{x},t) \\
&\leq V_1(\tilde{x},t) + \tilde{\theta}^T\phi\phi^T\tilde{\theta} + \beta M^2(1+\mu M^2)|\tilde{\theta}||p| \\
&= V_1(\tilde{x},t) + |e_y|^2 + \beta M^2(1+\mu M^2)|\tilde{\theta}||p| \\
&\leq -\exp(-T)\delta\tilde{\theta}^T\tilde{\theta} + |e_y|^2 + \beta M^2(1+\mu M^2)|\tilde{\theta}||p| \qquad (6.8) \\
&=: Y_1(\tilde{x},e_y).
\end{aligned}$$

Note that $Y_0(\tilde{x},e_y) = 0$ implies $p = 0$ and $e_y = 0$, which implies

$$Y_1(\tilde{x},e_y) = -\exp(-T)\delta\tilde{\theta}^T\tilde{\theta} \leq 0.$$

Also note that $Y_0(\tilde{x},e_y) = Y_1(\tilde{x},e_y) = 0$ implies $p = 0$ and $\tilde{\theta} = 0$. Finally, note that V_0 is time-invariant, the maps $(\tilde{x},t) \mapsto V_1(\tilde{x},t)$ and $(\tilde{x},t) \mapsto \phi^T(t)\tilde{\theta}$ are each locally bounded in $\tilde{x}$ uniformly in t, and both Y_0 and Y_1 are continuous. Thus, the conditions of Matrosov's theorem [77] hold, and we conclude that the origin of (6.4) is UGAS. ■

Theorem 7 *Under Assumption 15, with $\mathcal{N}_t$ given by* (6.2)*, if $\beta \geq 2\gamma/\mu$, the point (θ^*,θ^*) is uniformly globally asymptotically stable for* (6.3)*.*

Proof: Recalling that $\tilde{\theta} = \theta - \theta^*$, let $p \coloneqq \vartheta - \theta$ and $\tilde{x} \coloneqq (\tilde{\theta},p)$. Reusing notation from the proof of Theorem 6, we will use Matrosov's theorem [77] to establish that the

origin is UGAS for the system

$$\dot{\tilde{x}} = \tilde{f}(\tilde{x}, t) \coloneqq \begin{bmatrix} \beta p \\ -\beta p - \dfrac{\gamma}{\mathcal{N}_t} \nabla_\theta L_t \left(\tilde{\theta} + \theta^* \right) \end{bmatrix}, \tag{6.9}$$

which will imply that (θ^*, θ^*) is UGAS for (6.3). To begin, consider the Lyapunov function candidate (6.5), which is radially unbounded, positive definite, and continuously differentiable. Observing that the right-hand side of (6.9) can be obtained by multiplying the right-hand side of (6.4) by $1/\mathcal{N}_t$, we have from (6.6) that, for all $(\tilde{x}, t) \in \mathbb{R}^{2n} \times \mathbb{R}_{\geq 0}$ and for $\beta \geq 2\gamma/\mu$,

$$\begin{aligned} &\left\langle \nabla V_0(\tilde{x}), \tilde{f}(\tilde{x}, t) \right\rangle \\ &\quad \leq \frac{1}{\mathcal{N}_t} \left\{ -\frac{2\beta}{\gamma} |p|^2 - |e_y|^2 \right\} \\ &\quad = \frac{1}{1 + \mu \phi^T \phi} \left\{ -\frac{2\beta}{\gamma} |p|^2 - \tilde{\theta}^T \phi \phi^T \tilde{\theta} \right\} \\ &\quad =: Y_0(\tilde{x}, \phi) \leq 0, \end{aligned} \tag{6.10}$$

and hence the origin of (6.9) is uniformly globally stable. Next, we establish uniform global attractivity by building Matrosov functions as follows. Let V_1 be defined as in (6.7) so that, following the steps leading up to (6.8), we may write, for all $(\tilde{x}, t) \in \mathbb{R}^{2n} \times \mathbb{R}_{\geq 0}$,

$$\begin{aligned} &\frac{\partial V_1(\tilde{x}, t)}{\partial t} + \frac{\partial V_1(\tilde{x}, t)}{\partial \tilde{x}} f(\tilde{x}, t) \\ &\quad \leq -\exp(-T) \delta \tilde{\theta}^T \tilde{\theta} + \tilde{\theta}^T \phi \phi^T \tilde{\theta} + \beta M^2 |\tilde{\theta}| |p| \\ &\quad =: Y_1(\tilde{x}, \phi). \end{aligned}$$

Note that $Y_0(\tilde{x}, \phi) = 0$ implies $p = 0$ and $\phi^T \tilde{\theta} = 0$, which implies

$$Y_1(\tilde{x}, \phi) = -\exp(-T)\delta\tilde{\theta}^T\tilde{\theta} \leq 0.$$

Also note that $Y_0(\tilde{x}, \phi) = Y_1(\tilde{x}, \phi) = 0$ implies $p = 0$ and $\tilde{\theta} = 0$. Finally, note that V_0 is time-invariant, the maps $(\tilde{x}, t) \mapsto V_1(\tilde{x}, t)$ and $(\tilde{x}, t) \mapsto \phi(t)$ are each locally bounded in $\tilde{x}$ uniformly in t, and both Y_0 and Y_1 are continuous. Thus, the conditions of Matrosov's theorem [77] hold, and we conclude that the origin of (6.9) is UGAS. ■

Theorems 6 and 7 also establish uniform global exponential stability (UGES), due to linearity of the systems (6.1) and (6.3) and the fact that UGAS is equivalent to UGES for linear time-varying systems [79, Thm. 58.7].

Our assumptions differ from those of [71] only in regards to the regressor's properties. Namely, the analyses previously reported in [71, Thm. 2] and [71, Remark 8] require that the regressor has a bounded time derivative, whereas our analyses do not require differentiability of the regressor but instead require that it be persistently exciting. As a consequence, the previous analyses can establish only that the output error $e_y \coloneqq \phi^T\tilde{\theta}$ tends to 0 and not necessarily uniformly, whereas Theorems 6 and 7 establish that the parameter error $\tilde{\theta}$ tends to 0 uniformly.

6.3 Concurrent learning for high-order tuners

6.3.1 Stability analysis

Let $\{(\phi(t_k),\ y^*(t_k))\}_{k=1}^N$ be a sequence of recorded data. Define $B : \mathbb{R}^n \times \mathbb{R}_{\geq 0} \to \mathbb{R}^n$ as

$$B(\theta, \mu) \coloneqq \sum_{k=1}^{N} \frac{\phi(t_k)}{1 + \mu \phi^T(t_k)\phi(t_k)} \left(\phi^T(t_k)\theta - y^*(t_k)\right). \tag{6.11}$$

In (6.1), we implement concurrent learning (CL) in the sense of, e.g., [69], [80], and [78], as follows:

$$\dot{x} = f(x,t) \coloneqq \begin{bmatrix} -\beta(\theta - \vartheta)\mathcal{N}_t \\ -\gamma\left(\nabla_\theta L_t(\theta) + \mathcal{N}_t B(\theta, \mu)\right) \end{bmatrix}, \tag{6.12}$$

where $\mathcal{N}_t$ and μ are given by (6.2), and β and γ are positive real numbers. The B-term involves a factor of $\mathcal{N}_t$ for reasons that will become clear in the stability analysis.

In (6.3), we implement CL as follows:

$$\dot{x} = f(x,t) \coloneqq \begin{bmatrix} -\beta(\theta - \vartheta) \\ -\gamma\left(\frac{1}{\mathcal{N}_t}\nabla_\theta L_t(\theta) + B(\theta, \mu)\right) \end{bmatrix}, \tag{6.13}$$

where $\mathcal{N}_t$ and μ are given by (6.2), and β and γ are positive real numbers.

UGAS properties for (6.12) and (6.13) can be shown if the data satisfies the following property, which is characterized by the subsequent lemma.

Assumption 16 *The regressor data $\{\phi(t_k)\}_{k=1}^N$ is sufficiently rich (SR) in the sense that the matrix*

$$\mathcal{D} \coloneqq [\phi(t_1),\ \phi(t_2),\ \cdots,\ \phi(t_N)] \in \mathbb{R}^{n \times N}$$

has rank n.

Lemma 6.3.1 *For a given $\mu \in \mathbb{R}_{\geq 0}$, Assumption 16 holds if and only if there exists $\delta_\mu \in \mathbb{R}_{>0}$ such that*

$$P_\mu \coloneqq \sum_{k=1}^{N} \frac{\phi(t_k)\phi^T(t_k)}{1+\mu\phi^T(t_k)\phi(t_k)} \geq \delta_\mu I_n.$$

Proof: Let $\mu \in \mathbb{R}_{\geq 0}$ be given. First, we show the forward implication. Assuming that $\mathcal{D}$ has rank n, it follows that, for any non-zero $x \in \mathbb{R}^n$, there exists $k \in \{1, \ldots, N\}$ such that $\phi^T(t_k)x \neq 0$. (If it were not true, the columns of $\mathcal{D}$ would not span $\mathbb{R}^n$.) In other words, for any non-zero $x \in \mathbb{R}^n$, there exists k such that $x^T\phi(t_k)\phi^T(t_k)x > 0$. It follows that, for any non-zero $x \in \mathbb{R}^n$, $x^T P_\mu x > 0$, and hence there exists $\delta_\mu \in \mathbb{R}_{>0}$ (which generally depends on μ) such that $x^T P_\mu x \geq \delta_\mu$. Next, we show the reverse implication. Assuming that there exists $\delta_\mu \in \mathbb{R}_{>0}$ such that $P_\mu \geq \delta_\mu I_n$, it follows that, for any non-zero $x \in \mathbb{R}^n$, there exists $k \in \{1, \ldots, N\}$ such that $x^T\phi(t_k)\phi^T(t_k)x > 0$. That is, there exists k such that $\phi^T(t_k)x \neq 0$. Then, because x is an arbitrary non-zero vector in $\mathbb{R}^n$, it follows that there are n linearly independent columns of $\mathcal{D}$. ■

Theorem 8 *Under Assumption 16, if $\beta \geq 2\gamma/\mu$, the point (θ^*, θ^*) is UGAS for* (6.12).

Proof: Let $\tilde{\theta} \coloneqq \theta - \theta^*$, $p \coloneqq \vartheta - \theta$, and $\tilde{x} \coloneqq (\tilde{\theta}, p)$. Due to the fact that $y^*(t_k) = \phi^T(t_k)\theta^*$, we have that $B(\theta, \mu) = P_\mu\tilde{\theta}$, and (reusing notation from previous proofs) (6.12) can be written as

$$\dot{\tilde{x}} = \tilde{f}(\tilde{x}, t) \coloneqq \begin{bmatrix} \beta\mathcal{N}_t p \\ -\beta\mathcal{N}_t p - \gamma\left(\nabla_\theta L_t(\tilde{\theta}+\theta^*) + \mathcal{N}_t P_\mu\tilde{\theta}\right) \end{bmatrix}. \tag{6.14}$$

To show that (θ^*, θ^*) is UGAS for (6.12), it suffices to show that the origin of (6.14) is

UGAS. Consider the Lyapunov function candidate

$$V(\tilde{x}) \coloneqq \frac{1}{\gamma}\left|\tilde{\theta}+p\right|^2+\frac{1}{\gamma}|p|^2+\frac{2}{\beta}\tilde{\theta}^T P_\mu \tilde{\theta}, \tag{6.15}$$

which is radially unbounded, positive definite, and continuously differentiable. Following steps similar to those leading up to (6.6), it can be shown that, for all $(\tilde{x},t)\in\mathbb{R}^{2n}\times\mathbb{R}_{\geq 0}$ and for $\beta\geq 2\gamma/\mu$,

$$\begin{aligned}
&\left\langle \nabla V(\tilde{x}), \tilde{f}(\tilde{x},t)\right\rangle \\
&\leq -\frac{2\gamma}{\beta}|p|^2-|e_y|^2-2\mathcal{N}_t\left\langle\tilde{\theta},P_\mu\tilde{\theta}\right\rangle-4\mathcal{N}_t\left\langle p,P_\mu\tilde{\theta}\right\rangle \\
&\quad+\mathcal{N}_t\left\langle\frac{4}{\beta}P_\mu\tilde{\theta},\ \beta p\right\rangle \\
&\leq -2\mathcal{N}_t\tilde{\theta}^T P_\mu\tilde{\theta}-\frac{2\beta}{\gamma}|p|^2 \\
&\leq -2\tilde{\theta}^T P_\mu\tilde{\theta}-\frac{2\beta}{\gamma}|p|^2=:Y(\tilde{x}).
\end{aligned} \tag{6.16}$$

Due to Lemma 6.3.1, Y is negative definite. Hence, V is a Lyapunov function for (6.14), and the origin of (6.14) is UGAS. ■

Theorem 9 *Under Assumption 16, with $\mathcal{N}_t$ given by* (6.2)*, if $\beta\geq 2\gamma/\mu$, the point (θ^*,θ^*) is UGAS for* (6.13)*.*

Proof: Let $\tilde{\theta}\coloneqq\theta-\theta^*$, $p\coloneqq\vartheta-\theta$, and $\tilde{x}\coloneqq(\tilde{\theta},p)$. Due to the fact that $y^*(t_k)=\phi^T(t_k)\theta^*$, we have that $B(\theta,\mu)=P_\mu\tilde{\theta}$ for any $\mu\in\mathbb{R}_{\geq 0}$, and (reusing notation from previous proofs) (6.13) can be written as

$$\dot{\tilde{x}}=\tilde{f}(\tilde{x},t)\coloneqq\begin{bmatrix}\beta p\\ -\beta p-\gamma\left(\frac{1}{\mathcal{N}_t}\nabla_\theta L_t(\tilde{\theta}+\theta^*)+P_\mu\tilde{\theta}\right)\end{bmatrix}. \tag{6.17}$$

To show that (θ^*, θ^*) is UGAS for (6.13), it suffices to show that the origin of (6.17) is UGAS. Consider the Lyapunov function candidate (6.15), which is radially unbounded, positive definite, and continuously differentiable. Observing that the right-hand side of (6.17) can be obtained by multiplying the right-hand side of (6.14) by $1/\mathcal{N}_t$, we have from (6.16) that, for all $(\tilde{x}, t) \in \mathbb{R}^{2n} \times \mathbb{R}_{\geq 0}$ and for $\beta \geq 2\gamma/\mu$,

$$\begin{aligned}
&\left\langle \nabla V(\tilde{x}), \tilde{f}(\tilde{x}, t) \right\rangle \\
&\quad \leq -2\tilde{\theta}^T P_\mu \tilde{\theta} - \frac{2\beta}{\gamma \mathcal{N}_t} |p|^2 \\
&\quad \leq -2\tilde{\theta}^T P_\mu \tilde{\theta} - \frac{2\beta}{\gamma(1+\mu M^2)} |p|^2 =: Y(\tilde{x}).
\end{aligned}$$

Due to Lemma 6.3.1, Y is negative definite. Hence, V is a Lyapunov function for (6.17), and the origin of (6.17) is UGAS. ■

One benefit of the CL feature is that it can be implemented using only the sampled data, mitigating the practical costs that may be incurred by continuously collecting data online. For example, the following system can be interpreted as a novel high-order tuner which does not require continuous online measurement of $\phi(t)$ and $y(t)$:

$$\dot{x} = f(x, t) := \begin{bmatrix} -\beta(\theta - \vartheta) \\ -\gamma B(\theta, \mu) \end{bmatrix}. \tag{6.18}$$

In this case, an additional advantage is that the UGAS property can be established under no restriction on the relative magnitudes of β, γ, and μ.

Theorem 10 *Under Assumption 16, for any positive β and γ, and for any nonnegative μ, the point (θ^*, θ^*) is UGAS for* (6.18).

Proof: Let $\tilde{\theta} := \theta - \theta^*$, $p := \vartheta - \theta$, and $\tilde{x} := (\tilde{\theta}, p)$. Due to the fact that $y^*(t_k) = \phi^T(t_k)\theta^*$, we have that $B(\theta, \mu) = P_\mu \tilde{\theta}$ for any $\mu \in \mathbb{R}_{\geq 0}$, and (reusing notation from

previous proofs) (6.18) can be written as

$$\dot{\tilde{x}} = \tilde{f}(\tilde{x}, t) \coloneqq \begin{bmatrix} \beta p \\ -\beta p - \gamma P_\mu \tilde{\theta} \end{bmatrix}. \tag{6.19}$$

To show that (θ^*, θ^*) is UGAS for (6.18), it suffices to show that the origin of (6.19) is UGAS. Consider the Lyapunov function candidate

$$V(\tilde{x}) \coloneqq \frac{1}{2}|\tilde{\theta} + p|^2 + \frac{1}{2}|p|^2 + \frac{\gamma}{\beta}\tilde{\theta}^T P_\mu \tilde{\theta},$$

which is radially unbounded, positive definite, and continuously differentiable. For all $\tilde{x} \in \mathbb{R}^{2n}$, we have

$$\begin{aligned} \left\langle \nabla V(\tilde{x}), \tilde{f}(\tilde{x}, t) \right\rangle &= \left\langle \tilde{\theta} + p + \frac{2\gamma}{\beta} P_\mu \tilde{\theta}, \beta p \right\rangle \\ &\quad - \langle \tilde{\theta} + 2p, \beta p + \gamma P_\mu \tilde{\theta} \rangle \\ &= \langle p, 2\gamma P_\mu \tilde{\theta} \rangle - \gamma \tilde{\theta}^T P_\mu \tilde{\theta} - \beta |p|^2 - \langle 2p, \gamma P_\mu \tilde{\theta} \rangle \\ &= -\gamma \tilde{\theta}^T P_\mu \tilde{\theta} - \beta |p|^2 =: Y(\tilde{x}). \end{aligned}$$

Due to Lemma 6.3.1, Y is negative definite. Hence, V is a Lyapunov function for (6.19), and the origin of (6.19) is UGAS. ■

As remarked in Section 6.2, UGAS is equivalent to UGES for linear time-varying systems, and therefore Theorems 8, 9, and 10 also establish UGES, due to linearity of the systems (6.12), (6.13), and (6.18).

6.3.2 Online implementation

Standard analyses of stability and convergence for CL methods assume the availability of recorded (offline) data that satisfies a rank condition similar to Assumption 16 [81], [69], and the same assumption is made in Theorems 6-10. In the absence of such data, CL can be implemented via online criteria that aim to ensure that the rank condition is satisfied after executing the algorithm for some period of time. When evaluating the performance of high-order tuners in Section 6.5, the simple online criterion of [82, Sec. IV] is considered. Namely, the number of recorded data points at time t is denoted $N(t)$, and a new data point is added to the data set $\{(\phi(t_k),\ y^*(t_k))\}_{k=1}^{N(t)}$ at time t if the following condition is satisfied for some user-specified parameter $\varepsilon \in \mathbb{R}_{>0}$:

$$\frac{|\phi(t) - \phi(t_{N(t)})|^2}{|\phi(t)|} \geq \varepsilon. \tag{6.20}$$

The data set is initialized as $\{(\phi(t_1),\ y^*(t_1))\}$ with $t_1 = 0$ and $N(0) = 1$. The condition (6.20) is evaluated until $N(t)$ reaches a user-specified maximum, an integer $\overline{N} \geq n$. Equation (6.11) is implemented in a time-dependent fashion, i.e., with N replaced by $N(t)$, and it becomes time-independent after $N(t)$ reaches $\overline{N}$.

For this online implementation of CL, the stability analysis is beyond the scope of the current work and, to our knowledge, has not been pursued in previous studies of CL methods. Previous studies of online implementations have focused not on stability analysis of the resulting dynamics but on showing that, in certain circumstances, an online criterion ensures that a rank-condition is satisfied in finite time or that the convergence rate of the resulting dynamics is maximized after a rank-condition has been met [82].

6.4 Soft-reset methods for high-order tuners

For applications that demand high efficiency and precision, we explore the possibility that resetting the state $\vartheta - \theta$ to zero under certain conditions can benefit performance, motivated by works such as [26] and [40]. Defining f as in (6.12), we incorporate resets in (6.12) via a soft-reset approach, similar to ideas proposed in [40] and [28], resulting in a differential inclusion given by

$$\varphi(x,t) \coloneqq \langle \vartheta - \theta,\ \nabla_\theta L_t(\theta) \rangle, \tag{6.21a}$$

$$\dot{x} \in f(x,t) + \beta_r \Big(\mathrm{SGN}(\varphi(x,t)) + 1 \Big) \begin{bmatrix} -(\theta - \vartheta)\mathcal{N}_t \\ 0 \end{bmatrix}, \tag{6.21b}$$

where $\beta_r \in \mathbb{R}_{>0}$. The mapping 'SGN' is the set-valued sign mapping, i.e., $\mathrm{SGN}(s)$ is equal to $s/|s|$ when $s \neq 0$ and $\mathrm{SGN}(0) = [-1, 1]$. Consequently, when $\varphi(x,t) < 0$, (6.21) behaves like (6.12). On the other hand, when $\varphi(x,t) > 0$, the reset behavior becomes active, causing (6.21) to behave like (6.21) but with β increased to a value of $\beta + 2\beta_r$. Based on these observations, a UGAS result for (6.21) can be obtained under the same conditions of Theorem 8, following similar steps in the proof and making use of Lyapunov conditions for differential inclusions.

Defining f as in (6.13), soft resets are implemented in (6.13) according to the following differential inclusion:

$$\varphi(x,t) \coloneqq \left\langle \vartheta - \theta,\ \frac{1}{\mathcal{N}_t} \nabla_\theta L_t(\theta) \right\rangle, \tag{6.22a}$$

$$\dot{x} \in f(x,t) + \beta_r \Big(\mathrm{SGN}(\varphi(x,t)) + 1 \Big) \begin{bmatrix} -(\theta - \vartheta) \\ 0 \end{bmatrix}, \tag{6.22b}$$

with $\beta_r \in \mathbb{R}_{>0}$. A UGAS result for (6.22) can be obtained using similar observations as

those made above for (6.21), following similar steps as in the proof of Theorem 9 and making use of Lyapunov conditions for differential inclusions.

In contrast with the soft-reset approach, the authors of [78] have studied various hard-reset approaches in high-order algorithms for parameter identification.

6.5 Numerical results

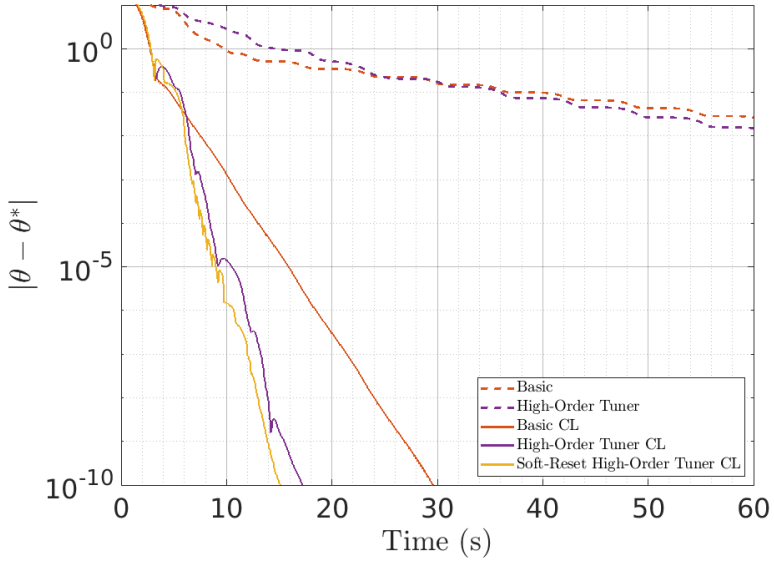

Figure 6.1: Evolution of the parameter error norm over time, for the algorithms having an unnormalized gradient term.

Figure 6.1 compares the efficiency of the basic gradient method given by

$$\dot{\theta} = -\nabla_\theta L_t(\theta) \tag{6.23}$$

and of the high-order tuner given by (6.1), along with their respective CL counterparts

given by

$$\dot{\theta} = -\gamma \left(\nabla_\theta L_t(\theta) + B(\theta, 0) \right) \tag{6.24}$$

and equation (6.12), using the online implementation described in Section 6.3.2 with $\varepsilon = 1$ and $\overline{N} = 10$. The soft-reset system is given by (6.21). Following [70, Sec. 5.7.1], we set $\phi(t) = [1,\ 1+3\sin(t),\ 1+3\cos(t)]^T$ for all $t \geq 0$ and randomly initialize the value of θ. We initialize ϑ at the same value as θ. For all algorithms, $\gamma = 0.1$, and $\mu = 0.2$. For all high-order tuners, we set $\beta = 1$ to satisfy the requirements of Theorems 6 and 8. These parameter values are intended to match those chosen in [70, Sec. 5.7]. For the soft-reset system, $\beta_r = 4$. All systems are implemented by Euler discretization with a stepsize of 10^{-3}.

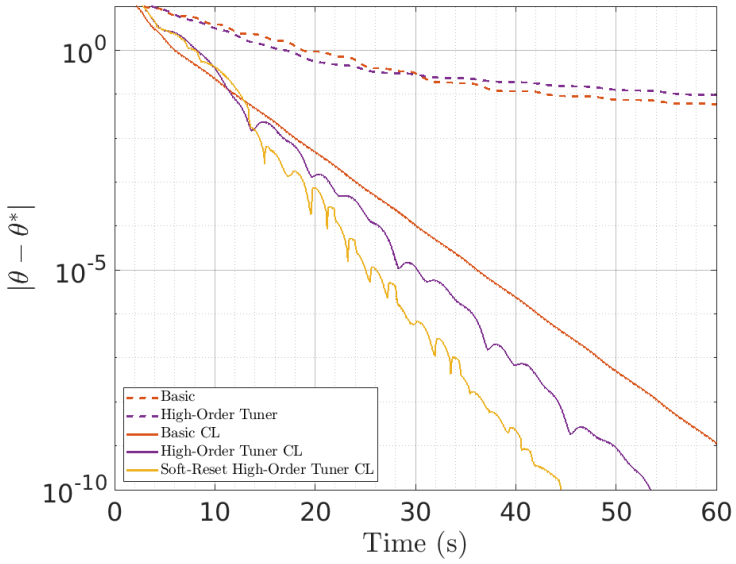

Figure 6.2: Evolution of the parameter error norm over time, for the algorithms having a normalized gradient term.

Under the same conditions as in Figure 6.1, Figure 6.2 compares the efficiency of the

basic normalized gradient method given by

$$\dot{\theta} = -\frac{\gamma}{\mathcal{N}_t}\nabla_\theta L_t(\theta) \tag{6.25}$$

and of the high-order tuner given by (6.3), along with their respective CL counterparts given by

$$\dot{\theta} = -\gamma\left(\frac{1}{\mathcal{N}_t}\nabla_\theta L_t(\theta) + B(\theta,\mu)\right) \tag{6.26}$$

and equation (6.13). To satisfy the requirements of Theorems 7 and 9, the values of β, γ, μ, and β_r are chosen to be the same as in the experiment shown by Figure 6.1.

Chapter 7

Hybrid Heavy-Ball Systems: Reset Methods for Optimization with Uncertainty

Momentum methods for convex optimization often rely on precise choices of algorithmic parameters, based on knowledge of problem parameters, in order to achieve fast convergence, as well as to prevent oscillations that could severely restrict applications of these algorithms to cyber-physical systems. To address these issues, we propose two dynamical systems, named the Hybrid Heavy-Ball System and Hybrid-inspired Heavy-Ball System, which employ a feedback mechanism for driving the momentum state toward zero whenever it points in undesired directions. We describe the relationship between the proposed systems and their discrete-time counterparts, deriving conditions based on linear matrix inequalities for ensuring exponential rates in both continuous time and discrete time. We provide numerical LMI results to illustrate the effects of our reset mechanisms on convergence rates in a setting that simulates uncertainty of problem parameters. Finally, we numerically demonstrate the efficiency and avoidance of oscillations of the proposed systems when solving both strongly convex and non-strongly convex problems.

7.1 Introduction

Convex optimization problems are becoming increasingly challenging as they find broader applications in cyber-physical systems, where they often bring stringent requirements on the efficiency and robustness of the algorithms that are used to solve them. In theory and in practice, the efficient convergence of iterative algorithms for convex optimization can be achieved through the use of momentum, as in the sense of Nesterov's method [83, Ch. 2]. In particular, for certain strongly convex problems, one theoretically significant aspect of Nesterov's method is that it achieves an efficient degradation of its convergence rate as the conditioning of the problem tends to infinity [84, Sec. 4.5]. However, in order to maintain such a property, the algorithmic parameters, namely the stepsize and momentum parameter, must be selected according to a specific formula dependent on the problem parameters. When such parameters are unavailable, Nesterov's method, as well as other momentum methods, not only lose their theoretical guarantees of efficiency but also suffer from oscillations in their trajectories that hinder their convergence in practice [85]. Moreover, such oscillations can make momentum methods unreliable for applications in feedback-based optimization [54] [57], where the algorithm is used in feedback interconnection with a physical system and can thereby jeopardize the safety of that system when experiencing oscillations.

Oscillations in momentum methods have been addressed with reset mechanisms [86] [87] [88], many of which involve scheduling the times at which the resets occur without using any feedback information about the state of the algorithm but instead by using knowledge or estimates of certain problem parameters, which are often uncertain or entirely unknown in practice. In contrast, the adaptive reset mechanisms of [85] offer conditions that can be computed straightforwardly at each iteration using state information to determine the instants of reset. Although the theoretical guarantees of efficiency

under the adaptive mechanism of [85] are difficult to extend beyond quadratic objectives, the proposed reset conditions raise analogies with reset systems in control theory, especially those that have benefited from the use of hybrid systems theory [15], suggesting opportunities to analyze and design novel optimization algorithms with resets within a hybrid systems framework, as done in [89].

Our work builds on the themes of [89] and [15] in order to determine whether or not (and to what extent) a feedback-based reset mechanism can either improve or degrade the efficiency and robustness to uncertainty of momentum methods. First, we introduce a hybrid dynamical system, referred to as the Hybrid Heavy-Ball Method (HHBM), that incorporates momentum in its flows and uses an adaptive mechanism to reset the momentum to zero whenever it points away from the negative gradient of the objective function. We also introduce a differential inclusion, referred to as the Hybrid-inspired Heavy-Ball Method (HiHBM), that uses a similar mechanism to adjust the amount of damping of the momentum. These two systems serve as vehicles for investigating the effects of reset mechanisms in existing momentum methods and for deriving novel momentum methods that are useful for their robustness to uncertainty. Toward these goals, we first derive linear matrix inequality (LMI) conditions for HHBM to achieve exponential convergence in the continuous-time sense for the case of strongly convex quadratic objectives, in order to relate our proposed ideas to an existing result on linear reset systems [90]. Using insights gained from the proof, we formulate analogous LMI conditions, assuming only strong convexity, for a general class of discrete-time systems whose special cases include discretizations of HHBM, HiHBM, and several other dynamical systems of interest in optimization, including the Hybrid Hamiltonian Algorithm of [89]. Our discrete-time analysis generalizes known LMI conditions in the literature on momentum methods, extending prior results from time-invariant systems to systems that feature switching behaviors based on state-feedback information.

We show numerically that our LMI conditions can be used to compute feasible exponential rates for the proposed family of discrete-time systems, revealing that the proposed reset laws derived from HHBM and HiHBM can mitigate the deterioration of rates caused by uncertainty about problem parameters. The computations suggest that the reset laws do not quite preserve the rate guarantees of Nesterov's method when assuming perfect knowledge of problem parameters; on the other hand, we demonstrate that the discrete-time analogues of HHBM and HiHBM show promise in achieving fast convergence and reduction of oscillations without requiring precise tuning of algorithmic parameters, in contrast to Nesterov's method. Finally, we compare the performance of the considered methods for a non-strongly convex objective to show that our proposed algorithms exhibit similar advantages over existing methods as in the strongly convex case, even when existing methods are tuned extensively by experiment.

7.2 Modeling heavy-ball systems with resets

Consider the problem

$$\min_{q\in\mathbb{R}^n} \ \phi(q) \tag{7.1}$$

under the following assumption:

Assumption 17 *The objective* $\phi : \mathbb{R}^n \to \mathbb{R}$

1. *attains* $\phi^* := \min_{q\in\mathbb{R}^n} \phi(q) > -\infty$,
2. *is continuously differentiable,*
3. *has compact sublevel sets,*

4. has an L-Lipschitz[1] *gradient* $\nabla\phi$,

5. is invex [29], i.e., satisfies

$$\mathcal{Q}^* \coloneqq \{q \in \mathbb{R}^n : \phi(q) = \phi^*\} = \{q \in \mathbb{R}^n : \nabla\phi(q) = 0\}.$$

For the purpose of computing a solution to (7.1), we propose algorithms that are extensions of the following system, referred to as a heavy-ball system with parameter $K \in \mathbb{R}_{>0}$, denoted HB(K) and with state denoted $x \coloneqq (q, p)$:

$$\dot{x} = \begin{bmatrix} p \\ -Kp - \nabla\phi(q) \end{bmatrix}. \tag{7.2}$$

We propose the Hybrid Heavy-Ball Method (HHBM) with parameter $K \in \mathbb{R}_{>0}$, denoted HHB(K), which is a hybrid system [10, Ch. 2] with state $z \coloneqq (x, \tau)$, with $x \coloneqq (q, p)$, with flow map and jump map

$$\begin{aligned} \dot{x} = f_0(x) &\coloneqq \begin{bmatrix} p \\ -Kp - \nabla\phi(q) \end{bmatrix}, \quad \dot{\tau} = 1, \\ x^+ = g_0(x) &\coloneqq \begin{bmatrix} q \\ 0 \end{bmatrix}, \qquad\qquad \tau^+ = 0, \end{aligned} \tag{7.3a}$$

with flow set $\mathcal{F}$ given by

$$\begin{aligned} \mathcal{F}_0 &\coloneqq \{(q, p) \in \mathbb{R}^{2n} : \langle \nabla\phi(q), p\rangle \leq 0\}, \\ \mathcal{F} &\coloneqq \left(\mathbb{R}^{2n} \times [0, \underline{T}]\right) \cup \left(\mathcal{F}_0 \times [\underline{T}, \infty)\right), \quad \underline{T} \in \mathbb{R}_{>0}, \end{aligned} \tag{7.3b}$$

[1] *A function is said to be L-Lipschitz if it is Lipschitz continuous with Lipschitz constant L.*

and jump set $\mathcal{J}$ given by

$$\begin{aligned}\mathcal{J}_0 &\coloneqq \{(q,p) \in \mathbb{R}^{2n} : \ \langle \nabla\phi(q), p\rangle \geq 0\},\\ \mathcal{J} &\coloneqq \mathcal{J}_0 \times [\underline{T}, \infty).\end{aligned} \tag{7.3c}$$

The parameter $\underline{T}$ provides temporal regularization in the sense of [90] to avoid purely discrete-time solutions. Without the regularization, the fact that $\mathcal{F}_0 \cap \mathcal{J}_0 \neq \emptyset$ would allow for solutions [10, Def 2.6] that jump indefinitely. Note that, for sufficiently small $\underline{T}$, the special case HHB(0) is closely related to the Hybrid Hamiltonian Algorithm [89].

We also propose a differential inclusion referred to as the Hybrid-inspired Heavy-Ball Method (HiHBM) with parameters $\{\underline{K}, \overline{K}\} \in \mathbb{R}^2$ satisfying $0 < \underline{K} \leq \overline{K}$, denoted HiHB($\underline{K}$, $\overline{K}$), with state $x \coloneqq (q,p)$ and dynamics given by

$$\dot{x} \in F(x) \coloneqq \begin{bmatrix} p \\ -\kappa(x)p - \nabla\phi(q) \end{bmatrix}, \tag{7.4a}$$

$$\begin{aligned}\kappa(x) &\coloneqq \kappa(x; \underline{K}, \overline{K})\\ &\coloneqq \begin{cases} \overline{K} & \text{if } \langle \nabla\phi(q), p\rangle > 0,\\ \underline{K} & \text{if } \langle \nabla\phi(q), p\rangle < 0,\\ \left[\underline{K}, \overline{K}\right] & \text{if } \langle \nabla\phi(q), p\rangle = 0. \end{cases}\end{aligned} \tag{7.4b}$$

For any $K \in \mathbb{R}_{>0}$, HiHB(K, K) is equivalent to HB(K).

Under Assumption (17), it can be shown that $\mathcal{Q}^*$ is uniformly globally asymptotically stable [10, Def. 3.6] for the system (7.3), with the proof being similar to that of [89, Thm. 1]. An analogous result can be obtained for (7.4). However, we focus here on studying exponential rates of convergence.

7.3 Continuous-time exponential rates

A differentiable function ϕ is said to be μ-strongly convex if, for some $\mu \in \mathbb{R}_{>0}$, it holds that, for all $x, y \in \mathbb{R}^n$,

$$\phi(y) \geq \phi(x) + \nabla\phi(x)^T(y-x) + \frac{\mu}{2}|y-x|^2.$$

We use the following property of strongly convex functions with Lipschitz gradient, which is established in [91, Eq. 3.27] as a special case of [84, Lemma 6].

Lemma 7.3.1 *Let $\phi : \mathbb{R}^n \mapsto \mathbb{R}$ be μ-strongly convex with L-Lipschitz gradient. Defining*

$$M_{\mu,L} \coloneqq \begin{bmatrix} -\frac{\mu L}{\mu+L} I_n & \frac{1}{2} I_n \\ \frac{1}{2} I_n & -\frac{1}{\mu+L} I_n \end{bmatrix}, \tag{7.5}$$

it holds that, for all $v, w \in \mathbb{R}^n$,

$$\begin{bmatrix} v-w \\ \nabla\phi(v) - \nabla\phi(w) \end{bmatrix}^T M_{\mu,L} \begin{bmatrix} v-w \\ \nabla\phi(v) - \nabla\phi(w) \end{bmatrix} \geq 0. \tag{7.6}$$

We now establish a result regarding exponential convergence of HHBM.

Theorem 11 *For $K \in \mathbb{R}_{>0}$, let*

$$\begin{aligned} A &\coloneqq \begin{bmatrix} 0 & I_n \\ 0 & -KI_n \end{bmatrix}, \quad A_R \coloneqq \begin{bmatrix} I_n & 0 \\ 0 & 0 \end{bmatrix}, \\ B &\coloneqq \begin{bmatrix} 0 \\ -I_n \end{bmatrix}, \qquad\qquad C \coloneqq \begin{bmatrix} I_n \\ 0 \end{bmatrix}^T. \end{aligned} \tag{7.7}$$

Consider a μ-strongly convex quadratic function ϕ satisfying Assumption (17) with unique

global minimum denoted q^*, and let $x^* \coloneqq (q^*, 0)$. Defining $M_{\mu,L}$ by (7.5), suppose that there exist $\alpha, \varepsilon, \sigma_\phi, \sigma_1, \sigma_2 \in \mathbb{R}_{>0}$ and a positive definite $P \in \mathbb{R}^{2n\times 2n}$ such that the matrices

$$
\begin{aligned}
M_{\mathcal{F}} &\coloneqq \begin{bmatrix} PA + A^TP + 2\alpha P & PB \\ B^TP & 0 \end{bmatrix}, \\
M_{\mathcal{J}} &\coloneqq \begin{bmatrix} A_R^TPA_R - P & 0 \\ 0 & 0 \end{bmatrix}, \\
M_{\phi} &\coloneqq \begin{bmatrix} C^T & 0 \\ 0 & I_n \end{bmatrix} M_{\mu,L} \begin{bmatrix} C & 0 \\ 0 & I_n \end{bmatrix}, \\
M_{\varepsilon} &\coloneqq \begin{bmatrix} \varepsilon I_n & 0 & 0 \\ 0 & \varepsilon I_n & -\frac{1}{2}I_n \\ 0 & -\frac{1}{2}I_n & 0 \end{bmatrix}, \quad M_0 \coloneqq M_{(\varepsilon=0)}
\end{aligned}
\tag{7.8}
$$

satisfy

$$M_{\mathcal{F}} + \sigma_\phi M_\phi + \sigma_1 M_\varepsilon \leq 0, \tag{7.9a}$$

$$M_{\mathcal{J}} - \sigma_2 M_0 \leq 0. \tag{7.9b}$$

Then, there exist $\underline{T}^*, c \in \mathbb{R}_{>0}$ such that, for all $\underline{T} \in (0, \underline{T}^*)$, the solutions of HHB(K) satisfy

$$|x(t,j) - x^*| \leq c|x_0 - x^*| \exp\left(-\frac{\alpha}{\mathrm{cond}(P)}t\right) \tag{7.10}$$

for each initial condition $x(0,0) \coloneqq x_0 \in \mathcal{F} \cup \mathcal{J}$ and for all $(t,j) \in \mathrm{dom}\, x$. Here, $cond(P) \coloneqq \lambda_{max}(P)/\lambda_{min}(P)$, where $\lambda_{max}(P)$ and $\lambda_{min}(P)$ denote the largest and smallest eigenvalues of P, respectively.

Proof: Define

$$\tilde{x} \coloneqq x - x^*, \qquad \tilde{q} \coloneqq q - q^*,$$
$$e \coloneqq (\tilde{x}, u), \qquad u \coloneqq \nabla\phi(q).$$

We aim to apply [90, Thm. 2] to the system whose state is $\tilde{x}$. To do so, we first observe that, under the given assumptions on ϕ, there exists a positive definite matrix $\tilde{Q}$ such that $\nabla\phi(q) = \tilde{Q}(q - q^*) = \tilde{Q}\tilde{q}$, so that the flow map and jump map for the system with state $\tilde{x}$ can be written as

$$\tilde{A} \coloneqq \begin{bmatrix} 0 & I_n \\ -\tilde{Q} & -KI_n \end{bmatrix}, \tag{7.11a}$$
$$\tilde{f}_0(\tilde{x}) = \tilde{A}\tilde{x}, \tag{7.11b}$$
$$\tilde{g}_0(\tilde{x}) = A_R\tilde{x}, \tag{7.11c}$$

with A_R given by (7.7). Then, letting $\tilde{\phi}(\tilde{q}) \coloneqq (1/2)\left|\tilde{Q}^{1/2}\tilde{q}\right|^2$, the flow set (7.3b) and jump set (7.3c) can be expressed in terms of $\tilde{x} \coloneqq (\tilde{q}, p)$ by observing that $(q, p) = (\tilde{q} + q^*, p)$ and that

$$\nabla_{\tilde{q}}\tilde{\phi}(\tilde{q}) = \nabla_q\phi(q), \quad \forall q \in \mathbb{R}^n. \tag{7.12}$$

For brevity, we omit the subscript of ∇ herein.

First, note that [90, Assumption 1] holds because g_0 in (7.11c) satisfies $g_0(\tilde{x}) = A_R\tilde{x} \in \mathcal{F}$. To satisfy the condition [90, Eq. 20], take $V(\tilde{x}) \coloneqq \tilde{x}^T P\tilde{x}$. Then, to show that [90, Eq. 22] is satisfied, multiply (7.9b) by e^T and e on the left and right, respectively, and

observe that

$$e^T M_0 e = -p^T \nabla \phi(q) \leq 0, \quad \forall (q,p) \in \mathcal{J}.$$

Then, (7.12) ensures that [90, Eq. 22] holds for all points in the jump set of the system whose state is $\tilde{x}$.

Next, to show that [90, Eq. 21] is satisfied, define

$$\mathcal{F}_\varepsilon \coloneqq \{(\tilde{q},p) \in \mathbb{R}^{2n} : \; p^T \nabla \tilde{\phi}(\tilde{q}) - \varepsilon \left(|\tilde{q}|^2 + |p|^2\right) \leq 0\}. \tag{7.13}$$

Then, multiply (7.9) by e^T and e on the left and right, respectively. From (7.12), we have the inequality

$$e^T M_\varepsilon e = -p^T \nabla \tilde{\phi}(\tilde{q}) + \varepsilon |\tilde{x}|^2 \geq 0, \quad \forall \tilde{x} \in \mathcal{F}_\varepsilon,$$

which implies that

$$e^T \left(M_{\mathcal{F}} + \sigma_\phi M_\phi\right) e \leq 0, \quad \forall \tilde{x} \in \mathcal{F}_\varepsilon.$$

Then, observe that $e^T M_\phi e$ is equal to the left-hand side of (7.6) when $v = q$ and $w = q^*$. Hence, Lemma 7.3.1 can be applied to obtain $e^T M_\phi e \geq 0$. It follows from the previous inequality that

$$e^T M_{\mathcal{F}} e \leq 0, \quad \forall \tilde{x} \in \mathcal{F}_\varepsilon.$$

Expanding the left-hand side yields

$$\frac{\partial V}{\partial \tilde{x}} \tilde{A}\tilde{x} \leq -2\alpha V(\tilde{x}) \leq -2\alpha\lambda_{\min}(P)|\tilde{x}|^2, \quad \forall \tilde{x} \in \mathcal{F}_\varepsilon.$$

Furthermore, the condition [90, Eq. 20] is satisfied according to $V(\tilde{x}) \leq \lambda_{\max}(P)|\tilde{x}|^2$. Thus, letting $a_2 \coloneqq \lambda_{\max}(P)$ and $a_3 \coloneqq 2\alpha\lambda_{\min}(P)$, [90, Thm. 2.1] ensures that there exists $\underline{T}^* \in \mathbb{R}_{>0}$ such that, for all $\underline{T} \in (0, \underline{T}^*)$ and for all $x_0 \in \mathcal{F} \cup \mathcal{J}$, the solutions x of HHB(K) are such that $\tilde{x}$ converges to zero with an exponential rate of $a_3/(2a_2) = 2\alpha\lambda_{\min}(P)/(2\lambda_{\max}(P)) = \alpha/\mathrm{cond}(P)$. ■

The role of M_ε in Theorem 11 motivates the results of the next section, where we take advantage of a similar approach in order to arrive at LMI conditions that are more numerically tractable and interpretable than (7.9). See 7.5.1 for more discussion on the feasibility of (7.9).

7.4 Discrete-time exponential rates

7.4.1 Discrete-time dynamic equations

Throughout this section, we assume that ϕ is a μ-strongly convex function satisfying Assumption 17. For certain choices of β, the following system, with state $x \coloneqq (q, p)$ and parameter $\epsilon \in \mathbb{R}_{>0}$, can be viewed as a discretization of the systems studied in the previous sections:

$$\begin{aligned} q_{k+1} &= q_k + \epsilon p_{k+1}, \\ p_{k+1} &= \beta(x_k)p_k - \epsilon\nabla\phi(q_k). \end{aligned} \tag{7.14}$$

Setting $\beta \equiv 1-\epsilon K$, the system (7.14) is a discretization of HB(K) defined in (7.2), which we refer to as Polyak's method. On the other hand, defining β to be

$$\begin{aligned}\beta(x_k) &:= \beta(x_k; \underline{\beta}, \overline{\beta}) \\ &:= \begin{cases} \overline{\beta} := 1 - \epsilon \underline{K} & \text{if } \langle \nabla\phi(q_k), p_k \rangle < 0, \\ \underline{\beta} := 1 - \epsilon \overline{K} & \text{if } \langle \nabla\phi(q_k), p_k \rangle \geq 0, \end{cases}\end{aligned} \tag{7.15}$$

(7.14) is a discretization of HiHB($\underline{K}$, $\overline{K}$) and is referred to as HiHB-Pol with parameters $0 \leq \underline{\beta} \leq \overline{\beta} \leq 1$. For the case of $\underline{\beta} = 0$ and $\overline{\beta} = 1 - \epsilon K$ in (7.15), the resulting system in (7.14) is a discretization of HHB(K) and is referred to as HHB-Pol with parameter $\overline{\beta}$. Thus, HHB-Pol is a special case of HiHB-Pol.

Note that, when discretizing HHB(K), there is no need to account for τ and $\underline{T}$. To see why, consider the case of $\underline{\beta} = 0$ and $\overline{\beta} = 1-\epsilon K$ in (7.15), and observe that, for any k such that $\nabla\phi(q_k) \neq 0$, and for sufficiently small ϵ, $\langle \nabla\phi(q_{k+1}), p_{k+1} \rangle = -\epsilon \nabla\phi(q_k)^T \nabla\phi(q_{k+1}) \simeq -\epsilon |\nabla\phi(q_k)| < 0$. Thus, $\beta(x_k) = \underline{\beta}$ implies that $\beta(x_{k+1}) = \overline{\beta}$. In other words, assuming sufficiently small ϵ, whenever x_k reaches a "jump" state, it immediately returns to a "flow" state and remains in "flow" states for some iterations thereafter. In this sense, HHB-Pol naturally models the temporally regularized system HHB(K) by having trajectories in which each "jump" is followed by a period of "flow".

Remark 7.4.1 *The form* (7.14) *has been referred to as a two-step or multi-step discretization [92], which is related to symplectic integration [93]. From this viewpoint, other systems of interest in optimization can be obtained from* (7.14)*. Setting* $\underline{\beta} = 0$ *and* $\overline{\beta} = 1$ *in* (7.15)*,* (7.14) *becomes a discretization of the Hybrid Hamiltonian Algorithm of [89]. Setting* $\beta \equiv 1$*,* (7.14) *is a symplectic integration of Hamiltonian flow, i.e., the left-hand variant of [93, Thm. 3.3]. Related systems are found in [92, Eq. 26] and [94, Sec. 2].*

The results of the next section will be applicable to two different discretizations of HHBM, one based on Polyak's method and another based on Nesterov's method [83], which we now describe. These two discretizations will also be possible for HiHBM. First, the system (7.14) can be rewritten to resemble Polyak's method in [95]:

$$q_{k+1} = q_k + \epsilon \left[\beta(x_k)p_k - \epsilon\nabla\phi(q_k)\right], \tag{7.16a}$$

$$p_{k+1} = \frac{q_{k+1} - q_k}{\epsilon}. \tag{7.16b}$$

We have already described above how special cases of this system correspond to discretizations of HHBM and HiHBM.

Next, note that, for strongly convex objectives, the continuous-time limit of Polyak's method is the same differential equation as the continuous-time limit of Nesterov's method [96]. Hence, we also consider the following system to be a discretization of our proposed hybrid and hybrid-inspired systems:

$$q_{k+1} = q_k + \epsilon \left[\beta(x_k)p_k - \epsilon\nabla\phi(q_k + \epsilon\beta(x_k)p_k)\right], \tag{7.17a}$$

$$p_{k+1} = \frac{q_{k+1} - q_k}{\epsilon}. \tag{7.17b}$$

For the case $\beta \equiv 1 - \epsilon K$, we simply refer to (7.17) as Nesterov's method with parameter $K \in \mathbb{R}_{>0}$. On the other hand, defining β as in (7.15), the system (7.17) is a discretization of HiHBM and is referred to as HiHB-Nes. Then, for the special case of $\underline{\beta} = 0$ and $\overline{\beta} = 1 - \epsilon K$ in (7.15), the system (7.17) is a discretization of HHBM, referred to as HHB-Nes.

In subsequent sections, it will be convenient to define the stepsize parameter $h \coloneqq \epsilon^2$, which appears as the coefficient of the gradient in the above discrete-time systems.

7.4.2 LMI conditions

Toward the goal of deriving LMI conditions for exponential convergence, consider the system

$$x_{k+1} = \hat{A}x_k + \hat{B}u_k, \qquad y_k = \hat{C}x_k, \tag{7.18a}$$

$$u_k = \nabla\phi(y_k), \qquad \xi_k = \hat{E}x_k, \tag{7.18b}$$

having a fixed point (x^*, u^*, y^*, ξ^*) that satisfies $\xi^* = q^* \coloneqq \arg\min_{q\in\mathbb{R}^n} \phi(q)$ and

$$x^* = \hat{A}x^* + \hat{B}u^*, \qquad y^* \coloneqq \hat{C}x^*,$$

$$u^* \coloneqq \nabla\phi(y^*), \qquad \xi^* = \hat{E}x^*.$$

We now begin rewriting (7.16a) and (7.17a) in the form (7.18). For the system (7.16a), we define a set of system matrices in (7.18) for each case of the switching law (7.15). Specifically, we set $x_k = (q_{k-1}, q_k)$ and, letting $h \coloneqq \epsilon^2$, we have

$$\begin{aligned} \hat{A} &= \begin{bmatrix} 0 & I_n \\ -\overline{\beta}I_n & (\overline{\beta}+1)I_n \end{bmatrix}, \quad \hat{B} = \begin{bmatrix} 0 \\ -hI_n \end{bmatrix}, \\ \hat{C} &= \begin{bmatrix} 0 \\ I_n \end{bmatrix}^T, \qquad \hat{E} = \begin{bmatrix} 0 \\ I_n \end{bmatrix}^T. \end{aligned} \tag{7.20}$$

Then, define $(\hat{A}_R, \hat{B}_R, \hat{C}_R, \hat{E}_R)$ in the same way but with $\overline{\beta}$ replaced by $\underline{\beta}$. (In this case, $\hat{B} = \hat{B}_R$, $\hat{C} = \hat{C}_R$, and $\hat{E} = \hat{E}_R$.) The subscript R indicates that these matrices represent the iterations that correspond to the (continuous-time) instants at which HHBM "resets" its p-state.

For the system (7.17a), define

$$(\hat{A}, \hat{B}, \hat{E}) \text{ as in (7.20)}, \quad \hat{C} = \begin{bmatrix} -\overline{\beta} I_n \\ (\overline{\beta} + 1) I_n \end{bmatrix}^T. \tag{7.21}$$

Then, define $(\hat{A}_R, \hat{B}_R, \hat{C}_R, \hat{E}_R)$ in the same way but with $\overline{\beta}$ replaced by $\underline{\beta}$. (In this case, $\hat{B} = \hat{B}_R$, and $\hat{E} = \hat{E}_R$.)

For convenience, we use the following notation to distinguish between the "non-reset" and "reset" regions in the state-space of our proposed systems:

$$\begin{aligned} S = &\{x = (x_1, x_2) \in \mathbb{R}^{2n} : \\ &\langle \nabla \phi(\hat{C}x),\ x_2 - x_1 \rangle < 0\}, \end{aligned} \tag{7.22a}$$

$$\begin{aligned} S_R = &\{x = (x_1, x_2) \in \mathbb{R}^{2n} : \\ &\langle \nabla \phi(\hat{C}x),\ x_2 - x_1 \rangle \geq 0\}. \end{aligned} \tag{7.22b}$$

These sets reflect the switching law (7.15) but with p_k scaled by ϵ (which does not change the nature of the law because $\epsilon > 0$). Then, combining the system matrices of (7.20) or (7.21) with (7.18), we have a representation that can capture either system (7.16) or

system (7.17), respectively, making both systems amenable to our LMI-based analysis:

$$x_k \in S \implies \begin{cases} x_{k+1} &= \hat{A}x_k + \hat{B}u_k, \\ y_k &= \hat{C}x_k, \\ u_k &= \nabla\phi(y_k), \\ \xi_k &= \hat{E}x_k, \end{cases} \tag{7.23a}$$

$$x_k \in S_R \implies \begin{cases} x_{k+1} &= \hat{A}_R x_k + \hat{B}_R u_k, \\ y_k &= \hat{C}_R x_k, \\ u_k &= \nabla\phi(y_k), \\ \xi_k &= \hat{E}_R x_k. \end{cases} \tag{7.23b}$$

We now have the ingredients to establish the following.

Theorem 12 *Let ϕ be a μ-strongly convex function satisfying Assumption 17 with minimizer denoted q^*. With system matrices $(\hat{A}, \hat{B}, \hat{C}, \hat{E})$ given by either* (7.20) *or* (7.21)*, define the matrices*

$$M_P \coloneqq \begin{bmatrix} \hat{A}^T P \hat{A} - \rho^2 P & \hat{A}^T P \hat{B} \\ \hat{B}^T P \hat{A} & \hat{B}^T P \hat{B} \end{bmatrix},$$

$$\Sigma_1 \coloneqq \begin{bmatrix} \hat{E}\hat{A} - \hat{C} & \hat{E}\hat{B} \\ 0 & I_n \end{bmatrix}, \quad \Sigma_2 \coloneqq \begin{bmatrix} \hat{C} - \hat{E} & 0 \\ 0 & I_n \end{bmatrix},$$

$$N_1 \coloneqq \Sigma_1^T \begin{bmatrix} \frac{L}{2} I_n & \frac{1}{2} I_n \\ \frac{1}{2} I_n & 0 \end{bmatrix} \Sigma_1,$$

$$N_2 \coloneqq \Sigma_2^T \begin{bmatrix} \frac{-\mu}{2} I_n & \frac{1}{2} I_n \\ \frac{1}{2} I_n & 0 \end{bmatrix} \Sigma_2,$$

$$N_3 \coloneqq \begin{bmatrix} \hat{C} & 0 \\ 0 & I_n \end{bmatrix}^T \begin{bmatrix} \frac{-\mu}{2} I_n & \frac{1}{2} I_n \\ \frac{1}{2} I_n & 0 \end{bmatrix} \begin{bmatrix} \hat{C} & 0 \\ 0 & I_n \end{bmatrix},$$

$$M_1 \coloneqq N_1 + N_2, \quad M_2 \coloneqq N_1 + N_3,$$

$M_3 = M_\phi$ *as defined by* (7.8),

$$M \coloneqq \begin{bmatrix} 0 & 0 & \frac{1}{2} I_n \\ 0 & 0 & -\frac{1}{2} I_n \\ \frac{1}{2} I_n & -\frac{1}{2} I_n & 0 \end{bmatrix}. \tag{7.24}$$

Define $(M_{P,R}, M_{1,R}, M_{2,R}, M_{3,R})$ *in the same way except with system matrices* $(\hat{A}_R, \hat{B}_R, \hat{C}_R, \hat{E}_R)$. *Suppose that there exist* $a, \lambda, \lambda_R, \sigma, \sigma_R \in \mathbb{R}_{>0}$, $\rho \in (0, 1]$, *and a positive definite* $P \in \mathbb{R}^{2n \times 2n}$ *such that*

$$\begin{aligned} M_P + a\rho^2 M_1 + a(1-\rho^2) M_2 \\ + \lambda M_3 + \sigma M \leq 0, \end{aligned} \tag{7.25a}$$

$$\begin{aligned} M_{P,R} + a\rho^2 M_{1,R} + a(1-\rho^2) M_{2,R} \\ + \lambda_R M_{3,R} - \sigma_R M \leq 0. \end{aligned} \tag{7.25b}$$

Then, for each initial condition $x_0 \in \mathbb{R}^{2n}$, *there exists* $c \in \mathbb{R}_{>0}$ *such that the trajectory of* (7.18) *satisfies*

$$\phi(\xi_k) - \phi(\xi^*) \leq c\rho^{2k}$$

for all $k \in \mathbb{Z}_{\geq 0}$. *In particular,*

$$c = \frac{1}{a} \left(a(\phi(\xi_0) - \phi^*) + (x_0 - x^*)^T P (x_0 - x^*) \right).$$

Proof: With $\xi \coloneqq \hat{E}x$, we will show that the function V_k given by

$$\begin{aligned} P_k &\coloneqq \rho^{-2k}P, \quad a_k \coloneqq a\rho^{-2k}, \\ V_k(x) &\coloneqq \rho^{-2k}\left(a(\phi(\xi)-\phi^*) + (x-x^*)^T P(x-x^*)\right) \end{aligned} \tag{7.26}$$

satisfies

$$V_{k+1}(x_{k+1}) \leq V_k(x_k), \tag{7.27}$$

for every iteration k of (7.23), from which it follows that

$$a_k(\phi(\xi_k)-\phi^*) \leq V_k(x_k) \leq V_0(x_0),$$

and therefore,

$$\phi(\xi_k)-\phi^* \leq \left(\frac{V_0(x_0)}{a}\right)\rho^{2k}.$$

First, with u defined by (7.18) and letting

$$e_k \coloneqq [x_k - x^* \quad u_k - u^*]^T, \tag{7.28}$$

we note that M in (7.24) satisfies

$$e_k^T M e_k \geq 0, \quad \forall k \text{ s.t. } x_k \in S, \tag{7.29a}$$

$$e_k^T M e_k \leq 0, \quad \forall k \text{ s.t. } x_k \in S_R. \tag{7.29b}$$

Now, consider any k such that $x_k \in S$. Multiply (7.25a) by e_k^T and e_k on the left and

right, respectively. Then, observe that (7.29a) implies

$$\sigma e_k^T M e_k \geq 0, \tag{7.30}$$

while Lemma 7.3.1 implies

$$\lambda e_k^T M_3 e_k \geq 0, \tag{7.31}$$

and therefore,

$$e_k^T \left(M_P + a\rho^2 M_1 + a(1-\rho^2) M_2 \right) e_k \leq 0. \tag{7.32}$$

Letting

$$M_{P_k} \coloneqq \begin{bmatrix} \hat{A}^T P_{k+1} \hat{A} - P_k & \hat{A}^T P_{k+1} \hat{B} \\ \hat{B}^T P_{k+1} \hat{A} & \hat{B}^T P_{k+1} \hat{B} \end{bmatrix},$$

multiply the previous inequality by ρ^{-2k-2} to obtain

$$e_k^T \left(M_{P_k} + a_k M_1 + (a_{k+1} - a_k) M_2 \right) e_k \leq 0. \tag{7.33}$$

We will use (7.33) momentarily.

Next, from [91, Lemma 4.1], we have

$$\phi(\xi_{k+1}) - \phi(\xi_k) \leq e_k^T M_1 e_k, \tag{7.34}$$

$$\phi(\xi_{k+1}) - \phi^* \leq e_k^T M_2 e_k. \tag{7.35}$$

Multiply (7.34) by a_k, multiply (7.35) by $(a_{k+1} - a_k)$, and then add the resulting inequal-

ities to obtain

$$\begin{aligned} &a_{k+1}(\phi(\xi_{k+1}) - \phi^*) - a_k(\phi(\xi_k) - \phi^*) \\ &\quad \leq e_k^T \left(a_k M_1 + (a_{k+1} - a_k) M_2\right) e_k. \end{aligned} \tag{7.36}$$

Combine this inequality with the fact that

$$\begin{aligned} e_k^T M_{P_k} e_k = &(x_{k+1} - x^*)^T P_{k+1} (x_{k+1} - x^*) \\ &- (x_k - x^*)^T P_k (x_k - x^*) \end{aligned}$$

to obtain

$$\begin{aligned} &V_{k+1}(x_{k+1}) - V_k(x_k) \\ &\quad \leq e_k^T \left(M_{P_k} + a_k M_1 + (a_{k+1} - a_k) M_2\right) e_k. \end{aligned} \tag{7.37}$$

Combining this inequality with (7.33), we have shown that (7.27) holds for all k such that $x_k \in S$.

Finally, for any k such that $x_k \in S_R$, we may show (7.27) using the same steps above, replacing (M_P, M_1, M_2, M_3) with $(M_{P,R}, M_{1,R}, M_{2,R}, M_{3,R})$ and replacing (7.30) with

$$-\sigma_R e_k^T M e_k \geq 0,$$

which follows from (7.29b). Because $S \cup S_R = \mathbb{R}^{2n}$, we have shown that (7.27) holds for all k. ■

Theorem 12 is a generalization of [91, Thm 3.2], extending the class of systems from those of the form (7.18) to those of the form (7.23).

7.5 Numerical results

7.5.1 LMI solutions

We now demonstrate how Nesterov's method is impacted by uncertainty about the problem parameters (μ, L) and how HHB-Nes (7.17) shows some promise for mitigating these effects. For simplicity, we use the notation β in this section for both the β parameter of Nesterov's method as well as the $\overline{\beta}$ parameter of HHB-Nes. We are interested in a setting in which the stepsize parameter h and momentum parameter β deviate significantly from the optimal values (h^*, β^*), by which we mean the values dependent on (μ, L) that have been shown in, e.g., [84, Proposition 12], to be optimal with respect to the class of μ-strongly convex objectives with L-Lipschitz gradient. Specifically, for both Nesterov's method and HHB-Nes, we set $h = 1/(2L)$ and $\beta = 1 - 0.1\sqrt{h}$, which makes h an underestimate of h^* and makes β close to 1 but still increasing with L.

To obtain a value of ρ from the LMI (7.25), we perform a bisection search on ρ, solving the resulting LMI for each fixed value of $\rho \in [0, 1]$. From the discussion in [84, Sec. 4.2], the structure of the system matrices in (7.21) ensures that the LMI (7.25) holds with $n \geq 1$ being the dimension of dom ϕ if and only if it holds for $n = 1$. So, we attempt to solve the LMI only for $n = 1$ here. For each fixed ρ, the LMI is solved by SeDuMi 1.3 in Matlab 2020*a*. The resulting values of ρ for $\mu = 1$ and $L \in [1, 100]$ are shown by the top two curves in Figure 7.1a in tuning (h, β) causes ρ to deteriorate significantly for Nesterov's method, while HHB-Nes mitigates these impacts. For Nesterov's method, we use the LMI in [91, Thm 3.2] of which Theorem 12 is an extension. The bottom two curves in Figure 7.1b depict the case $(h, \beta) = (h^*, \beta^*)$, showing that, when the algorithmic parameters are tuned with perfect knowledge of (μ, L), HHBM does not necessarily preserve the scaling behavior of ρ with respect to L/μ, which is a desirable property of Nesterov's method [84, Sec. 4.5]. The experiment is repeated for HiHB-Nes

with $\underline{\beta} = 1 - \sqrt{h}$ in Figure 7.1b, which shows that HiHB-Nes trades off between the behaviors of HHB-Nes and Nesterov's method.

We pursued similar experiments for HHB-Pol, in which the LMI (7.25) was able to show that, for various choices (and sequences of choices) of algorithmic parameters, HHB-Pol achieves nearly the same convergence rate as Polyak's method across a variety of values of L/μ. In particular, setting $\mu = 1$ and using parameters that are (locally) optimal for the strongly convex setting [84, Sec. 4.2], HHB-Pol achieves the same convergence rate as Polyak's method up to the value of L at which rates can no longer be guaranteed for Polyak's method, reproducing the curve in [84, Figure 5] labelled "LMI (sector)". These results suggest that HHB-Pol at least preserves the rates achievable by Polyak's method, even if it does not improve on those rates for any particular value of L/μ.

The continuous-time LMI (7.9) is difficult to solve (performing a bisection search for $\alpha \in [10^{-6}, 100]$) unless the $B = [0 \ -I_n]^T$ matrix is replaced by $[-I_n \ -I_n]^T$, in which case the LMI is feasible for a restrictive range of values for L/μ, and the rates are difficult to compare with those of the heavy-ball differential equation. We leave it to future research to determine the permissible modifications to (A, B, C, M_ε) that could play a role in improving the feasibility of LMI conditions such as (7.9).

7.5.2 Example: strongly convex quadratic objective

In this section, we show examples of how HHBM can prevent oscillations from appearing in the trajectory of $\phi(q)$ that are caused by having a poorly tuned pair (h, β). In particular, we consider a problem with strongly convex quadratic objective $\phi(q) \coloneqq \frac{1}{2}q^T Q q + b^T q$, with $L/\mu = 10^3$, and with Q and b randomly generated as described at the end of this subsection. As in the previous section, we intentionally use a smaller value of h than recommended in theory ($h = 10^{-4}$), forcing $\beta = 1 - \sqrt{h}K$ to take values very close

to 1. As a consequence, it is more intuitive to discuss the parameters of the algorithms in terms of K rather than β, which we do in Figure 7.2, where $K = 1.97$ roughly corresponds to the value that yields the fastest convergence rate for Polyak's method and Nesterov's method for the given h and given (Q, b) (determined experimentally). Figure 7.2 shows that the convergence rates of both Polyak's method and Nesterov's method deteriorate significantly when K underestimates the desirable value of 1.97. Furthermore, due to the large L/μ, the only way to remove the oscillations from the trajectory of Polyak's method is to increase K to the point at which the asymptotic convergence rate is significantly slower than seen in Figure 7.2a. In contrast, HHBM achieves the same asymptotic rates as the other two methods when $K = 1.97$, while it exhibits both faster asymptotic rates and fewer oscillations when K underestimates the desirable value.

We do not include HiHBM in Figure 7.2 because the chosen stepsize is sufficiently small that the performance of HiHBM can be made to resemble that of HHBM very closely by choosing $\overline{K}$ sufficiently large. The appeal of HiHBM will instead be conveyed in the next section.

It is important to note that the advantages of HHBM and HiHBM are specific to the situation simulated above, in which the optimal algorithmic parameters are unavailable, especially when h is too small and β is too large. In our experiments, we have found situations where Polyak's method and Nesterov's method do not exhibit oscillations when using their respective optimally tuned parameters, and in these situations, our proposed algorithms essentially achieve the same asymptotic convergence rates (and lack of oscillations) as their classic counterparts. These observations are compatible with our LMI computations of the previous section, which suggested that our algorithms do not improve on the rates of their classic counterparts when optimal algorithmic parameters are available.

We use the following approach to generate a random matrix with a specific condition

number L/μ. In fact, we consider only $\mu = 1$. First, generate a random $n \times n$ matrix. Then, take the singular value decomposition USV^T, and replace S with $\hat{S}$, where $\hat{S}$ has diagonal entries σ_i for $i \in \{1, \ldots, n\}$ satisfying $\sigma_{\min} = 1$ and $\sigma_{\max} = \sqrt{L}$, with each of the remaining $n-2$ diagonal entries being uniformly distributed on $[1, \sqrt{L}]$. Let $\hat{Q} = U\hat{S}V^T$, and take $Q \coloneqq \hat{Q}\hat{Q}^T$ to be the matrix that defines ϕ. To generate b, we take each of its entries to be uniformly distributed on $[-100, 100]$. Initial conditions are randomly generated in the same way as b. We have verified that the behaviors in Figure 7.2 persist across several random trials.

7.5.3 Example: logistic regression

In this section, we show that our proposed algorithms may have advantages even when applied to problems that are more general than those considered in our analyses. We consider a problem of logistic regression, common in statistical data analysis and machine learning [97, Ch. 4]. Figure 7.3 compares convergence rates for a problem of logistic regression with dataset (Θ, b), where $\Theta \in \mathbb{R}^{n \times m}$ has columns denoted Θ_i and entries randomly drawn with standard normal distribution, and each component b_i of b is uniformly randomly drawn from $\{-1, 1\}$. The dataset has $m = 1000$ observations. The objective is

$$\phi(q) = \sum_{i=1}^{m} \log\left(1 + \exp\left(-b_i \Theta_i^T q\right)\right). \tag{7.38}$$

The objective is convex but not strictly convex. However, on any compact set, it satisfies the μ-PL condition [98, Eq. 3] for some constant μ (see [98, Sec. 2.3] for a discussion).

The stepsizes of gradient descent, Nesterov's method, and Polyak's method were tuned via bisection search. For Polyak's method, the best stepsize was chosen from a broad range of values, with the value of β being tuned via bisection search for each

stepsize considered. For Nesterov's method, we use the standard sequence of values for β intended for the class of general convex objectives [83, Sec. 2.2], namely the sequence $\alpha_k(1-\alpha_k)/\left[\alpha_k^2+\alpha_{k+1}\right]$ where α_k satisfies $\alpha_{k+1}^2=(1-\alpha_{k+1})\alpha_k^2$ (here, the initialization of β had negligible effect). For HiHBM, we set $\underline{K}=0$, while the stepsize and $\overline{K}$ were tuned in the same way that the stepsize and β were tuned for HBM (which resulted in the same ϵ found for HBM). For HHBM, the stepsize and $\underline{K}$ were tuned in the same way that the stepsize and $\overline{K}$ were tuned for HiHBM, resulting in the same stepsize found for Nesterov's method and $\underline{K}=0$.

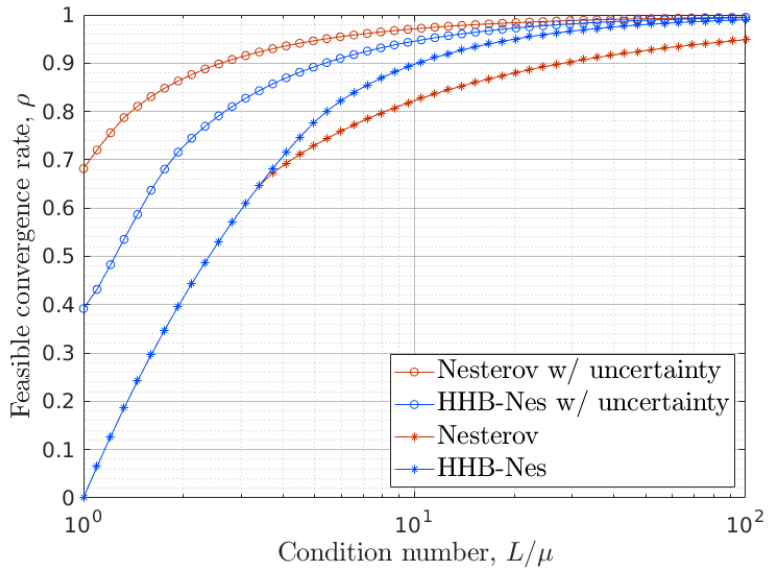

(a) $\underline{\beta} = 0$

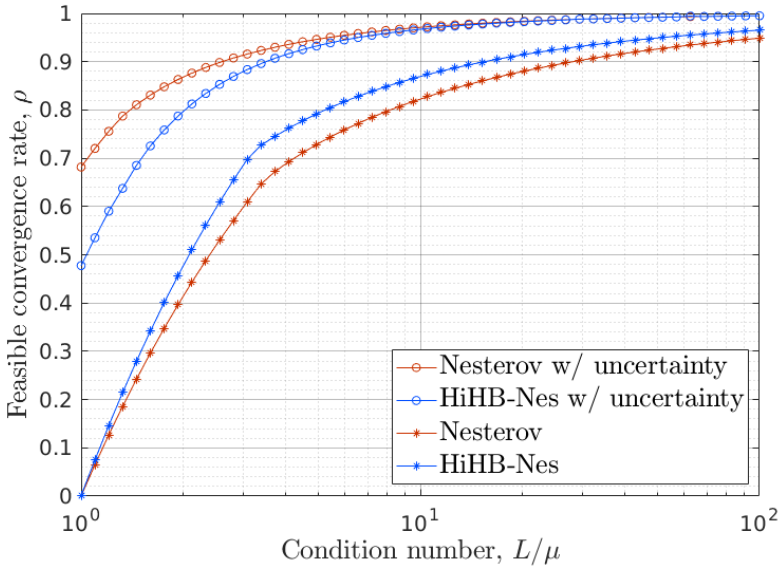

(b) $\underline{\beta} = 1 - \sqrt{h}$

Figure 7.1: Values of ρ obtained from Thm. 12 for HHB-Nes and HiHB-Nes and from [91, Thm 3.2] for Nesterov's method. The circled curves indicate uncertainty about (μ, L) in tuning (h, β), as described in Sec. 7.5.1. The starred curves indicate that h and β are tuned with perfect knowledge of (μ, L), using [84, Proposition 12].

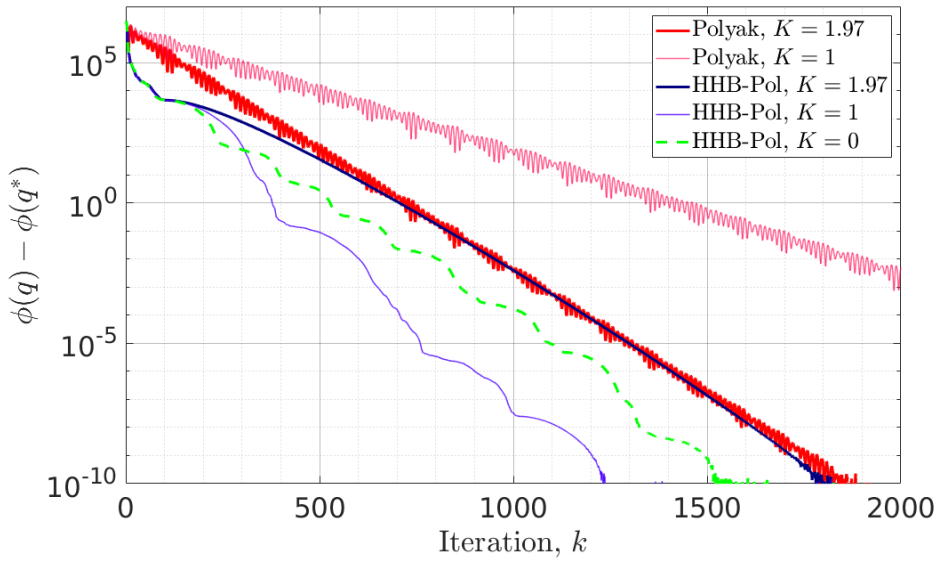

(a)

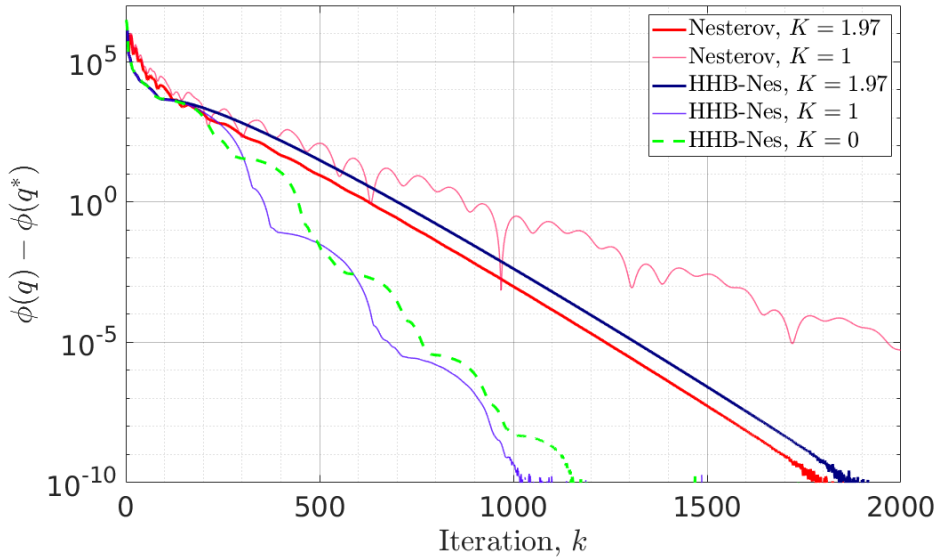

(b)

Figure 7.2: The value of $\phi(q) - \phi(q^*)$ versus iteration k, where ϕ is a strongly convex quadratic objective, and q^* is the minimizer of ϕ computed by Matlab's "quadprog" function.

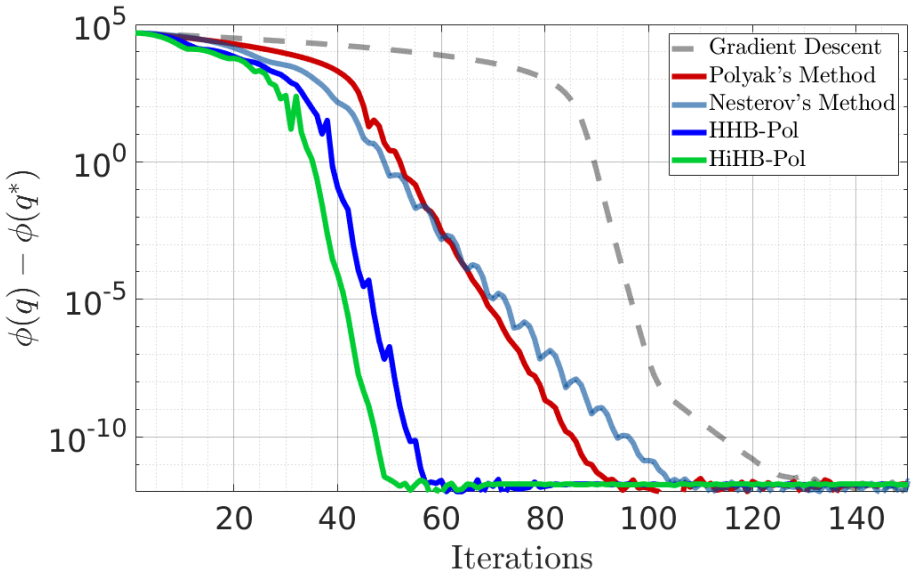

Figure 7.3: The value of $\phi(q) - \phi(q^*)$ versus iteration k, where ϕ is the logistic regression objective (7.38), and q^* is the minimizer of ϕ computed by gradient descent.

Chapter 8

Nonconvex Optimization via Resets and Stochasticity

In previous chapters, gradient-based optimization dynamics have been interpreted as dynamical systems and control systems, enabling the use of tools from stability theory for studying convergence and performance. This interpretation can be extended to discrete-time systems having both stochasticity and set-valued right-hand sides, which have been shown to be useful for nonconvex problems. The resulting dynamics are modeled as stochastic difference inclusions, for which stability analysis can be carried out using invariance principles. In this chapter, we make use of recent developments in Lyapunov-like analyses for gradient-based algorithms in nonconvex optimization, enabling the use of an invariance principle for establishing a probabilistic notion of asymptotic stability for the set of global minimizers of a not-necessarily-convex but suitably smooth objective function.

8.0.1 Introduction

Optimization problems with nonconvex objectives are becoming increasingly prevalent in large-scale signal processing, data analysis, and machine learning [99, Ch. 7-10]. In these areas, the training of deep neural networks is an especially prevalent application

in which nonconvex objectives arise. Moreover, multi-agent systems such as UAV teams [100], [101] may require decentralized training of neural networks using data collected online in a changing and uncertain environment, where robustness to noise becomes crucial. In centralized settings, nonconvex problems have often been tackled using iterative first-order optimization algorithms [99, Ch. 3], [102, Ch. 4], which are discrete-time dynamical systems that update their states using only information about the first-order gradient of the objective function, and possibly the objective function value, at each iteration. Well-known examples include gradient descent and momentum-based methods such as the Accelerated Gradient Method [103, Ch. 3]; see [104], [102], and [99] for other examples. Unlike the convex setting, the nonconvex setting often calls for certain modifications to the dynamics of first-order methods in order to ensure efficient convergence in theory and in practice. Two such modifications that have been shown to be especially effective include the injection of stochastic perturbations and the resetting of momentum variables [105]. Each of these two modifications gives rise to its own challenges in the analysis of convergence, and the challenges are further complicated when combining the two modifications.

On one hand, due to the presence of saddle points in a variety of nonconvex objectives that arise in applications, theoretical research has taken an interest in studying the efficiency with which first-order algorithms escape from saddle points. When establishing such guarantees, the introduction of a stochastic perturbation to the dynamic equation has been crucial to the analysis. For example, in [106], a random vector is added to the state of the gradient descent algorithm before executing each update, resulting in an algorithm referred to as Perturbed Gradient Descent that is shown to escape from saddle points and, in particular, to converge to a neighborhood of a second-order stationary point with high probability. Here, a second-order stationary point is defined as a point where the first-order gradient vanishes and where the second-order gradient (assumed

to be Lipschitz continuous) is positive semidefinite. In the subsequent work of [107], a similar perturbation applied to the Accelerated Gradient Method yields the Perturbed Accelerated Gradient Method, which is shown to converge more efficiently to second-order stationary points than Perturbed Gradient Descent.

On the other hand, the training of deep neural networks is a nonconvex optimization problem in which momentum-based methods, such as the Accelerated Gradient Method and its derivative methods, have been shown experimentally to be crucial in achieving practical efficiency of convergence; see, for example, [108]. In this context, each momentum-based method has its advantages and disadvantages according to the design of its dynamics and the selection of the (possibly time-varying or state-dependent) algorithmic parameters such as the stepsize. Due to the complexity and poor conditioning of the optimization landscape, the design of dynamics and algorithmic parameters becomes crucial to preventing severe fluctuations in an algorithm's trajectory that may significantly degrade its efficiency. In momentum-based methods, such fluctuations are often addressed using reset mechanisms, which are mechanisms that reset the momentum variable to zero when certain conditions are met. Resets have been shown experimentally to greatly improve on the efficiency of momentum-based methods when training deep neural networks [105]. Although the literature on this subject has historically used the term "restarting", we use the term "resetting" to maintain the analogy with control systems that is central to our work.

Various reset mechanisms have been proposed and analyzed for momentum-based methods, such as those in [109], [86], [88], [87], and [85]. The mechanisms differ in terms of the conditions that trigger the resets, some of which are periodic or based on the number of iterations, while others are based on state-dependent conditions involving the objective and/or gradient. Existing analyses have provided estimates for convergence rates on a case-by-case basis, depending on the specific reset mechanism and class of

objective functions considered. On the other hand, hybrid systems theory has recently led to a framework that enables systematic study of convergence rates for a broad class of state-dependent reset mechanisms and for strongly convex objectives [26]. Central to this work is a hybrid system referred to as the Hybrid Heavy-Ball Method, for which there are discrete-time implementations that recover the Accelerated Gradient Method and Polyak's Heavy-Ball Method as special cases. The resets in these discrete-time systems are motivated by the type of reset condition studied in [85] and therefore make use of state-dependent conditions for switching the value of the momentum parameter at each iterate. One of the basic requirements for analyzing robust stability in such systems is outer semicontinuity of the right-hand side of the dynamic equations [110], and for this reason, the state-dependent momentum parameter must be modeled as a set-valued mapping and the resulting dynamics modeled by a difference inclusion. When stochasticity is incorporated in this model, invariance principles can be used to establish a probabilistic notion of stability, namely uniform global asymptotic stability in probability.

In this chapter, robust stability properties of perturbed gradient methods with resetting are established by modeling the dynamics as a stochastic difference inclusion and thereby enabling the use of invariance principles that have been developed for such systems [111], [110]. These works have established conditions under which guarantees of asymptotic stability are robust against arbitrarily small disturbances to the algorithmic state or dynamics, and hence, these guarantees are especially relevant in the aforementioned decentralized optimization problems, where numerical imprecisions may arise from limited communication bandwidth, quantized or sparsified data, and other factors that can potentially be detrimental to the convergence properties of decentralized gradient-based algorithms [112], [113]. In Section 8.1, we give both verbal and mathematical descriptions of the class of dynamics to be considered. Then, in Section 8.2, we show uniform global asymptotic stability in probability (UGASp) of the set of global minimiz-

ers for a class of not-necessarily-convex objective functions having Lipschitz continuous first and second derivatives.

8.1 A stochastic difference inclusion for global nonconvex optimization

8.1.1 Algorithmic overview

We study a stochastic difference inclusion that models a broad class of algorithms for global optimization of nonconvex objective functions. At a high level, our model is constructed from a deterministic subsystem and a stochastic subsystem, whose dynamic equations have right-hand sides given by maps G_c and G_d, respectively.

The deterministic subsystem of our model, represented by G_c, is constructed from two algorithms, referred to as the accelerated gradient method (AG) and the negative curvature exploitation method (NCE), respectively represented by maps G_a and G_b. AG is widely known to be useful for first-order convex optimization. However, when AG is applied to nonconvex problems, it can be difficult to identify a Lyapunov function for the purpose of analyzing stability properties of the resulting algorithmic dynamics. Combining AG with NCE enables us to identify such a Lyapunov function in nonconvex settings. This approach has been taken in [107].

Meanwhile, the stochastic subsystem, represented by G_d, employs stochastic updates at time instances governed by a periodically resetting timer variable τ. This stochastic feature of our model is intended to capture the behavior of algorithms that employ state perturbations or random reinitialization strategies, which are often used in practice to facilitate escape from local minima, maximizers, and saddle points in nonconvex settings.

8.1.2 Algorithmic description

Let v be a placeholder for an i.i.d. sequence of random variables having a distribution assigning positive probability to every open subset of $\mathbb{R}^n$. We study stability properties of the following stochastic difference inclusion having state variable $x \coloneqq (q, p, \tau)$ with $q \in \mathbb{R}^n$, $p \in \mathbb{R}^n$, and $\tau \in \mathbb{Z}_{\geq 0}$:

$$x^+ = G(x, v), \qquad x \in D, \tag{8.1}$$

where G and D will be defined below.

We consider the system (8.1) to be a model for algorithms that iteratively seek solutions of the following problem:

$$\min_{q' \in \mathbb{R}^n} f(q'), \tag{8.2}$$

where the objective function $f : \mathbb{R}^n \to \mathbb{R}$ is assumed to achieve a minimum in $\mathbb{R}^n$, and it is assumed that f has certain properties of smoothness and unboundedness to be described in Sec. 8.2.

We define G and D as follows, using positive numbers s, η, γ, and θ, along with positive integers $T_{\min}$ and $T_{\max}$, whose restrictions will be stated in the stability analysis of Sec. 8.2:

$$\begin{aligned}
y(q,p) &\coloneqq q + (1-\theta)p, \\
\mathcal{D}_a &\coloneqq \Big\{ (q,p) \in \mathbb{R}^{2n} : \\
&\qquad f(q) \geq f(y(q,p)) + \langle \nabla f(y(q,p)), q - y(q,p) \rangle - \frac{\gamma}{2} |q - y(q,p)|^2 \Big\}, \\
\mathcal{D}_{b,1} &\coloneqq \Big\{ (q,p) \in \overline{\mathbb{R}^{2n} \setminus \mathcal{D}_a} : \ |p|^2 \geq s \Big\},
\end{aligned}$$

$$\mathcal{D}_{b,2} \coloneqq \left\{(q,p) \in \overline{\mathbb{R}^{2n} \setminus \mathcal{D}_a} : \ |p|^2 \leq s\right\},$$

$$\mathcal{D}_b \coloneqq \mathcal{D}_{b,1} \cup \mathcal{D}_{b,2},$$

$$\mathcal{D} \coloneqq \mathcal{D}_a \cup \mathcal{D}_b,$$

$$D_a \coloneqq \mathcal{D}_a \times \{0, \ldots, T_{\min}\}, \tag{8.3a}$$

$$D_{b,1} \coloneqq \mathcal{D}_{b,1} \times \{0, \ldots, T_{\min}\}, \tag{8.3b}$$

$$D_{b,2} \coloneqq \mathcal{D}_{b,2} \times \{0, \ldots, T_{\min}\}, \tag{8.3c}$$

$$D_b \coloneqq \mathcal{D}_b \times \{0, \ldots, T_{\min}\}, \tag{8.3d}$$

$$D_c \coloneqq \mathcal{D} \times \{0, \ldots, T_{\min}\}, \tag{8.3e}$$

$$D_d \coloneqq \mathcal{D} \times \{T_{\min}, \ldots, T_{\max}\}, \tag{8.3f}$$

$$D \coloneqq D_c \cup D_d, \tag{8.3g}$$

$$g(q,p) \coloneqq y(q,p) - \eta \nabla f(y(q,p)),$$

$$G_a(x) \coloneqq \begin{bmatrix} g(q) \\ g(q) - q \\ \tau + 1 \end{bmatrix}, \tag{8.3h}$$

$$G_{b,1}(x) \coloneqq \begin{bmatrix} q \\ 0 \\ \tau + 1 \end{bmatrix}, \tag{8.3i}$$

$$G_{b,2}(x) \coloneqq \begin{bmatrix} \arg\min \left\{ f(q') : \ q' \in \left\{ q + s\frac{p}{|p|}, \ q - s\frac{p}{|p|} \right\} \right\} \\ 0 \\ \tau + 1 \end{bmatrix}, \tag{8.3j}$$

$$G_b(x) \coloneqq \begin{cases} G_{b,1}(x) & \forall x \in D_{b,1} \setminus D_{b,2} \\ G_{b,2}(x) & \forall x \in D_{b,2} \setminus D_{b,1} \\ G_{b,1}(x) \cup G_{b,2}(x) & \forall x \in D_{b,1} \cap D_{b,2}, \end{cases} \tag{8.3k}$$

$$G_c(x) \coloneqq \begin{cases} G_a(x) & \forall x \in D_a \setminus D_b \\ G_b(x) & \forall x \in D_b \setminus D_a \\ G_a(x) \cup G_b(x) & \forall x \in D_a \cap D_b, \end{cases} \tag{8.3l}$$

$$G_d(x,v) \coloneqq \begin{bmatrix} \arg\min_{q' \in \{q,v\}} f(q') \\ 0 \\ 0 \end{bmatrix}, \tag{8.3m}$$

$$G(x,v) \coloneqq \begin{cases} G_c(x) & \forall x \in D_c \setminus D_d \\ G_d(x,v) & \forall x \in D_d \setminus D_c \\ G_c(x) \cup G_d(x,v) & \forall x \in D_c \cap D_d. \end{cases} \tag{8.3n}$$

Note that, in (8.3j), if $p = 0$, the expression $p/|p|$ is considered to be 0.

8.2 Stability analysis

Our main result relies on the following assumptions regarding the function f in (8.2).

Assumption 18 *The function f is twice differentiable, and there exist positive numbers ℓ and ρ such that, for all $q_1, q_2 \in \mathbb{R}^n$,*

$$|\nabla f(q_1) - \nabla f(q_2)| \leq \ell |q_1 - q_2|, \tag{8.4a}$$

$$\left|\nabla^2 f(q_1) - \nabla^2 f(q_2)\right| \leq \rho |q_1 - q_2|. \tag{8.4b}$$

Let $\mathcal{Q}^*$ denote the set of solutions to the problem (8.2), and let f^* denote the value of f on $\mathcal{Q}^*$.

Assumption 19 *The set $\mathcal{Q}^*$ is compact, and the function f is radially unbounded with respect to $\mathcal{Q}^*$.*

Consider the continuous function $V : \mathbb{R}^{2n} \times \{0, \ldots, T_{\max}\} \to \mathbb{R}$ given by

$$V(x) \coloneqq f(q) - f^* + \frac{1}{2\gamma}|p|^2, \tag{8.5}$$

which is positive definite and radially unbounded with respect to $\mathcal{A} \coloneqq \mathcal{Q}^* \times \{0\} \subset \mathbb{R}^{2n}$.

Equation (8.5) is motivated by the work of [107], which provides key lemmas for our analysis.

Lemma 8.2.1 *If f is a differentiable function satisfying* (8.4a) *for some $\ell > 0$, and if $\eta \leq 1/(2\ell)$, $\theta \in [2\eta\gamma, 1/2]$ with $\gamma > 0$, and $T_{\min} \in \mathbb{Z}_{>0}$, it holds that*

$$V(G_a(x)) \leq V(x) \qquad \forall x \in D_a. \tag{8.6}$$

Proof: The result follows from the proof of [107, Lemma 9]. Note that the proof of [107, Lemma 9] is carried out under the condition given by [107, Eq. 8], which is compatible with our definition of D_a in (8.3a), despite this condition not being made explicit in the statement of [107, Lemma 9]. ■

Lemma 8.2.2 *Given a function f satisfying Assumption 18, $T_{\min} \in \mathbb{Z}_{>0}$, and any positive numbers γ and s, it holds that*

$$\max_{g \in G_b(x)} V(g) \leq V(x) \qquad \forall x \in D_b. \tag{8.7}$$

Proof: The result follows from the proof of [107, Lemma 10]. Note that the proof of [107, Lemma 10] accounts for the case $|p| = s$, despite this case not being explicitly accounted for in the algorithmic descriptions of [107, Alg. 2] or [107, Alg. 3]. ■

The following lemmas ensure fulfillment of some standard requirements for analyzing stability in stochastic difference inclusions.

Lemma 8.2.3 *The set-valued mapping $S : \mathbb{R}^n \rightrightarrows \mathbb{R}^{4n+2}$ given by*

$$S(v) \coloneqq \text{graph}(G(\cdot, v)) \coloneqq \{(x, y) \in \mathbb{R}^{4n+2} : y \in G(x, v)\} \quad \forall v \in \mathbb{R}^n \tag{8.8}$$

is outer semicontinuous and closed-valued.

Proof: By continuity of f, $(x, v) \mapsto G_d(x, v)$ is outer semicontinuous. By construction, it follows that $(x, v) \mapsto G(x, v)$ is outer semicontinuous. By [114, Thm. 5.7(a)], it follows that S is closed-valued. To show that S is outer semicontinuous, consider a sequence $\{(v_i, x_i, y_i)\}_{i=1}^{\infty}$ having a limit denoted $(\overline{v}, \overline{x}, \overline{y})$ and satisfying $(x_i, y_i) \in S(v_i)$ for all i. By outer semicontinuity of G, we have $\overline{y} \in G(\overline{x}, \overline{v})$. It follows that $(\overline{x}, \overline{y}) \in S(\overline{v})$. ■

Lemma 8.2.4 *The mapping S in* (8.8) *is measurable.*

Proof: By Lemma 8.2.3 and [114, Prop. 5.11(a)], we have that, for every $\zeta \in \text{range}(S) = \mathbb{R}^{4n+2}$, $v \mapsto |\zeta|_{S(v)}$ is lower semicontinuous and therefore measurable. It follows by [114, Thm. 14.3(j)] that S is measurable. ■

Theorem 13 *Under Assumptions 18 and 19, if $\eta \leq 1/(2\ell)$, $\theta \in [2\eta\gamma, 1/2]$ with $\gamma > 0$, $T_{\max} \geq T_{\min} \in \mathbb{Z}_{>0}$, and $s > 0$, the set $\mathcal{Q}^* \times \{0\} \times \{0, \ldots, T_{\max}\}$ is UGASp for the system* (8.1)*.*

Proof: We make use of an invariance principle for stochastic difference inclusions [110, Thm. 8]. To do so, we first note that, by construction, the map G in (8.3n) is locally bounded, and the map $v \mapsto \text{graph}(G(\cdot, v))$ is measurable with closed values, by Lemmas 8.2.3 and 8.2.4. Next, we show that

$$\int_{\mathbb{R}^n} \max_{g \in G(x,v)} V(g)\mu(dv) \leq V(x) \qquad \forall x \in D. \tag{8.9}$$

From Lemmas 8.2.1 and 8.2.2, along with the definitions of D_c and G_c in (8.3e) and (8.3l), respectively, we have

$$\max_{g \in G_c(x)} V(g) \leq V(x) \qquad \forall x \in D_c. \tag{8.10}$$

From (8.10) and the definitions of D_d, D, G_d, and G in (8.3f), (8.3g), (8.3m), and (8.3n), respectively, we have

$$\max_{g \in G(x,v)} V(g) \leq V(x) \qquad \forall x \in D,\ v \in \mathbb{R}^n, \tag{8.11}$$

and therefore, (8.9) holds.

Next, we show that there does not exist an almost surely complete solution of (8.1) that remains in a non-zero level set of V almost surely. Due to the fact that a stochastic update is caused by G_d at least once every $T_{\max}$ time steps, it suffices to show that those updates cause a decrease in the expected value of V from points outside of $\mathcal{A} \coloneqq \mathcal{Q}^* \times \{0\}$. To do so, let $\mathbb{B} \coloneqq \{q \in \mathbb{R}^n : |q| \leq 1\}$, and note that, given points $(q,p) \in \mathbb{R}^{2n} \setminus \mathcal{A}$ and $(q^*,p^*) \in \mathcal{A}$, there exists $\varepsilon > 0$ such that, for all $\hat{q} \in q^* + \varepsilon\mathbb{B}$, $f(\hat{q}) \leq f(q) - \varepsilon$. Then, for all $x \coloneqq (q,p,\tau) \in (\mathbb{R}^{2n} \setminus \mathcal{A}) \times \{0,\dots,T_{\max}\}$, it holds that

$$\begin{aligned}
&\int_{\mathbb{R}^n} \max_{g \in G_d(x,v)} V(g)\mu(dv) \\
&\qquad = \mu(q^* + \varepsilon\mathbb{B})(f(q) - \varepsilon) \\
&\qquad\qquad + (1 - \mu(q^* + \varepsilon\mathbb{B}))f(q) \\
&\qquad = f(q) - \mu(q^* + \varepsilon\mathbb{B})\varepsilon \\
&\qquad \leq V(x) - \mu(q^* + \varepsilon\mathbb{B})\varepsilon.
\end{aligned}$$

Due to the assumption that μ assigns non-zero measure to every open subset of $\mathbb{R}^n$, it

follows that there does not exist an almost surely complete solution of (8.1) that remains in a non-zero level set of V almost surely. ■

Chapter 9

Conclusion

In this dissertation, we have introduced soft-reset controllers for nonlinear and multi-agent systems, especially those that have nonlinear optimization objectives, by modeling them as differential inclusions and thereby enabling their stability analysis through the use of tools such as invariance principles and passivity. Conditions have been established on the data of a given hard-reset controller under which its soft-reset implementation enjoys desired passivity and stability properties, and these conditions have been extended to the multi-agent case for the problem of leader-follower target-seeking formation control. Specific soft-reset controllers have been proposed for feedback-based steady-state optimization of linear time-invariant and passive plants. In a separate thread of research, high-order tuners for parameter identification have been analyzed under persistent excitation conditions and then augmented with concurrent learning in order to relax those conditions. Soft resetting was then proposed for the resulting high-order tuners with concurrent learning. In all of the aforementioned cases, numerical results illustrated the advantages of soft-reset approaches over standard approaches. Finally, discrete-time reset systems have been proposed as iterative algorithms for convex and nonconvex optimization. For strongly convex problems, the effects of resetting on exponential rates of convergence have been studied through the use of linear matrix inequalities, while for nonconvex problems, stability properties have been established for a class of stochasti-

cally perturbed gradient methods with resetting.

We have focused on unconstrained optimization problems, but it would be of interest to investigate the handling of constraints. In continuous time, optimization constraints can encode requirements on states, inputs, and outputs that play an important role in the safety and reliably of the robotic and vehicular systems that we have emphasized in our proposed applications. In both continuous and discrete time, constraints can encode requirements on the relationship between decision variables that are computed by networked agents in a decentralized fashion, ensuring that network-wide optimality conditions are met in the absence of centralized coordination [115]. Constraints can potentially be addressed using techniques such as projected gradients and anti-windup control [116] [117], which fit into the framework of differential inclusions that we have employed in our study of soft-reset systems.

High-order tuners are applicable to certain adaptive control problems [76], although concurrent learning and resetting have not been explored in these cases. It would be of interest to incorporate concurrent learning in high-order tuners for adaptive control and investigate applications of soft resetting for such methods, motivated by the prevalence of gradient methods in adaptive control and the effectiveness of soft resetting in other settings where gradient methods have played a significant role. Similar gradient methods also arise in actor-critic algorithms for approximate dynamic programming and reinforcement learning [64], where momentum-based methods have been explored but not with soft resetting [118].

Our linear matrix inequalities for certifying exponential rates of convergence in reset systems can be refined using the general framework of integral quadratic constraints, potentially giving rise to more refined rate estimates. In this dissertation, we have made use of only one special case of such constraints. Linear matrix inequalities have also been useful for certifying convergence rates of stochastic gradient methods [119] and there-

fore provide opportunities for studying interactions between resetting and stochasticity. Moreover, we have focused on applying resets to the Heavy-Ball Method, but future research may reveal that resetting can benefit other optimization algorithms in which momentum variables are present, such as the Triple Momentum Method [36].

Finally, it would be of interest to investigate conditions under which soft-reset systems enjoy desirable properties other than passivity or stability, such as dissipativity or contractivity. Such properties would be desirable in the sense that, much like passivity, they are useful in multi-agent systems, adaptive systems, optimization algorithms, and many other applications [120] [121] [122] [123] [124] [125] [126]. Initial efforts have already been made in this direction with regard to input-to-state stability of soft-reset systems [127], and we are optimistic that future research on soft-reset systems will be as fruitful.

Bibliography

[1] J. C. Clegg, *A nonlinear integrator for servomechanisms*, *Transactions A.I.E.E.* **77 (Part II)** (1958) 41–42.

[2] K. Krishnan and I. Horowitz, *Synthesis of a non-linear feedback system with significant plant-ignorance for prescribed system tolerances*, *International Journal of Control* **19** (1974), no. 4 689–706.

[3] I. Horowitz and P. Rosenbaum, *Non-linear design for cost of feedback reduction in systems with large parameter uncertainty*, *International Journal of Control* **21** (1975), no. 6 977–1001.

[4] C. V. Hollot, *Revisiting Clegg integrators: periodicity, stability and IQCs*, in *IFAC Proceedings*, vol. 30, pp. 31–38, 1997.

[5] H. Hu, Y. Zheng, Y. Chait, and C. V. Hollot, *On the zero-input stability of control systems with Clegg integrators*, in *Proceedings of the 1997 American Control Conference*, vol. 1, pp. 408–410, 1997.

[6] C. V. Hollot, Y. Zheng, and Y. Chait, *Stability analysis for control systems with reset integrators*, in *Proceedings of the 36th IEEE Conference on Decision and Control*, vol. 2, pp. 1717–1719 vol.2, 1997.

[7] H. Hu, Y. Zheng, C. V. Hollot, and Y. Chait, *On the stability of control systems having Clegg integrators*, in *Topics in Control and its Applications*. Springer, London, 1999.

[8] Q. Chen, C. V. Hollot, and Y. Chait, *Stability and asymptotic performance analysis of a class of reset control systems*, in *Proceedings of the 39th IEEE Conference on Decision and Control*, pp. 251–256, 2000.

[9] O. Beker, C. Hollot, Y. Chait, and H. Han, *Fundamental properties of reset control systems*, *Automatica* **40** (2004), no. 6 905 – 915.

[10] R. Goebel, R. Sanfelice, and A. Teel, *Hybrid Dynamical Systems: Modeling, Stability, and Robustness*. Princeton University Press, 2012.

[11] D. Nesic, L. Zaccarian, and A. R. Teel, *Stability properties of reset systems*, *Automatica* **44** (2008), no. 8 2019–2026.

[12] D. Nesic, A. R. Teel, and L. Zaccarian, *Stability and performance of SISO control systems with first-order reset elements*, *IEEE Transactions on Automatic Control* **56** (2011), no. 11 2567–2582.

[13] A. Baños and A. Barreiro, *Reset Control Systems*. Springer, 2012.

[14] W. Aangenent, G. Witvoet, W. Heemels, M. van de Molengraft, and M. Steinbuch, *Performance analysis of reset control systems*, *International Journal of Robust and Nonlinear Control* **20** (2010), no. 11 1213–1233.

[15] C. Prieur, I. Queinnec, S. Tarbouriech, and L. Zaccarian, *Analysis and synthesis of reset control systems*, *Foundations and Trends® in Systems and Control* **6** (2018), no. 2-3 117–338.

[16] R. T. Bupp, D. S. Bernstein, V. Chellaboina, and W. M. Haddad, *Resetting virtual absorbers for vibration control*, *J. Vibr. Control* **6** (2000) 61–83.

[17] W. Haddad, V. Chellaboina, Q. Hui, and S. Nersesov, *Energy- and entropy-based stabilization for lossless dynamical systems via hybrid controllers*, *IEEE Transactions on Automatic Control* **52** (2007), no. 9 1604–1614.

[18] W. Haddad, V. Chellaboina, and S. Nersesov, *Impulsive and Hybrid Dynamical Systems*. Princeton University Press, 2006.

[19] K. J. Astrom and B. M. Bernhardsson, *Comparison of Riemann and Lebesgue sampling for first order stochastic systems*, in *Proceedings of the 41st IEEE Conference on Decision and Control*, pp. 2011–2016, 2002.

[20] P. Tabuada, *Event-triggered real-time scheduling of stabilizing control tasks*, *IEEE Trans. Automat. Control* **52** (2007), no. 9 1680–1685.

[21] A. Bisoffi, R. Beerens, W. Heemels, H. Nijmeijer, N. van de Wouw, and L. Zaccarian, *To stick or to slip: A reset pid control perspective on positioning systems with friction*, *Annual Reviews in Control* **49** (2020) 37–63.

[22] R. Beerens, A. Bisoffi, L. Zaccarian, H. Nijmeijer, W. P. M. H. Heemels, and N. Van De Wouw, *Reset PID design for motion systems with Stribeck friction*, Research Report Rapport LAAS n° 20015, Eindhoven university of technology ; Rijksuniversiteit te Groningen ; LAAS-CNRS ; University of Trento ; ASML, Jan., 2020.

[23] M. Cerdeira, P. Falcón, E. Delgado, and A. Barreiro, *Reset controller design based on error minimization for a lane change maneuver*, *Sensors* **18** (2018), no. 7.

[24] A. Costas, M. Cerdeira-Corujo, A. Barreiro, E. Delgado, and A. Baños, *Car platooning reconfiguration applying reset control techniques*, in *2016 IEEE 21st International Conference on Emerging Technologies and Factory Automation (ETFA)*, pp. 1–8, 2016.

[25] S. van Loon, B. Hunnekens, W. Heemels, N. van de Wouw, and H. Nijmeijer, *Split-path nonlinear integral control for transient performance improvement*, *Automatica* **66** (2016) 262–270.

[26] J. H. Le and A. R. Teel, *Hybrid heavy-ball systems: Reset methods for optimization with uncertainty*, in *2021 American Control Conference (ACC)*, pp. 2236–2241, 2021.

[27] M. Baradaran Hosseini, J. H. Le, and A. R. Teel, *Analyzing the effect of persistent asset switches on a class of hybrid-inspired optimization algorithms*, in *2021 American Control Conference (ACC)*, pp. 3422–3427, 2021.

[28] A. R. Teel, *Continuous-time implementation of reset control systems*, in *Trends in Nonlinear and Adaptive Control – A tribute to Laurent Praly for his 65th birthday*, Lecture Notes in Control and Information Sciences. Springer, 2021.

[29] A. Ben-Israel and B. Mond, *What is invexity?*, *The ANZIAM Journal* **28** (1986), no. 1 1–9.

[30] S. Boyd and L. Vandenberghe, *Convex Optimization*. Cambridge University Press, 2004.

[31] E. P. Ryan, *A universal adaptive stabilizer for a class of nonlinear systems*, *Systems & Control Letters* **16** (1991), no. 3 209 – 218.

[32] E. P. Ryan, *An integral invariance principle for differential inclusions with applications in adaptive control*, *SIAM Journal on Control and Optimization* **36** (1998), no. 3 960–980, [https://doi.org/10.1137/S0363012996301701].

[33] C.-J. Wan, D. Bernstein, and V. Coppola, *Global stabilization of the oscillating eccentric rotor*, *Nonlinear Dynamics* (1996) 49–62.

[34] M. Jankovic, D. Fontaine, and P. V. Kokotovic, *TORA example: cascade- and passivity-based control designs*, *IEEE Transactions on Control Systems Technology* **4** (1996), no. 3 292–297.

[35] H. Khalil, *Nonlinear Control*. Pearson Education, Inc., 2015.

[36] B. Van Scoy, R. A. Freeman, and K. M. Lynch, *The fastest known globally convergent first-order method for minimizing strongly convex functions*, *IEEE Control Systems Letters* **2** (2018), no. 1 49–54.

[37] C. Meissen, K. Klausen, M. Arcak, T. I. Fossen, and A. Packard, *Passivity-based formation control for UAVs with a suspended load*, *IFAC-PapersOnLine* **50** (2017), no. 1 13150–13155. 20th IFAC World Congress.

[38] K. Klausen, C. Meissen, T. I. Fossen, M. Arcak, and T. A. Johansen, *Cooperative control for multirotors transporting an unknown suspended load under environmental disturbances*, *IEEE Transactions on Control Systems Technology* **28** (2018), no. 2 653–660.

[39] K.-K. Oh, M.-C. Park, and H.-S. Ahn, *A survey of multi-agent formation control*, *Automatica* **53** (Mar., 2015) 424–440.

[40] J. H. Le and A. R. Teel, *Passive soft-reset controllers for nonlinear systems*, in *2021 60th IEEE Conference on Decision and Control (CDC)*, pp. 5320–5325, 2021.

[41] P. Köhler, *Double-integrator leader-follower networks: Sufficient conditions for connectivity maintenance*, Master's thesis, KTH Royal Institute of Technology, 2014.

[42] H. Bai, M. Arcak, and J. Wen, *Cooperative Control Design: A Systematic, Passivity-Based Approach.* Communications and Control Engineering. Springer New York, 2011.

[43] E. Nuño and R. Ortega, *Achieving consensus of Euler–Lagrange agents with interconnecting delays and without velocity measurements via passivity-based control*, *IEEE Transactions on Control Systems Technology* **26** (2018), no. 1 222–232.

[44] A. Donaire, J. G. Romero, and T. Perez, *Trajectory tracking passivity-based control for marine vehicles subject to disturbances*, *Journal of the Franklin Institute* **354** (2017), no. 5 2167–2182.

[45] N. Chopra and M. W. Spong, *Passivity-Based Control of Multi-Agent Systems*, pp. 107–134. Springer Berlin Heidelberg, Berlin, Heidelberg, 2006.

[46] T. Hatanaka, N. Chopra, M. Fujita, and M. W. Spong, *Passivity-Based Control and Estimation in Networked Robotics.* Communications and Control Engineering. Springer International Publishing Switzerland, 2015.

[47] X. Meng, L. Xie, and Y. C. Soh, *Reset control for synchronization of multi-agent systems*, *Automatica* **104** (2019) 189–195.

[48] G. Zhao, C. Hua, and X. Guan, *Reset control for consensus of multiagent systems with event-triggered communication*, *IEEE Transactions on Cybernetics* (2019) 1–10.

[49] M. Bürger, D. Zelazo, and F. Allgöwer, *Duality and network theory in passivity-based cooperative control*, *Automatica* **50** (2014), no. 8 2051–2061.

[50] M. Arcak, C. Meissen, and A. Packard, *Networks of Dissipative Systems: Compositional Certification of Stability, Performance, and Safety*. Springer Publishing Company, Incorporated, 1st ed., 2016.

[51] M. Li, S. Yamashita, T. Hatanaka, and G. Chesi, *Smooth dynamics for distributed constrained optimization with heterogeneous delays*, *IEEE Control Systems Letters* **4** (2020), no. 3 626–631.

[52] N. Biggs, *Algebraic Graph Theory*. Cambridge Mathematical Library. Cambridge University Press, 2nd ed., 1974.

[53] J. Wang and M. Xin, *Integrated optimal formation control of multiple unmanned aerial vehicles*, *IEEE Transactions on Control Systems Technology* **21** (2013), no. 5 1731–1744.

[54] A. Hauswirth, S. Bolognani, G. Hug, and F. Dörfler, *Timescale separation in autonomous optimization*, *IEEE Transactions on Automatic Control* **66** (2021), no. 2 611–624.

[55] L. S. P. Lawrence, J. W. Simpson-Porco, and E. Mallada, *Linear-convex optimal steady-state control*, *IEEE Transactions on Automatic Control* **66** (2021), no. 11 5377–5384.

[56] A. Hauswirth, S. Bolognani, G. Hug, and F. Dörfler, *Optimization algorithms as robust feedback controllers*, 2021. `https://arxiv.org/abs/2103.11329`.

[57] L. Ortmann, A. Hauswirth, I. Caduff, F. Dörfler, and S. Bolognani, *Experimental validation of feedback optimization in power distribution grids*, *Electric Power Systems Research* **189** (2020) 106782.

[58] L. Ortmann, C. Rubin, A. Scozzafava, J. Lehmann, S. Bolognani, and F. Dörfler, *Deployment of an online feedback optimization controller for reactive power flow optimization in a distribution grid*, 2023. `https://arxiv.org/abs/2305.06702`.

[59] G. Bianchin, J. I. Poveda, and E. Dall'Anese, *Online optimization of switched lti systems using continuous-time and hybrid accelerated gradient flows*, *Automatica* **146** (2022) 110579.

[60] G. Bianchin, J. Cortés, J. I. Poveda, and E. Dall'Anese, *Time-varying optimization of lti systems via projected primal-dual gradient flows*, *IEEE Transactions on Control of Network Systems* **9** (2022), no. 1 474–486.

[61] J. P. Hespanha, *Linear Systems Theory*. Springer Nature, 2021. ISBN13: 9780691179575.

[62] K. Narendra and A. Annaswamy, *Stable Adaptive Systems*. Dover Books on Electrical Engineering. Dover Publications, 2012.

[63] G. Tao, *Adaptive Control Design and Analysis*. Adaptive and Cognitive Dynamic Systems: Signal Processing, Learning, Communications and Control. Wiley, 2003.

[64] K. G. Vamvoudakis and F. L. Lewis, *Online actor–critic algorithm to solve the continuous-time infinite horizon optimal control problem*, *Automatica* **46** (2010), no. 5 878–888.

[65] J. I. Poveda, M. Benosman, and K. G. Vamvoudakis, *Data-enabled extremum seeking: A cooperative concurrent learning-based approach*, *International Journal of Adaptive Control and Signal Processing* **35** (2021), no. 7 1256–1284.

[66] J. E. Gaudio, T. E. Gibson, A. M. Annaswamy, M. A. Bolender, and E. Lavretsky, *Connections between adaptive control and optimization in machine learning*, in *2019 IEEE 58th Conference on Decision and Control (CDC)*, pp. 4563–4568, 2019.

[67] A. P. Morgan and K. S. Narendra, *On the uniform asymptotic stability of certain linear nonautonomous differential equations*, *SIAM J. Control Optimization* **15** (1977), no. 1 5–24.

[68] E. Panteley, A. Loria, and A. Teel, *Relaxed persistency of excitation for uniform asymptotic stability*, *IEEE Transactions on Automatic Control* **46** (2001), no. 12 1874–1886.

[69] G. Chowdhary and E. Johnson, *Concurrent learning for convergence in adaptive control without persistency of excitation*, in *49th IEEE Conference on Decision and Control (CDC)*, pp. 3674–3679, 2010.

[70] J. E. Gaudio, *Fast Learning and Adaptation in Control and Machine Learning*. PhD thesis, MIT, 2020.

[71] J. E. Gaudio, A. M. Annaswamy, M. A. Bolender, E. Lavretsky, and T. E. Gibson, *A class of high order tuners for adaptive systems*, *IEEE Control Systems Letters* **5** (2021), no. 2 391–396.

[72] A. S. Morse, *High-order parameter tuners for the adaptive control of nonlinear systems*, in *Robust Control* (L. D. Davisson, A. G. J. MacFarlane, H. Kwakernaak, J. L. Massey, Y. Z. Tsypkin, A. J. Viterbi, and S. Hosoe, eds.), (Berlin, Heidelberg), pp. 138–145, Springer Berlin Heidelberg, 1992.

[73] J. M. Moreu and A. M. Annaswamy, *A stable high-order tuner for general convex functions*, 2021. `https://arxiv.org/abs/2011.09996v3`.

[74] S. McDonald, Y. Cui, J. E. Gaudio, and A. M. Annaswamy, *A high-order tuner for accelerated learning and control*, 2021. https://arxiv.org/abs/2103.12868.

[75] J. E. Gaudio, A. M. Annaswamy, J. M. Moreu, M. A. Bolender, and T. E. Gibson, *Accelerated learning with robustness to adversarial regressors*, in *Proceedings of the 3rd Conference on Learning for Dynamics and Control* (A. Jadbabaie, J. Lygeros, G. J. Pappas, P. A. Parrilo, B. Recht, C. J. Tomlin, and M. N. Zeilinger, eds.), vol. 144 of *Proceedings of Machine Learning Research*, pp. 636–650, PMLR, 2021.

[76] A. M. Annaswamy, A. Guha, Y. Cui, J. E. Gaudio, and J. M. Moreu, *Online algorithms and policies using adaptive and machine learning approaches*, 2022. https://arxiv.org/abs/2105.06577v4.

[77] A. Loria, E. Panteley, D. Popovic, and A. Teel, *A nested Matrosov theorem and persistency of excitation for uniform convergence in stable nonautonomous systems*, *IEEE Transactions on Automatic Control* **50** (2005), no. 2 183–198.

[78] D. E. Ochoa, J. I. Poveda, A. Subbaraman, G. S. Schmidt, and F. R. Pour-Safaei, *Accelerated concurrent learning algorithms via data-driven hybrid dynamics and nonsmooth ODEs*, in *Proceedings of the 3rd Conference on Learning for Dynamics and Control*, pp. 866–878, PMLR, 2021.

[79] W. Hahn, *Stability of motion*. Springer, 1967.

[80] G. Chowdhary, T. Yucelen, M. Mühlegg, and E. N. Johnson, *Concurrent learning adaptive control of linear systems with exponentially convergent bounds*, *International Journal of Adaptive Control and Signal Processing* **27** (2013), no. 4 280–301.

[81] G. Chowdhary, *Concurrent learning for convergence in adaptive control without persistency of excitation*. PhD thesis, Georgia Institute of Technology, 2010.

[82] G. Chowdhary and E. Johnson, *A singular value maximizing data recording algorithm for concurrent learning*, in *Proceedings of the 2011 American Control Conference*, pp. 3547–3552, 2011.

[83] Y. Nesterov, *Introductory Lectures on Convex Optimization: A Basic Course*. Springer Publishing Company, Incorporated, 1 ed., 2014.

[84] L. Lessard, B. Recht, and A. Packard, *Analysis and design of optimization algorithms via integral quadratic constraints*, *SIAM Journal on Optimization* **26** (2016), no. 1 57–95, [https://doi.org/10.1137/15M1009597].

[85] B. O'donoghue and E. Candès, *Adaptive restart for accelerated gradient schemes*, *Found. Comput. Math.* **15** (June, 2015) 715–732.

[86] O. Fercoq and Z. Qu, *Adaptive restart of accelerated gradient methods under local quadratic growth condition*, *IMA Journal of Numerical Analysis* **39** (Mar., 2019) 2069–2095.

[87] V. Roulet and A. d'Aspremont, *Sharpness, restart and acceleration*, in *Advances in Neural Information Processing Systems 30* (I. Guyon, U. V. Luxburg, S. Bengio, H. Wallach, R. Fergus, S. Vishwanathan, and R. Garnett, eds.), pp. 1119–1129. Curran Associates, Inc., 2017.

[88] O. Fercoq and Z. Qu, *Restarting the accelerated coordinate descent method with a rough strong convexity estimate*, *Computational Optimization and Applications* **75** (Oct., 2019) 63–91.

[89] A. R. Teel, J. I. Poveda, and J. Le, *First-order optimization algorithms with resets and Hamiltonian flows*, in *58th IEEE Conference on Decision and Control (CDC)*, 2019.

[90] D. Nešić, L. Zaccarian, and A. R. Teel, *Stability properties of reset systems*, *Automatica* **44** (Aug., 2008) 2019–2026.

[91] M. Fazlyab, A. Ribeiro, M. Morari, and V. M. Preciado, *Analysis of optimization algorithms via integral quadratic constraints: Nonstrongly convex problems*, *SIAM J. Optimization* **28** (2018), no. 3 2654–2689.

[92] M. Muehlebach and M. I. Jordan, *Optimization with momentum: Dynamical, control-theoretic, and symplectic perspectives*, 2020. `https://arxiv.org/abs/2002.12493`.

[93] E. Hairer, C. Lubich, and G. Wanner, *Geometric Numerical Integration: Structure-Preserving Algorithms for Ordinary Differential Equations; 2nd ed.* Springer, Dordrecht, 2006.

[94] M. Muehlebach and M. Jordan, *A dynamical systems perspective on Nesterov acceleration*, in *Proceedings of the 36th International Conference on Machine Learning* (K. Chaudhuri and R. Salakhutdinov, eds.), vol. 97 of *Proceedings of Machine Learning Research*, (Long Beach, California, USA), pp. 4656–4662, PMLR, 09–15 Jun, 2019.

[95] B. Polyak, *Some methods of speeding up the convergence of iteration methods*, *USSR Computational Mathematics and Mathematical Physics* **4** (Jan., 1964) 1–17.

[96] B. Shi, S. S. Du, M. I. Jordan, and W. J. Su, *Understanding the acceleration phenomenon via high-resolution differential equations*, 2018. arXiv:1810.08907.

[97] T. Hastie, R. Tibshirani, and J. Friedman, *The Elements of Statistical Learning*. Springer Series in Statistics. Springer New York Inc., New York, NY, USA, 2001.

[98] H. Karimi, J. Nutini, and M. Schmidt, *Linear convergence of gradient and proximal-gradient methods under the Polyak-Lojasiewicz condition*, in *Machine Learning and Knowledge Discovery in Databases* (P. Frasconi, N. Landwehr, G. Manco, and J. Vreeken, eds.), (Cham), pp. 795–811, Springer International Publishing, 2016.

[99] P. Jain and P. Kar, *Non-convex optimization for machine learning*, *Found. Trends Mach. Learn.* **10** (Dec., 2017) 142–336.

[100] P. S. Bithas, E. T. Michailidis, N. Nomikos, D. Vouyioukas, and A. G. Kanatas, *A survey on machine-learning techniques for UAV-based communications*, *Sensors (Basel, Switzerland)* **19** (Nov, 2019) 5170.

[101] Y. Choi, M. Martel, S. I. Briceno, and D. N. Mavris, *Multi-UAV Trajectory Optimization and Deep Learning-based Imagery Analysis for a UAS-based Inventory Tracking Solution*. AIAA, 2019. https://arc.aiaa.org/doi/pdf/10.2514/6.2019-1569.

[102] L. Bottou, F. E. Curtis, and J. Nocedal, *Optimization methods for large-scale machine learning*, *SIAM Review* **60** (2018), no. 2 223–311, [https://doi.org/10.1137/16M1080173].

[103] S. Bubeck, *Convex optimization: Algorithms and complexity*, *Foundations and Trends® in Machine Learning* **8** (2015), no. 3-4 231–357.

[104] A. Beck, *First-Order Methods in Optimization*. Society for Industrial and Applied Mathematics, Philadelphia, PA, 2017.

[105] B. Wang, T. M. Nguyen, A. L. Bertozzi, R. G. Baraniuk, and S. J. Osher, *Scheduled restart momentum for accelerated stochastic gradient descent*, 2020. `https://arxiv.org/abs/2002.10583`.

[106] C. Jin, R. Ge, P. Netrapalli, S. M. Kakade, and M. I. Jordan, *How to escape saddle points efficiently*, in *Proceedings of the 34th International Conference on Machine Learning - Volume 70*, ICML'17, pp. 1724–1732, JMLR.org, 2017.

[107] C. Jin, P. Netrapalli, and M. I. Jordan, *Accelerated gradient descent escapes saddle points faster than gradient descent*, in *Proceedings of the 31st Conference On Learning Theory* (S. Bubeck, V. Perchet, and P. Rigollet, eds.), vol. 75 of *Proceedings of Machine Learning Research*, pp. 1042–1085, PMLR, 06–09 Jul, 2018.

[108] I. Sutskever, J. Martens, G. Dahl, and G. Hinton, *On the importance of initialization and momentum in deep learning*, in *Proceedings of the 30th International Conference on Machine Learning* (S. Dasgupta and D. McAllester,

eds.), vol. 28 of *Proceedings of Machine Learning Research*, (Atlanta, Georgia, USA), pp. 1139–1147, PMLR, 17–19 Jun, 2013.

[109] P. Giselsson and S. Boyd, *Monotonicity and restart in fast gradient methods*, in *53rd IEEE Conference on Decision and Control*, pp. 5058–5063, 2014.

[110] A. Subbaraman and A. R. Teel, *Recurrence principles and their application to stability theory for a class of stochastic hybrid systems*, *IEEE Transactions on Automatic Control* **61** (2016), no. 11 3477–3492.

[111] A. R. Teel, *A recurrence principle for stochastic difference inclusions*, *IEEE Transactions on Automatic Control* **60** (2015), no. 2 420–435.

[112] E. by: Peter Kairouz and H. B. McMahan, *Advances and open problems in federated learning*, *Foundations and Trends® in Machine Learning* **14** (2021), no. 1 –.

[113] T. Ben-Nun and T. Hoefler, *Demystifying parallel and distributed deep learning: An in-depth concurrency analysis*, *ACM Comput. Surv.* **52** (Aug., 2019).

[114] R. T. Rockafellar and R. J. Wets, *Variational Analysis*, vol. 317. Springer Berlin, Heidelberg, 1998.

[115] T. Yang, X. Yi, J. Wu, Y. Yuan, D. Wu, Z. Meng, Y. Hong, H. Wang, Z. Lin, and K. H. Johansson, *A survey of distributed optimization*, *Annual Reviews in Control* **47** (2019) 278 – 305.

[116] A. Hauswirth, F. Dörfler, and A. R. Teel, *On the differentiability of projected trajectories and the robust convergence of non-convex anti-windup gradient flows*, *IEEE Control. Syst. Lett.* **4** (2020), no. 3 620–625.

[117] A. Hauswirth, F. Dörfler, and A. R. Teel, *On the robust implementation of projected dynamical systems with anti-windup controllers*, in *2020 American Control Conference, ACC 2020, Denver, CO, USA, July 1-3, 2020*, pp. 1286–1291, IEEE, 2020.

[118] D. E. Ochoa and J. I. Poveda, *Accelerated continuous-time approximate dynamic programming via data-assisted hybrid control*, *IFAC-PapersOnLine* **55** (2022), no. 12 561–566. 14th IFAC Workshop on Adaptive and Learning Control Systems ALCOS 2022.

[119] B. Hu, S. Wright, and L. Lessard, *Dissipativity theory for accelerating stochastic variance reduction: A unified analysis of SVRG and Katyusha using semidefinite programs*, in *Proceedings of the 35th International Conference on Machine Learning* (J. Dy and A. Krause, eds.), vol. 80 of *Proceedings of Machine Learning Research*, pp. 2038–2047, PMLR, 10–15 Jul, 2018.

[120] M. Arcak, C. Meissen, and A. Packard, *Networks of Dissipative Systems: Compositional Certification of Stability, Performance, and Safety*. SpringerBriefs in Electrical and Computer Engineering. Springer International Publishing, 2016.

[121] B. Hu and L. Lessard, *Dissipativity theory for nesterov's accelerated method*, in *Proceedings of the 34th International Conference on Machine Learning - Volume 70*, ICML'17, pp. 1549–1557, JMLR.org, 2017.

[122] N. M. Boffi and J.-J. E. Slotine, *Implicit Regularization and Momentum Algorithms in Nonlinearly Parameterized Adaptive Control and Prediction*, *Neural Computation* **33** (03, 2021) 590–673, [https://direct.mit.edu/neco/article-pdf/33/3/590/1889460/neco_a_01360.pdf].

[123] Q. Jiao, H. Modares, F. L. Lewis, S. Xu, and L. Xie, *Distributed L_2-gain output-feedback control of homogeneous and heterogeneous systems*, *Automatica* **71** (2016) 361–368.

[124] P. J. Antsaklis, B. Goodwine, V. Gupta, M. J. McCourt, Y. Wang, P. Wu, M. Xia, H. Yu, and F. Zhu, *Control of cyber-physical systems using passivity and dissipativity based methods*, *European Journal of Control* **19** (2013), no. 5 379 – 388. The Path of Control.

[125] B. Brogliato, R. Lozano, B. Maschke, and O. Egeland, *Dissipative Systems Analysis and Control: Theory and Applications*. Springer, 2007.

[126] Z. Aminzare, B. Dey, E. N. Davison, and N. E. Leonard, *Cluster synchronization of diffusively coupled nonlinear systems: A contraction-based approach*, *Journal of Nonlinear Science* **30** (Oct, 2020) 2235–2257.

[127] M. Baradaran Hosseini, J. H. Le, and A. R. Teel, *Input-to-state stability of soft-reset systems with nonlinear data*, *Mathematics of Control, Signals, and Systems* (Feb, 2023).